A TYPOLOGY OF FOREDUNE TEXTURES:

SAND PATCHES AND CLIMATE CONTROLS

A Dissertation

by

WANSANG RYU

Submitted to the Office of Graduate Studies of
Texas A&M University
in partial fulfillment of the requirements for the degree of

DOCTOR OF PHILOSOPHY

Approved by:

Co-Chairs of Committee,	Douglas J. Sherman
	Vatche P. Tchakerian
Committee Members,	Steven M. Quiring
	Chris Houser
Head of Department,	Vatche P. Tchakerian

December 2012

Major Subject: Geography

ABSTRACT

Foredunes are formed and developed in association with vegetation. A bare sand area has been viewed as a measure of dune mobility or activity and researched in association with climate controls: particularly wind power, annual mean precipitation, and temperature, expressed in annual mean potential evapotranspiration. There has been no research that utilized the patterns of bare sand areas to classify foredune areas in coastal dune systems and investigated climate controls related to sand patch patterns, or "foredune textures" such as size, number, and distribution of sand patches.

Four foredune types were classified based on four landscape metrics (PLAND: percentage of bare sand area, PLADJ: proportion of like-adjacencies, NLSI: normalized landscape shape index, and ENN_RA: range of Euclidean nearest neighbor), by applying the concepts and methodologies of landscape ecology. Four climate variables (annual mean precipitation, annual mean potential evapotranspiration, Lancaster's mobility index, and the standard deviation of annual mean precipitation) were found to affect the foredune types and help in distinguishing one foredune type from another.

The amount of bare sand area on coastal foredune areas can be explained by annual mean precipitation (R^2 is 0.52 at the 99 % confidence level), standard deviation of precipitation (R^2 is 0.51 at the 99 % confidence level), and Lancaster's mobility index (R^2 is 0.37 at the 99 % confidence level) but wind variables such as drift potential do not explain much (R^2 is 0.04 at maximum). This suggests that dune activity or stabilization

in coastal dune systems is mainly controlled by vegetation cover, which is in turn affected by precipitation. Foredune textures can be a useful tool to predict foredune types in association with future climate change, and the optimal averaging period of precipitation for each bare sand area was seven years.

ACKNOWLEDGEMENTS

I would like to thank Dr. Douglas Sherman, one of my co-chairs. He has always been patient and supportive, and encouraged me when I was struggling with doing this research. He is not only my advisor for my academic career, but also a mentor for my life. I also would like to thank Dr. Vatche Tchakerian, Dr. Steven Quiring, and Dr. Chris Houser for their thoughtful comments and suggestions.

Numerous individuals have contributed to this research. Dr. Jangwhan Choi, Dr. Hosahng Rhew, Dr. Moochan Kim, Dr. Hyunmyung Cho, and Dr. Sangnam Ahn helped me to learn mathematics and computer programs such as Matlab, GrADS and Stada. Dr. Daehyun Kim has never hesitated to help me. Diana Vance helped me to refine this dissertation.

I am also very thankful to Pastor Hongil Lim and the members of Vision Mission Church for their warm encouragement and prayers. Pastor Wonil Lim has been my spiritual mentor since I was a teenager. I miss my parents, Jungwoong and Bongja, and my sister, Youngmi. They have always taken care of me and prayed for me.

I could not finish this long way without my wife, Okja, who I love most. She has been patient with me for so long, but has encouraged and loved me, and prayed for me in any situation. I am very thankful to God for giving my wife, my family, and those good people, and enabling me to finish my dissertation. Gig'em!

TABLE OF CONTENTS

Page

LIST OF FIGURES

Page

LIST OF TABLES

Page

1 INTRODUCTION

A foredune is the seawardmost feature of a coastal dune system, formed on the top of the backshore by an accumulation of sand being transported by wind above the threshold velocity (Hesp 2002). When wind approaches vegetation, wind speed decreases and wind-blown sand is trapped around vegetation and starts to accumulate (Hesp 1983). Hence, vegetation is important in forming foredunes and also providing a barrier that protects inland areas (Miller, Gornish, and Buckley 2010). In this way, wind (for sand transport), and precipitation and temperature, often expressed in potential evapotranspiration, (for vegetation cover) are considered the most fundamental variables for foredunes (Thomas and Leason, 2005). However, vegetated dunes are the most sensitive and fragile to any effect of changes (damages) of the components of the active littoral zone because the dunes retain the damages for a long time (Rust and Illenberger 1996). After the vegetation cover is damaged or destroyed by various climatic causes such as waves or washovers due to severe storms or hurricanes, prolonged drought, fire, or burial due to an excessive amount of sand transport (Hesp 2002), a bare sand area on the dunes allows the remobilization of sand from stabilized dunes (Van der Meulen and Salman 1996). In this manner, the extent of bare sand areas or active dune areas have been viewed as an index of dune activity or mobility and researched in an attempt to find the relationships between dune activity/mobility and recent climate variability (Thomas and Leason 2005; Hugenholtz and Wolfe 2005b; Tsoar 2005). On coastal dunes, bare sand areas have been researched mainly in association with blowouts or parabolic dunes

often focused on aeolian processes (Gares 1992; Gares and Nordstrom 1988; Hesp and Hyde 1996). On the other hand, on inland or desert dunes, most research on bare sand areas have been used as a measure of dune migration in association with climate variables such as wind, precipitation and potential evapotranspiration (Barchyn and Hugenholtz 2012; Hugenholtz et al. 2012; Nield and Baas 2008). For this reason, several researchers such as Lancaster (1988) and Tsoar (2005) created mobility indices (Bullard et al. 1997). The overall results of the research on dune mobility and its climate control were that areas with low vegetation cover during the dry season are more susceptible to aeolian processes.

Figure 1.1. Different patterns of bare sand on foredune areas: a) Plum Island, MA; b) Manzanita, OR; and c) Vandenberg, CA.

The patterns of bare sand on foredune areas are different at each site, and can be easily seen in aerial photographs (Figure 1.1). So not only the amount of bare sand area, but also the patterns of bare sand are thought to be meaningful on the foredunes. The

study of patterns has been a main subject in landscape ecology (Forman and Godron 1986) and perhaps, foredunes can be classified based on the size, shape, and distribution of sand patches by applying the concepts and methodology of landscape ecology. In this way, foredune texture is defined as the appearance or character of patches on a foredune, such as size, number, shape, and distribution of sand patches. Further, the relationships between bare sand patterns and climate can be explored. However, there has been no research on foredune classification based on the bare sand patterns and the relationships with climate on coastal sand dunes. If this is successful, we could better understand the development of foredunes in terms of pattern types and climate. Furthermore, this knowledge will enable us to estimate or predict foredune types in the future in association with climate change and vice versa.

The hypotheses of this study are:

I. The potential mobility and nature of foredune areas of coastal dune fields can be classified based on bare sand patterns.

II. The foredune types are related to climate variables such as wind, precipitation, potential evapotranspiration, and mobility indices.

III. The relationship between the foredune types and climate variables enables us to predict dune types through climate change.

The objectives of this study in support of testing the hypotheses mentioned above are:

I. To identify a diverse set of coastal foredunes in the U.S.

II. To quantify bare sand patterns of foredunes on the coastal dune fields of the United States using digital aerial photographs.

III. To classify foredune types based on the patterns of bare sand.

IV. To investigate which climate variables play an important role in controlling the foredune types.

V. To investigate how many years of climate data we need.

VI. To compare two mobility indices and find which one works better for this study.

VII. To examine how we can estimate or predict the development of foredunes in terms of the classified foredune types in association with climate change.

2 BACKGROUND

2.1 Chapter introduction

This chapter begins with an introduction to the foredune systems. The concept of dune mobility/activity and two mobility indices, Lancaster's (1988) and Tsoar's (2005), are described. The introductory concept of landscape ecology is discussed and then widely used software, Fragstats, is described. Details of this study to understand data collection and methods for this study are described; selection of study sites, identification of foredunes, identification of foredunes, image processing, Fragstats, climate data, dune/sand patch types, climate controls, and optimal climate data averaging period.

2.2 Foredune systems

Foredunes are the seawardmost feature of coastal sand dune systems, formed on the top of the backshore by an accumulation of sand (Hesp 2002). Sand transported by wind above threshold velocity starts to accumulate around vegetation, which slows the wind and deposits the sand. Once foredunes start to form as incipient dunes around clumps of vegetation or other materials such as rocks or wrack (Nordstrom, Jackson, and Korotky 2011), more vegetation grows on and around the foredunes and they increase in size and become ridges. Foredunes are breached or destroyed partly as a result of the destruction of vegetation by various causes such as waves or washovers during severe storms, trampling by humans or animals, vegetation loss because of prolonged droughts or fire, or burial by excessive amounts of sand transported by wind (Gares and Nordstrom 1988; Hesp 2002; Hesp and Hyde 1996). Blowouts, either elongated ones at

the front of foredunes or saucer-shaped ones on the top of the foredunes, help sand grains to move inland and allow the bare sand areas to expand laterally when wind exceeds threshold velocity (Hesp and Hyde 1996; Gares and Nordstrom 1995; Gares 1992). Those once destroyed foredunes recover through the regrowth of vegetation (Priestas and Fagherazzi 2010).

2.3 Dune mobility/activity

Research has been done to understand the relationship between dune mobility/activity or stabilization and climate variables (Chepil, Armbrust, and Siddoway 1963; Talbot 1984; Lancaster 1988; Tsoar 2005). Most research on dune mobility/activity were conducted in deserts of inland dune fields (Ash and Wasson 1983; Bullard et al. 1997; Hugenholtz and Wolfe 2005b; Lancaster 1988; Wasson 1984; Tsoar 2005). Research on dune mobility commonly considered wind power as a forcing factor and vegetation cover as a resisting factor. Vegetation cover is strongly linked to rainfall or rainfall efficiency (ratio of precipitation to evapotranspiration: PPT/PET), and so most equations for dune mobility/activity use wind power, precipitation, and actual or potential evapotranspiration (Bullard et al. 1997). Wind power is expressed in various ways such as the cube of the average wind speed (Thomas, Knight, and Wiggs 2005; Chepil, Armbrust, and Siddoway 1963), drift potential (Tsoar 2005), or percentage of wind above threshold velocity (Lancaster 1988). Precipitation (PPT) and potential evapotranspiration (PET) are often used together, PPT/PET, to express moisture efficiency (Wasson 1984; Lancaster 1988).

Although the term dune mobility implies dune migration (Hugenholtz et al. 2012), I use the term dune mobility rather than dune activity because I focus on Lancaster's (Lancaster 1988) and Tsoar's (Tsoar 2005) mobility indices and their concepts. However, the term "dune mobility" in this study means the potential for redistribution of sand rather than dune migration.

I chose Lancaster's mobility index because it is simple to calculate with basic climate data: wind speed, precipitation, and temperature, and has often been tested and applied in many environments (Muhs and Maat 1993; Lancaster and Helm 2000; Hugenholtz et al. 2012; Tsoar 2005; Hugenholtz and Wolfe 2005b). I also chose Tsoar's mobility index for this study because the concept of his mobility index is different from Lancaster's and the two indices can be compared. Tsoar (2005) suggested that moisture is not important in desert sand dunes because dune sand has the unique characteristics of high permeability, lack of cohesion, and big pore space, so that rainfall (PPT) and rainfall efficiency (P/PET) is not a decisive factor in dune mobility, but high wind power is. I will apply these two indices in my study to determine which index will be a better fit.

Lancaster's mobility index (MB) is calculated as follows:

$$MB = W / \left(\frac{P}{PE}\right)$$

where *W* is the percentage of time the wind is blowing above the threshold velocity (Vt/All in this study), P is Precipitation (PPT in this study), and PET is potential evapotranspiration. He found critical values of *MB* for the Namib sand sea and southwestern Kalahari: values of the index were >200 for fully active dunes with vegetation cover <10% and <50 for inactive dunes with vegetation cover >20%.

The percentage of the time the wind blew above threshold velocity (*W*), shown in the above equation, came from Fryberger's model (Fryberger and Dean 1979). Fryberger used drift potential to compare wind regimes with dune forms (barchanoid, linear, or star dunes) on a worldwide basis. Drift potential is wind power expressed in vector units. Wind roses were made based on drift potential for each direction of the total 16 compass directions to express graphically both the amount of drift potential and its directional variability. Using the model, Fryberger found that barchanoid dunes are linked to narrow unimodal wind roses, linear dunes are linked to bimodal roses, and star dunes are linked to complex roses. His model was useful for this study because the model provides information about how dune mobility can be affected by the amount of *W* or degree of wind convergence.

Tsoar's mobility index is calculated as follows:

$$MB_2 = \frac{DP}{1000 - \left(750\frac{RDP}{DP}\right)}$$

where DP is drift potential, a vector unit of wind power, and RDP is resultant drift potential, the magnitude of the vector results of drift potential from 16 compass directions.

2.4 Landscape ecology

Landscape is defined as "a heterogeneous land area composed of a cluster of interacting ecosystems that is repeated in similar form throughout" (Forman and Godron 1986). Overall, landscape ecology examines the physical environment and the ecological effects occurring in the environment. In other words, it analyzes the structures and

functions of a landscape, the interactions among the spatial elements such as energy flow, materials, and species, and the changes in the structure and function of the ecological landscape over time.

The concept of landscape ecology, first coined by Troll in 1939, through its theory, applications, and methodology has become one of the main interdisciplinary studies in geography and environmental sciences (Wu and Hobbs 2002; Forman 1995b). Landscape ecology has emerged in relation to the ecological mapping of vast areas because quantifying landscape structures is very important in landscape ecology research. So digital images and GIS technology are very useful for its analysis (McGarigal et al. 2002; Burel and Baudry 2003; Steiniger and Hay 2009).

Patch is a fundamental term in landscape ecology and is defined as a relatively homogeneous area that differs from its surroundings (Forman 1995a). In this study, a sand patch is defined as a bare sand area on remotely sensed images and can be a cell or a set of cells. A collection of patches of the same type is called a class. In this study, there are only two classes: "sand" and "other." The class "other" can be any feature other than bare sand such as vegetation, buildings, water bodies, etc. This study investigates patterns of sand patches in each coastal dune field. These sand patch patterns will be compared across all study sites and then classified into several sand patch types. In order to accomplish this goal, it is necessary to understand and apply the concepts and methodologies of landscape ecology in this study.

2.5 Characterization with Fragstats

Fragstats is a software program originally written by Barbara Marks and Kevin McGarigal in 1995 (McGarigal et al. 2002). It is designed to quantify landscape patterns for categorical maps and has been widely used in landscape ecology since then. Fragstats (version 2) was first publicly released in 1995, updated in 2002 (version 3), and updated again in 2012 (version 4). This latest version works with ArcGIS 10. In Fragstats the calculations of a number of statistics that characterize the concepts used in landscape ecology can be done quickly and easily at each level of an individual patch, class (all patches of the same type), and landscape (full extent of the data). Fragstats is very useful when working with digital images created through GIS programs. Statistics, called metrics in Fragstats, have been researched in many studies of landscape ecology (Li et al. 2001; Raines 2002; Luck and Wu 2002; Hargis, Bissonette, and David 1998; Uuemaa et al. 2009), so it is easy to understand the concepts, meanings, usages, and pros and cons of metrics that can be applied to studies.

2.6 Details of the study

2.6.1 Selection of study sites

In order for coastal dune systems to represent climate controls, they must be in a nearly natural state, minimally developed, or with little interference. Coastal dune fields have often been used for agriculture (timber, grazing, etc.), sand mining, military field training, or recreation (Nordstrom and Lotstein 1989), and most coastal dunes in the United States have been altered by human activities, which are discussed in many studies such as those by Cooper (1967), Capece (2001), Carls et al. (1990), Dolan et al.

(1973), and Savoy et al. (1985), and can be observed from aerial photographs. Therefore, dunes that have had severe interference inland, but not on the foredunes, or that have minimal evidence of human usage on the foredunes were accepted sites for this study. In addition, dunes selected for this study had to have substantial alongshore extent and total area.

2.6.2 Identification of foredunes

A foredune area is defined as a ridge that includes the dune toe, dune crest, and leeward side of the dune ridge, and is the most active feature of a dune system because it can change in a short period of time. From an image processing perspective, a foredune line is sometimes hard to detect on the aerial photographs. For these reasons, in this study, I decided that foredune areas are sections 100 m wide from the dune toe, which can sometimes include dune slacks and parts of secondary dunes. Foredune areas of a 100 m width are suitable because the 30 year-long climate data used in this study might show impacts not only on the current foredune ridges, but also on those more inland that might have been foredune ridges several decades ago.

2.6.3 Image processing

Fragstats uses categorical maps to calculate statistics, but original images such as aerial photographs contain a lot of information, so they should be processed into categorical images divided into classes. Image classification is a method of categorizing digital images through either a supervised or unsupervised classification (see chapter 3, Methodology, for the details). One of the disadvantages of image classification is that no perfect classification can be made. Therefore, users could use their own knowledge or

expertise or could use other photos or images as supplements to obtain classified images that correspond with the desired information classes.

2.6.4 Fragstats

This study calculates metrics at only the class level because it focuses only on a single class, "sand." Fragstats can calculate 109 metrics at the class level in different categories such as "area-edge," "shape," "core area," "contrast," and "aggregation." To understand the relationships between sand patches and climate, the amount of bare sand area on each dune field is the most straightforward and important metric. In addition, the shape (complexity) and distribution of sand patches are also metrics to be considered in order to understand bare sand structures in more detail. However, metrics in the category "core area" and "contrast" are not considered in this study. These two types of metrics are important in the study of ecosystems and ecology because of the "edge effect" in which the edges between patches can influence adjacent ecosystems in both or either abiotic or biotic environments (Murcia 1995). This study has only two patch types: "sand" and "other," so edge effect does not play a significant role. Thus, core area, which is an area after removal of edge depth (distance between patches), and edge contrast between patches was not considered. Although core area and contrast metrics were not considered in this study, edge density (ED) was calculated because it represents patch extent and complexity.

2.6.5 Climate data

Among all climate variables, moisture and wind are considered the most fundamental in aeolian research (Ash and Wasson 1983; Bullard et al. 1997; Chepil,

Armbrust, and Siddoway 1963; Lancaster 1988; Wiggs et al. 1995). Wind is directly involved in sand transport and moisture, which is expressed in rainfall (PPT) or rainfall efficiency (ratio of precipitation to potential evapotranspiration (PET), (PPT/PET), controls vegetation cover in dune systems. Wind data, especially at 10 m above the ground, which is the standard height for wind measurement, is the most difficult to obtain because not all weather stations measure wind data, and if they do, the height of anemometers is not provided in many cases. In addition, because wind is the most variable, even for a short period of time, the time period for collecting wind data is critical. Therefore, wind data provided from the NARR (North America Regional Reanalysis) are very useful because the wind is modeled at 10 m above ground and the time period for the wind data is every 3 hours. Temperature is frequently converted into PET to be coupled with precipitation in many studies (Hugenholtz and Wolfe 2005a, 2006; Lancaster 1988; Marin et al. 2005). PPT and temperature data were obtained from PRISM (Parameter-elevation Regressions on Independent Slopes Model). See 4.1.2, climate data in the Methodology chapter for more details of PRISM.

2.6.6 Dune/sand patch types

By viewing sand dune fields in the United State through aerial photographs it is not hard to find regional characteristics in terms of bare sand areas or sand patches. The most typical is sand patches on the dune fields of Southern California, where the sand patches are few and large (i.e. Santa Maria and Vandenberg). On the other hand, dune fields in Oregon consist of a large number of patches, but of small sizes. In addition, on the west coast, the orientation of sand patches tends to represent the prevailing wind,

west or northwest, but on the east coast, this pattern is rarely found. Patterns and structures of not only such easily visible patterns, but also those that are invisible or undetectable can be seen if they are quantified by statistics available in Fragstats. Analysis of the quantified sand patches enables us to find similarities and differences in the patch patterns of each dune field, and to cluster dune fields into several groups, if possible. The study of patch patterns or structures has been a subject in landscape ecology, so the application of this to geomorphology can provide a new perspective on the study of the texture or structure of geomorphological features at larger scales.

2.6.7 Climate controls

Climate variables such as precipitation, potential evapotranspiration, and wind regime play an important role in the initiation and development of coastal sand dunes (Marin et al. 2005; Hugenholtz and Wolfe 2005a; Chepil, Armbrust, and Siddoway 1963). In order for dunes to form, wind should be fast enough to move sand grains and blow onshore for some period of time. Vegetation slows down wind speed, helps moving sand to deposit around the vegetation, and the growth of vegetation helps to stabilize and maintain sand dunes. The amount of moisture controls vegetation growth and prolonged drought withers vegetation and helps bare sand areas expand inland.

However, little is known about how much and in what ways such climate variables affect the patterns and textures of sand patches. For example, at microscale, wind is the most important factor in sand transport, but how will wind affect larger spatial and temporal scales such as entire foredune areas and for several years to decades?

Such knowledge can provide a better understanding of the geomorphology and management of coastal sand dunes.

2.6.8 Optimal climate data averaging period

Thirty years is the time period for the calculation of normal climate (www.ncdc.noaa.gov), but what if available climate data is short of 30 years? How many years of climate data is needed to investigate the bare sand area on coastal sand dune systems? If the optimal number of years of averaged climate data is known, it is helpful in understanding the relationship between climate and the amount of bare sand areas with the least number of years of climate data. This study calculates cumulative averages of climate variables and tries to find the optimal period in association with bare sand patch patterns.

In a number of papers, relating climate data to dune mobility, active sand areas, or bare sand areas are used as a measure of dune mobility/activity, and climate periods depend on the availability of data. For example, Hugenholtz and Wolfe (2005b) and Levin (2011) evaluated the bare sand areas of dune activity with climate data for available years: Hugenholtz and Wolfe examined 24 years of wind speed and PPT:PET, and Levin explored 52 years of wind and 69 years of rainfall data.

3 STUDY SITES

In this study, the focus is on the nature of bare sand areas (patches) that occur within foredune systems only. This is because foredunes tend to be geomorphologically dynamic and represent the most recently formed dune system within a particular coastal system. The bare sand patches that occur landward of foredune systems may be the manifestation of any number of causes not necessarily related to local climate, especially in the 30 years of recent climate data that were used for this study. In most coastal environments it is difficult to determine the landward extent (in particular) of a foredune system using only aerial photographs. As an analytical expedient, therefore, I chose to delineate a representative width of 100 m perpendicular to a line along the seaward foredune toe. The created foredune "area" is deemed representative of the characteristics of the foredune sand patches in each studied environment. More details about the delineation are described in the methodology chapter.

Study sites were selected from the shorelines of the 48 contiguous United States using two fundamental criteria: 1) a site must be located within a dune system of substantial alongshore extent and total area; and 2) a site must display minimal or no human disturbance or development. Google Earth™ imagery was used to scan the coastline of the contiguous U.S., and, using the criteria above, 22 dune fields were identified for study (Figure 3.1). Among the 22 sites, four are in Oregon, eight in California (four in Southern California), one in Texas, one in Florida, two in North Carolina, one in Virginia, one in New Jersey, one in New York, and three in

Massachusetts. There are many other dune fields, but they do not satisfy both of the criteria. For instance, dune fields in Louisiana are too narrow to have extensive foredune ridges and many dune fields on the Florida coasts are too developed. For example the east side of the Santa Rosa Island dunes in the panhandle area of Florida is developed for residences and resorts and the west side is relatively natural but destroyed by many washovers.

The characteristics of each dune field are described below in terms of geography, geology, and climate. Some dune fields are described in groups, because they are located very close to each other and have similar characteristics.

Figure 3.1. Map of study sites

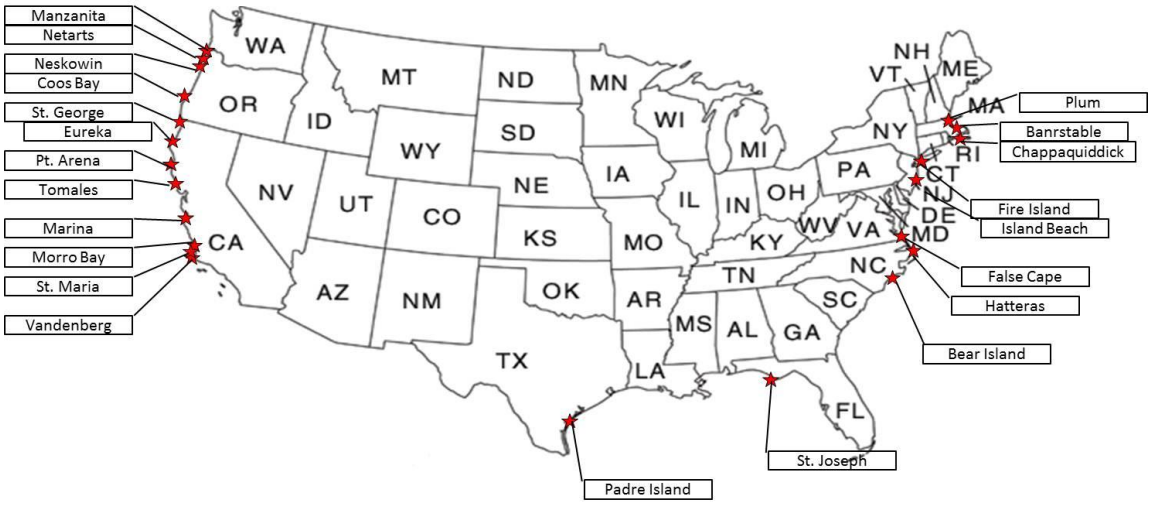

3.1 The Oregon coast

In Oregon, the dune fields at Manzanita, Netarts, Nestucca, and Coos Bay were selected for this study. The first three are on the northern coast of Oregon and their areas

are relatively small. The Coos Bay dune field is the southernmost and its area is the largest of any site in this study. Other Oregon dune fields are very small because the state's coastal strip is mountainous and provides little accommodation space.

The descriptions of the geology and climate of the Oregon coast are based on Cooper (1958) except as otherwise noted. Most of the shoreline in Oregon is rocky and irregular. The bars and spits usually associated with river mouths are small and scarce; as is found in Manzanita and Neskowin. Other large dune fields, for example dunes in the river mouths of the Siuslaw, Umpqua, and Coquille rivers have been developed for golf courses, cities, or recreation areas. The grain sizes of most particles in the dune fields of the Oregon coast fall between 0.125 and 0.50 mm.

According to Köppen's climate classifications (See Appendix, p.185), north Oregon is categorized as Cfb without precipitation deficiency, and the south is categorized as Cs, with a long dry summer season (Table 3.1). However, the difference between the temperature maximum and minimum in northern and southern in Oregon is small; 13.7°F in the north (North Head on the border between Washington and Oregon, 46°18'N) and 15.5°F at North Bend in Coos Bay, 43°25'N. The patterns of precipitation are similar throughout Oregon; abundant heavy winter precipitation and a summer deficiency in July and August. There is minimal coastal snow fall.

Average winds in Oregon vary with the seasons. In winter, the most common wind directions are from the south and east; in summer, they are from the west and northwest (Taylor and Hannan 1999). The average wind direction is south and southwest

in July, and north and northwest in January. In summer, onshore winds predominate; in winter, low velocity offshore winds are most frequent.

Figure 3.2. Map of the Northern Oregon Coast

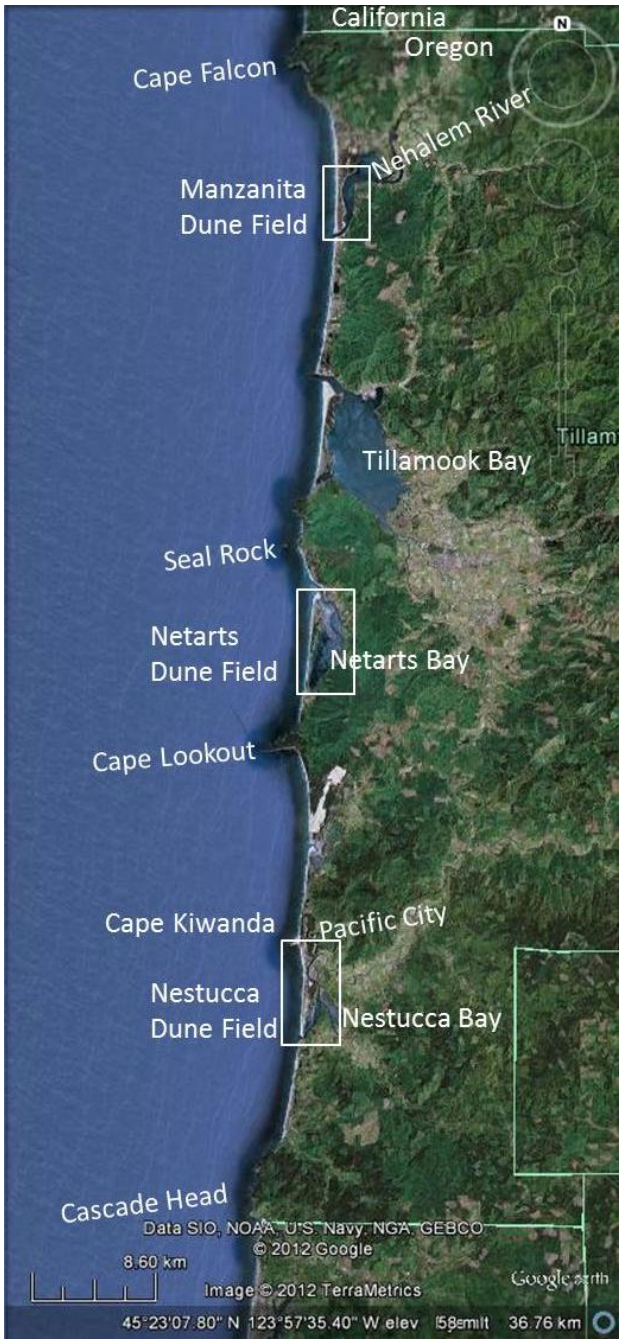

Table 3.1. Summary of climate & Köppen's climate classification. Precipitation data (1979-2008) were obtained from PRISM, and temperature and wind from NARR.

Site	Temperature				Precipitation				Wind Speed		Wind Direction		Köppen's classification
	Average		Range		Annual Total		Avg. Range		Avg.	Range	Average		
	°F	°C	°F	°C	in	cm	in	cm	m/s	m/s	deg	NEWS	
Manzanita, OR	52.6	11.3	16.2	8.9	77.3	196.3	15.6	39.7	5.9	2.9	272	W	Cfb
Netarts, OR	50.5	10.2	15.9	8.7	86.0	218.4	17.3	44.0	5.0	2.4	256	WSW	Cfb
Nestucca, OR	52.3	11.2	16.4	9.0	73.1	185.8	14.8	37.5	5.0	2.4	267	W	Cfb
Coos Bay, OR	52.7	11.4	14.2	7.8	66.5	168.9	15.4	39.1	6.1	3.3	267	W	Csb
St. George, CA	52.1	11.0	11.9	6.5	70.6	179.4	17.1	43.5	5.3	1.5	234	SW	Csb
Eureka, CA	52.9	11.5	10.8	5.9	40.7	103.5	10.9	27.7	6.0	2.0	306	NW	Csb
Pt. Arena, CA	53.1	11.6	11.2	6.2	41.1	104.3	12.7	32.2	7.0	2.0	259	W	Csb
Tomales, CA	59.0	14.9	19.2	10.6	34.1	86.7	12.0	30.4	5.6	2.2	316	NW	Csb
Marina, CA	56.7	13.6	10.8	5.9	16.8	42.6	5.4	13.7	3.5	0.8	273	W	Csb
Morro Bay, CA	55.9	13.2	8.2	4.5	17.3	44.0	6.1	15.6	5.3	1.5	297	WNW	Csb
St. Maria, CA	58.5	14.6	9.5	5.2	16.4	41.7	6.0	15.2	4.6	1.8	316	NW	Csb
Vandenberg, CA	59.7	15.2	12.2	6.7	16.1	41.0	5.9	15.1	5.6	2.2	298	WNW	Csb
Padre Island, TX	73.5	22.8	27.9	15.3	30.6	77.8	7.6	19.4	4.7	1.2	256	WSW	Cfa
St. Joseph, FL	68.3	20.0	29.2	16.1	58.6	148.9	9.8	24.8	3.7	1.5	321	NW	Cfa
Bear Island, NC	62.7	16.9	35.5	19.5	56.8	144.3	8.6	21.9	5.3	2.6	239	WSW	Cfa
Hatteras, NC	62.8	16.9	33.1	18.2	51.5	130.8	6.9	17.4	5.3	2.9	261	W	Cfa
False Cape, VA	60.1	15.5	37.7	20.7	46.1	117.2	7.0	17.8	4.3	1.7	341	NNW	Cfa
Island Beach, NJ	53.1	11.6	43.8	24.1	45.7	116.2	6.0	15.3	5.3	2.5	256	WSW	Dfa
Fire Island, NY	52.4	11.2	43.7	24.0	48.9	124.3	7.1	18.0	4.4	1.8	263	W	Dfa
Chappaquiddick, MA	50.5	10.2	39.8	21.9	48.3	122.8	6.7	16.9	4.9	2.0	267	W	Dfb
Barnstable, MA	49.5	9.6	41.3	22.7	44.3	112.6	6.6	16.7	5.8	2.8	262	W	Dfb
Plum, MA	47.4	8.5	43.7	24.0	48.3	122.8	7.8	19.8	5.2	1.3	119	ESE	Dfb

3.1.1 Manzanita

The Manzanita dune system is located at approximately 45° 40'N, 123° 56'W, backed by Nehalem Bay and located south of the city of Manzanita (Figure 3.3). The dune system is formed on a spit that is about 6 km in length, ranges from 0.3 to 0.6 km in width, and extends almost exactly from north to south. Cape Falcon is located at the

northern end of the spit (Figure 3.2) and a deflation plain lies behind the foredune (Peterson et al. 2011). European beach grass, or marram grass (*Ammophila arenaria*) was introduced and planted on the foredune during the 19th century (Nordstrom 2004). Largehead sedge (*Carex macrocephala* Willd.*)* is abundant and the coastal sand verbena (*Abronia latifolia* Escsch.) and two species of bur ragweed (*Franseria bipinnatifida* Nutt. and *F. chamissonis* Less.) are common on the foredune (Cooper 1958). The median grain diameter of this area is 0.32 mm (Komar, Carpenter, and McDougal 1995). Except for small roads, the dune field is little developed and well vegetated.

Climate descriptions are based on the analysis of 30 year data (1979-2008) from PRISM and NARR except as otherwise noted. The average temperature is 52.6°F (11.3°C) and the temperature range is 16.2°F (8.9°C) (Table 3.1). The total annual precipitation is 75.74 inches (192.4 cm). Summer precipitation is much less than that during winter (Figure 3.4), but this site falls in the Cfb category (Marine West Coast Climate), not in the Csb category (Mediterranean Dry-Summer Climate) according to Köppen's classification (Table 3.1), because even the driest summer month has more than 3 cm precipitation. The average annual wind speed is 5.9 m/s (Table 3.1). Winds are faster in winter and the annual range is only 2.9 m/s. Prevailing wind directions from April to October are from the west or northwest, shifting to southerly (SW ~ S) in winter (Figure 3.5). The annual average wind direction is west (273°) but stronger winds are south and southwest (Figure 3.6).

Figure 3.3. Map of Manzanita, OR. Foredune area (ca. 0.42 km^2) is in red box.

Figure 3.4. Average monthly precipitation and temperature in Manzanita, OR (1979-2008).

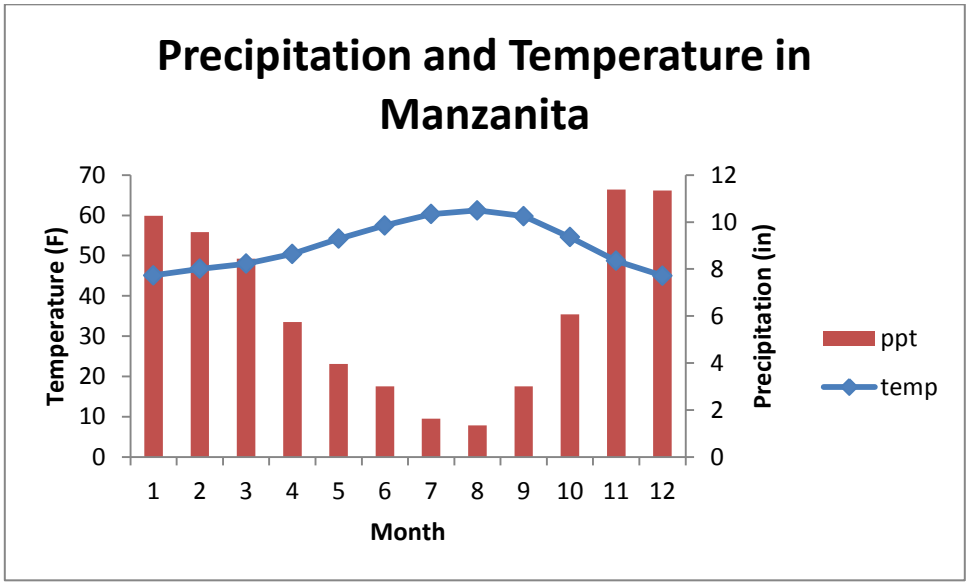

Figure 3.5. Average monthly wind speed and direction in Manzanita, OR (1979-2008).

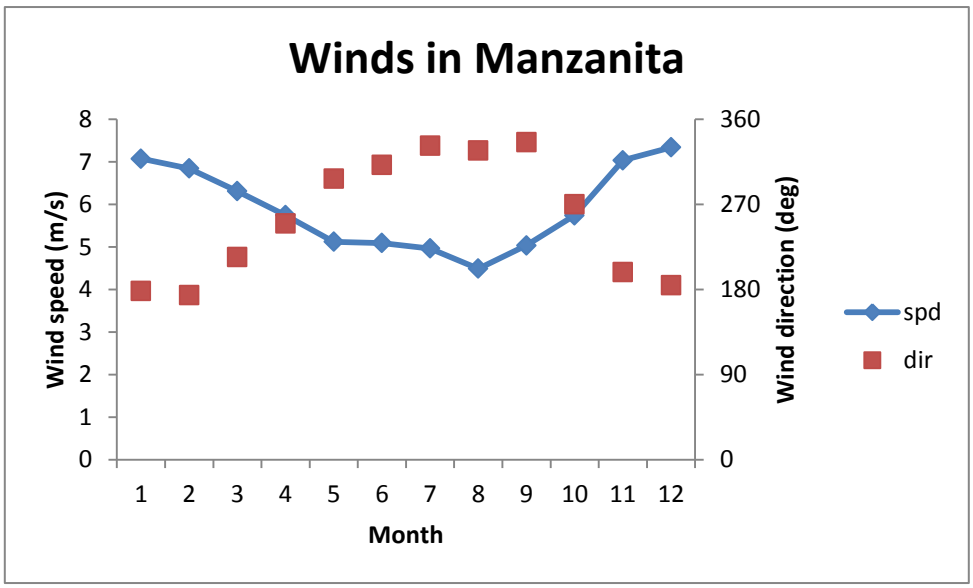

Figure 3.6. Wind rose in Manzanita, OR (1979-2008)

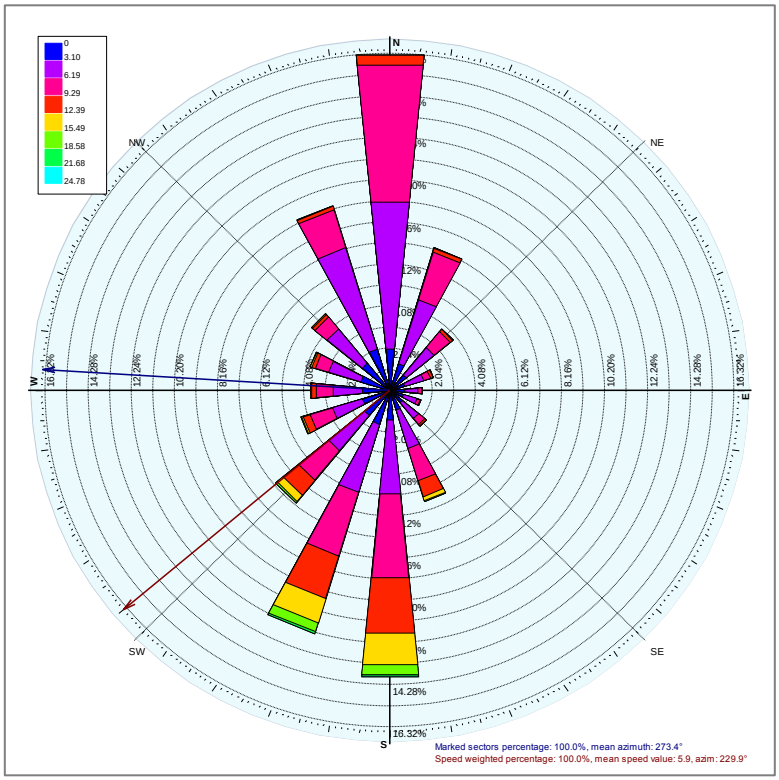

3.1.2 Netarts

The Netarts dune field is located at approximately 45° 25'N, 123° 57'W, backed by the Netarts Bay (Figure 3.7). The dune field is on a spit formed by longshore currents moving from south to north. It is about 7 km long, ranging from 0.1 – 1.0 km in width and extends north-northeastward. Headlands are on both sides of the spit; Seal Rock on the north and Cape Lookout on the south (Figure 3.2). On the spit, there are several remnants of ridges stabilized with forest. At the northern end, the spit is wide but low (~ 3 m in height) with many scattered bare sand areas, and covered with European beach grass (*Ammophila arenaria*) and occasional colonizing trees and shrubs (Bonacker,

Martin, and Frenkel 1979). The middle to southern part of the spit is well vegetated, especially with coniferous forest dominated by Sitka spruce (*Picea sitchensis*) (Losey 2005), and several blowouts are encroaching on the forest inland . Human interference is rare found in the dune field, however the spit was inhabited from A.D. 1300 until the mid- to late 1700s according to Losey (2005). Tidal marshes are at the southern end of the bay (Shennan et al. 1998). Blowouts are in the middle of the spit.

The temperature and precipitation patterns in Netarts are almost the same as at Manzanita (Figure 3.4 and Figure 3.8). The annual average temperature at this site is 50.5°F (10.2°C) and the temperature range is 15.9°F (8.7°C). The annual total precipitation is 90.4 inches (229.6 cm). This site falls in the Cfb category (Maritime West Coast Climate) according to Köppen's climate classification system (Table 3.1). The annual average wind speed is 5.0 m/s. Winds are faster in winter and its annual range is only 2.4 m/s. The annual average wind direction is west-southwest (257°) and the stronger winds are south and southwest (Figure 3.10). Wind direction in May is west-southwest, shifting to west-northwest or north-northwest through September, and ending up southerly in winter (Figure 3.9).

Figure 3.7. Map of Netarts, OR. Foredune area (ca. 0.59 km^2) is in red box.

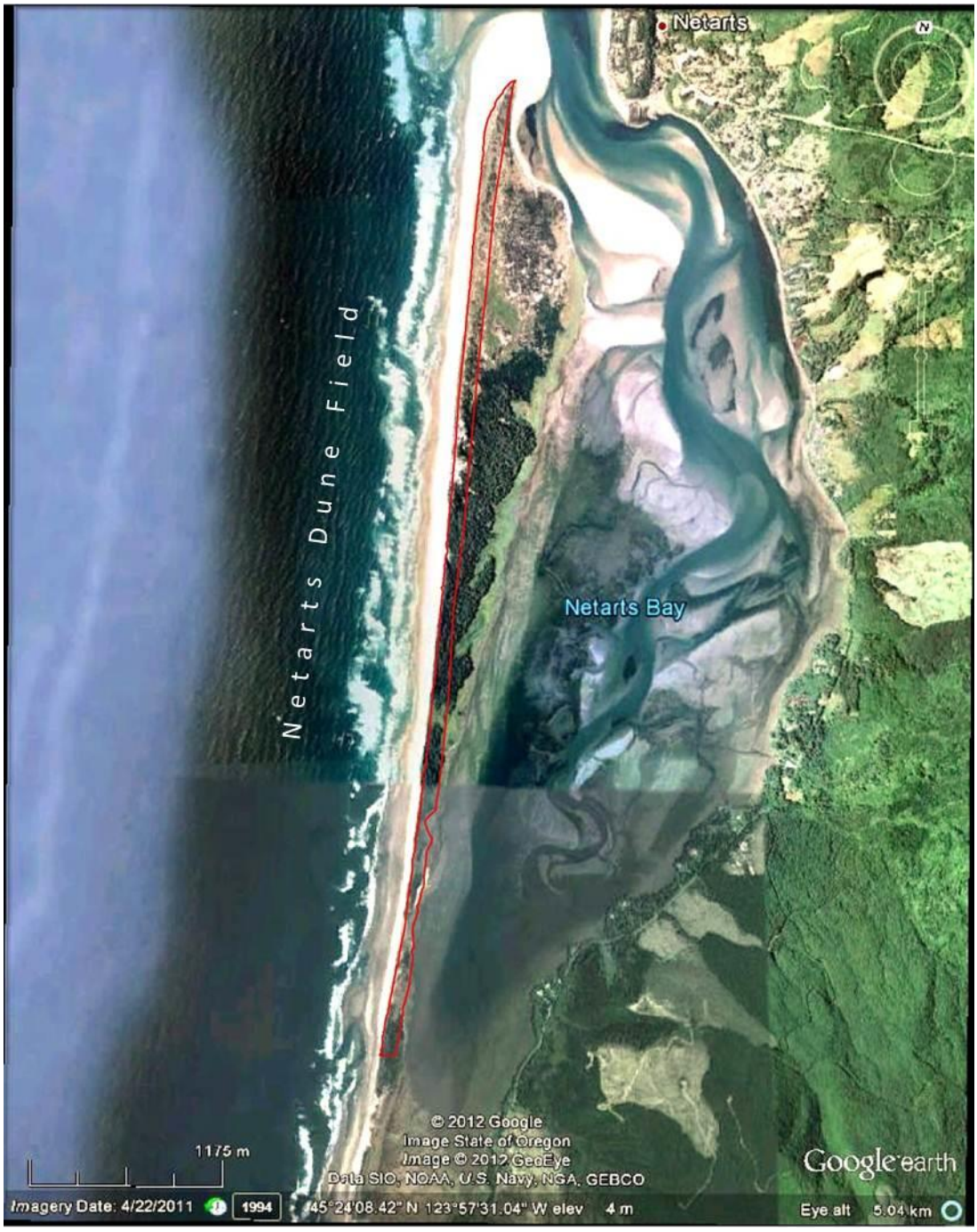

Figure 3.8. Average monthly precipitation and temperature in Netarts, OR (1979-2008)

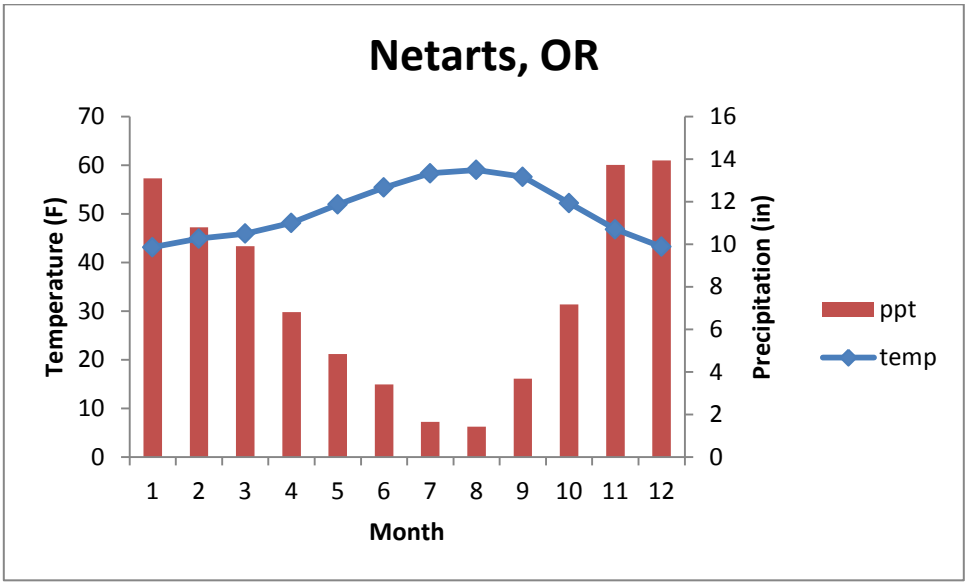

Figure 3.9. Average monthly wind speed and direction in Netarts, OR (1979-2008)

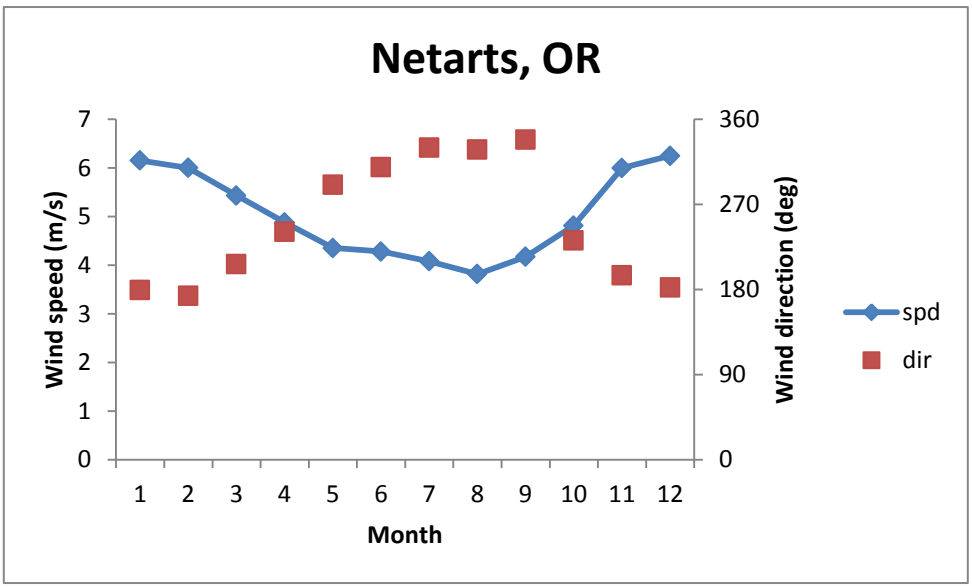

Figure 3.10. Wind rose in Netarts, OR (1979-2008)

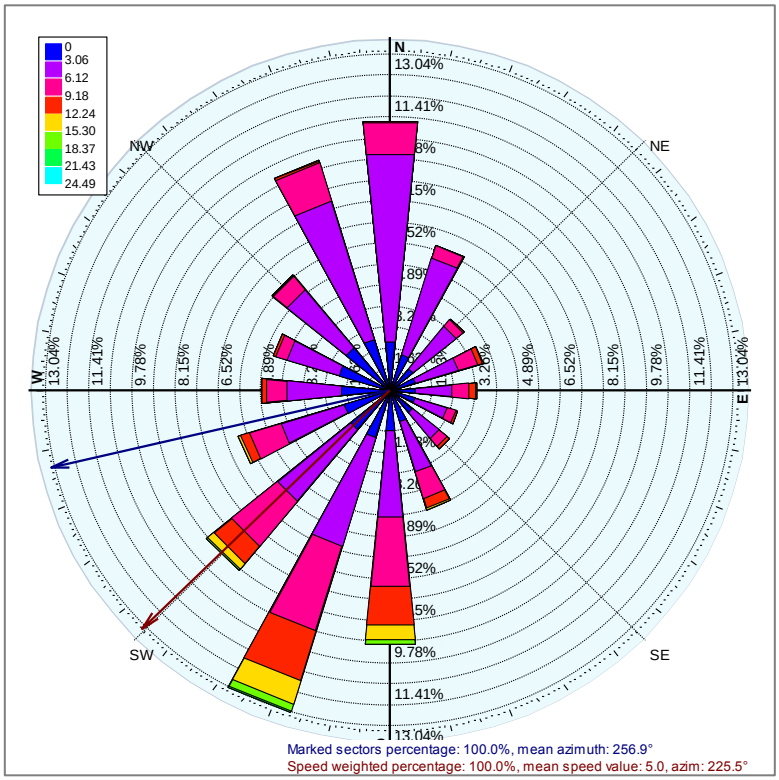

3.1.3 Nestucca

The Nestucca dune field is in the Bob Straub State Park located south of Pacific City (Figure 3.11). The dune field is about 4 km long, 0.2 – 1.0 km wide, formed at the mouth of the Nestucca River at the Nestucca Bay, and is on a spit at the south end. Its location is 45°11'N and 123°58'W. Although the northern end of the park is developed for recreation, the rest of the dune is little developed, except for some roads and parking lots. Haystack Rock and Cape Kiwanda (Figure 3.2) are located at the northern end of the dune fields and protect the weaker material behind them. Several remnants of parabolic dunes cut by the Nestucca River are located north of Pacific City (Figure 3.11),

and were stabilized with hardwood forest (Cooper 1958). The dune field on the peninsula has a well-developed and stabilized foredune, up to 7 m in height, and there is a large deflation area behind it with many bare sand areas but also with grass and hardwood cover. There is a tidal marsh between the dune field and the bay. The vegetation cover of this dune field is similar to that of the dune fields in northern Oregon (Cooper 1958).

Temperature and precipitation patterns at Nestucca are similar to those in the two other dune fields in northern Oregon (Figure 3.12). The annual average temperature at this site is 52.3°F (11.2°C) and the temperature range is 16.4°F (9.0°C). The annual total precipitation is 82.5 inches (209.6 cm). This site falls in the Cfb category (Maritime West Coast Climate) according to Köppen's climate classification system (Table 3.1). The annual average wind speed is 5.0 m/s. Winds are faster in winter with an annual range of 2.4 m/s. The annual average wind direction is west (268°), but wind directions fluctuate around the west throughout the year (west-southwest – west-northwest), which is different from the wind patterns of the two previous sites (Figure 3.13). In Manzanita and Netarts, northerly and southerly winds are more frequent and southerly winds are stronger, whereas in Nestucca westerly winds are more frequent and stronger (Figure 3.14).

Figure 3.11. Map of Nestucca, OR. Foredune area (ca. 0.25 km^2) is in red box.

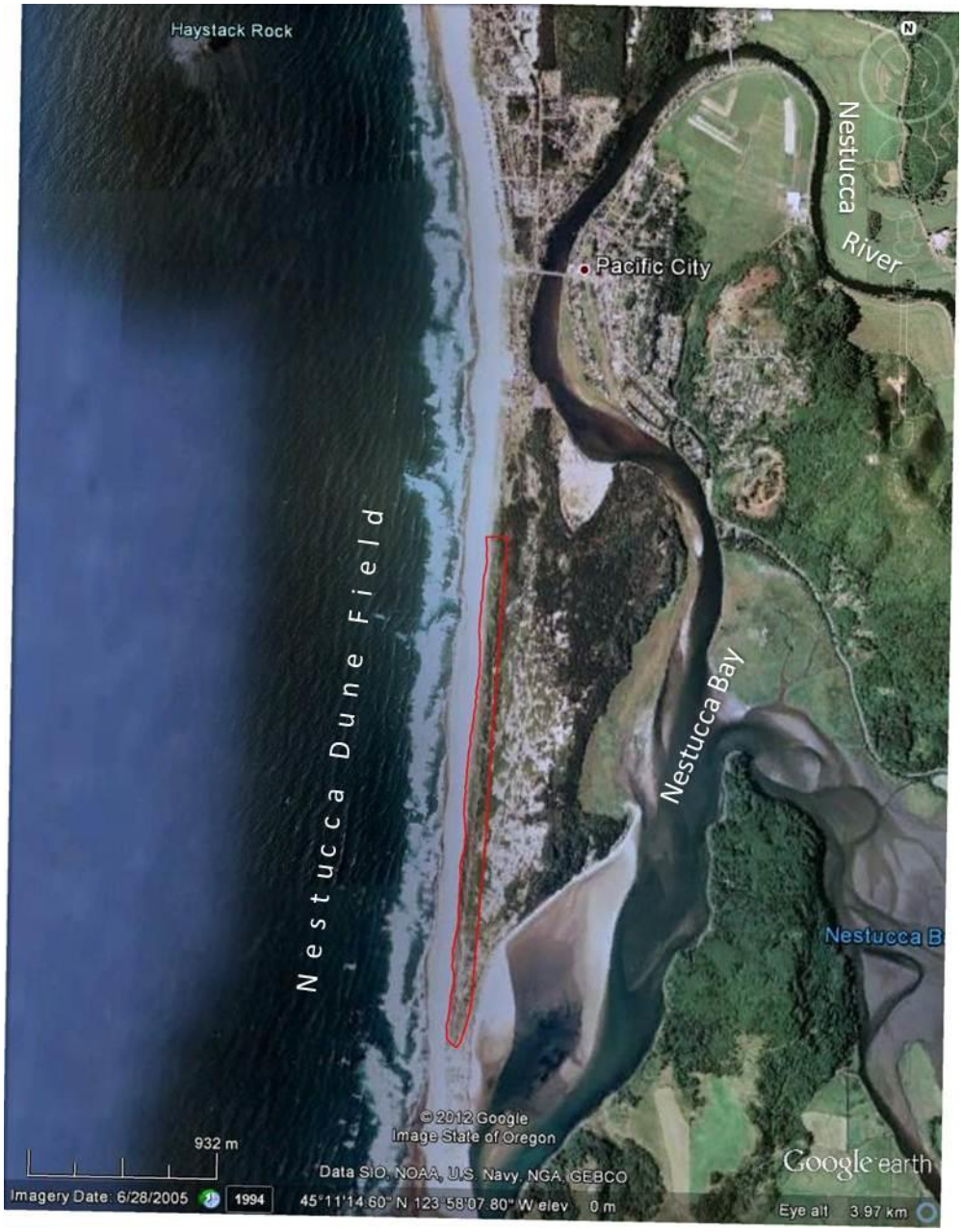

Figure 3.12. Average monthly precipitation and temperature in Nestucca, OR (1979-2008)

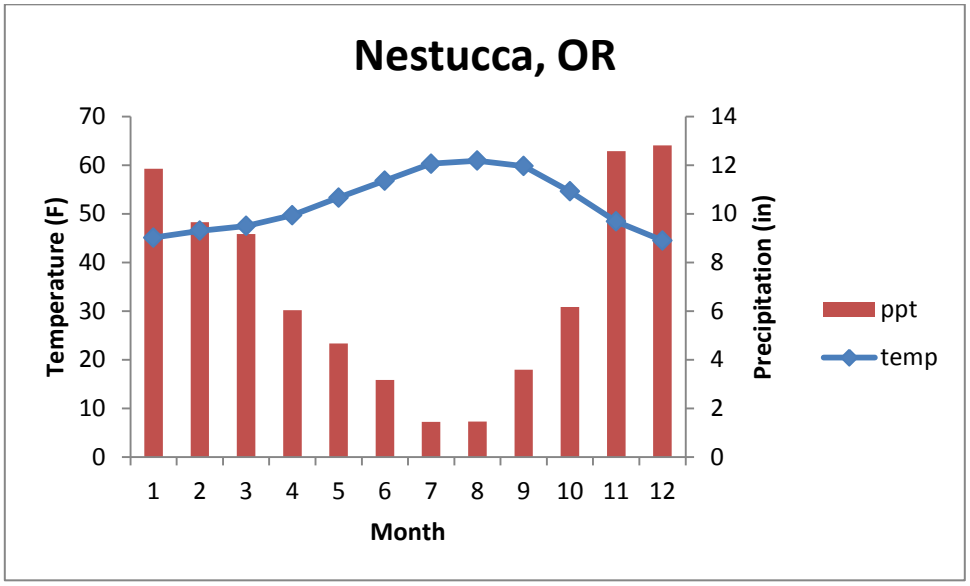

Figure 3.13. Average monthly wind speed and direction in Nestucca, OR (1979-2008)

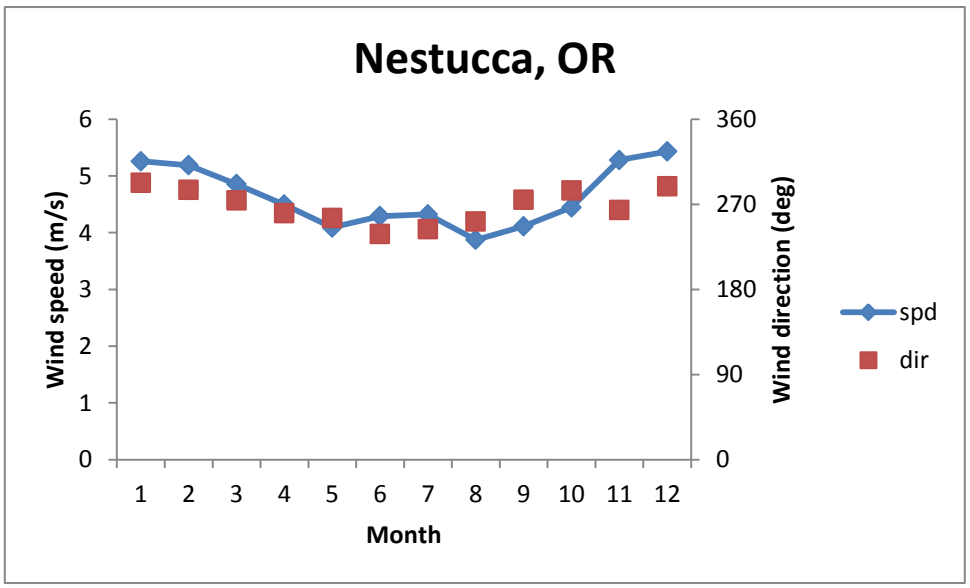

Figure 3.14. Wind rose in Nestucca, OR (1979-2008)

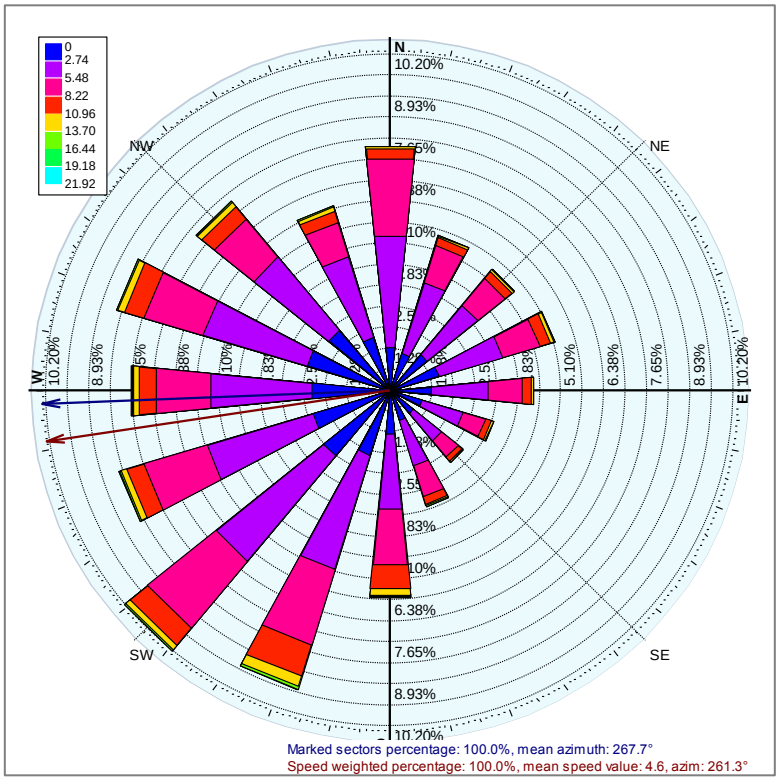

3.1.4 Coos Bay

The Coos Bay dune field is the largest dune complex in the United States. It extends 86 km from Cox Rock to the Coos Bay Inlet (Figure 3.15). Only the southern part, from Tenmile Creek to the Coos Bay Outlet was considered in this study. The site is located at 43°30'N and 124°14'W, is 18 km in length, and ranges from 1- 4 km in width.

There are three episodes of dune advance in the Coos Bay dune sheet (Cooper 1958). The first episode is stabilized ridges, hills, and isolated masses. The second advance, still represented locally, overpassed the stabilized ridges and invaded the

forests. The third episode is represented by the active foredune system in the west and will develop further.

As in other Oregon dune fields, European marram grass was introduced as a dune stabilizer in this area and spread rapidly so that a larger foredune was formed (Wiedemann 1998). Two active dune ridges (western and eastern) lie inland, behind the foredune. Between the two ridges is a deflation plain where there are several shallow lakes, some of which are of considerable size.

There are many roads and paths on the Coos Bay dune field that might have been created by off road vehicles on both active and stabilized dunes. However, the foredune area, which is defined as a 100 m width from the dune toe inland, has fewer sand patches than inland areas and contains roads for transportation and some parking lots. Most of the foredune is well vegetated but there are many small sand patches.

The annual average temperature in Coos Bay is 52.7°F (11.4°C) and the temperature range is 14.2°F (7.8°C) (Table 3.1). The annual total precipitation is 64.4 inches (163.7 cm), which is 10 to 20 inches less than that of the three northern sites in Oregon. This site falls in the Csb category (Maritime Dry-Summer Climate) according to Köppen's climate classification system because the driest summer month has less than 3 cm of precipitation. The annual average wind speed is 6.1 m/s. In winter winds are northwesterly and fast, and southwesterly in summer (Figure 3.17). Annual wind range is 3.3 m/s. Annual average wind direction is west (267°) (Figure 3.18) and monthly wind directions fluctuate around the west throughout the year (southwest – west-northwest).

Figure 3.15. Map of Coos Bay dune field, OR. Foredune area (ca. 1.62 km^2) is in red box.

Figure 3.16. Average monthly precipitation and temperature in Coos Bay, OR (1979-2008)

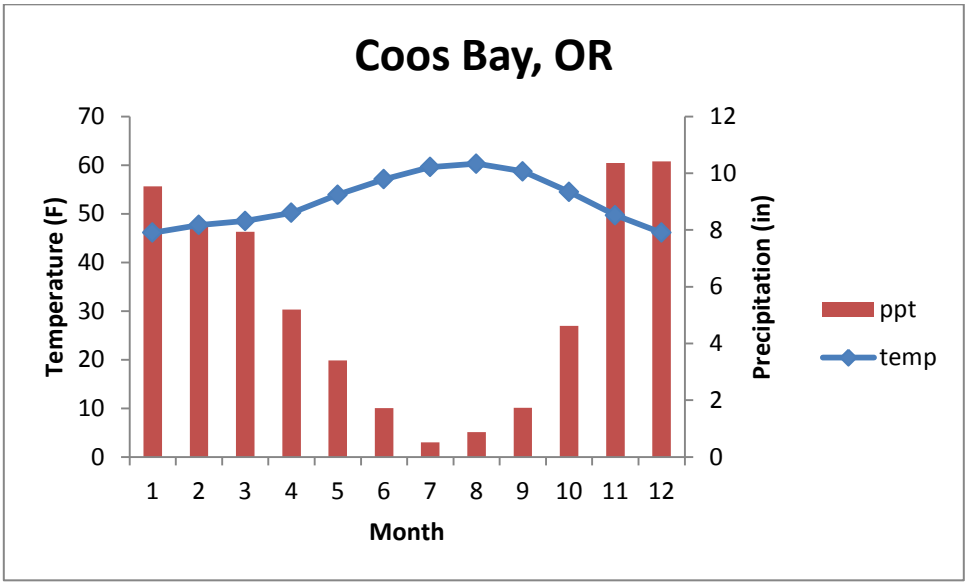

Figure 3.17. Average monthly wind speed and direction in Coos Bay, OR (1979-2008)

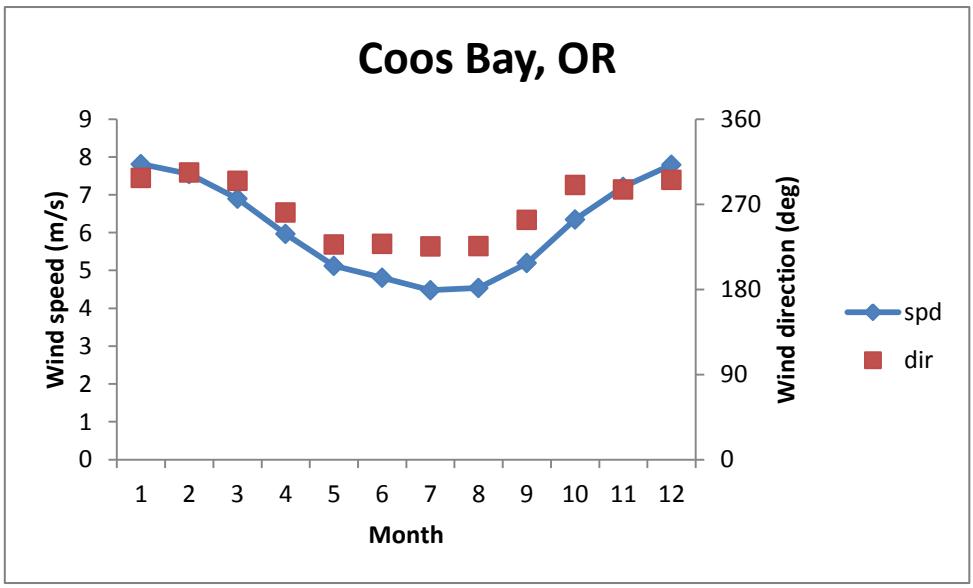

Figure 3.18 Wind rose in Coos Bay, OR (1979-2008)

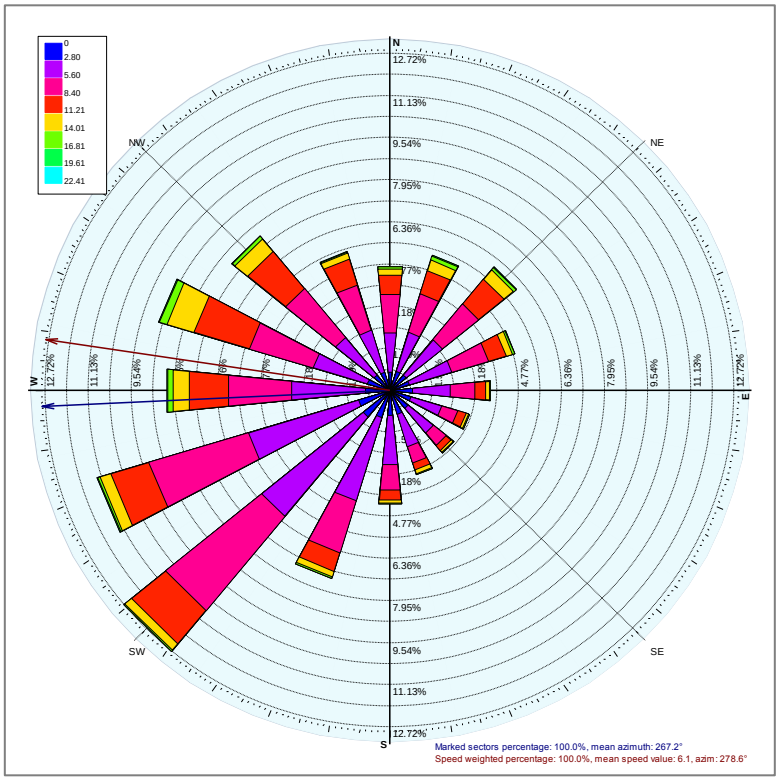

3.2 The California coast

Eight sites were chosen along the California coast for this study (Figure 3.1). Four of them are in northern California (Saint George, Eureka, Point Arena, and Tomales) and the rest are in southern California (Marina, Morro, Santa Maria, and Vandenberg). The descriptions of the geology of the California coast are based on Cooper (1967) except as otherwise noted. The California coast is mountainous, characterized by the California Coast Ranges that are continuous and parallel to the shoreline from Trinidad Head (the Eureka dune field) to Point Aguello (the Santa Maria dune field) (Figure 3.19). The mountains and valleys of the California coast are strongly

related to faults and the ridges and the mountains end at the coastline with projecting headlands composed of resistant rock. In association with these features, most dunes were developed on coastal plains of deltaic origin or on barrier spits. The primary sources of sediment for California beaches are from stream and headland erosions. Sand transport by littoral drift is predominantly southward. As seen along the Oregon coast, marram grass was introduced to the California coast in 1869 and spread rapidly.

All the California dune fields for this study are categorized as Csb (Mediterranean climate), with a mild temperature throughout the year and summer drought. The annual average temperatures do not vary substantially between sites. For instance, the temperature difference between the northernmost study site, St. George, (11.0 °C) and the southernmost, Vandenberg, (15.2°C) is only 4.2°C (Table 3.1). However, precipitation begins to decrease abruptly in Eureka. The annual precipitation difference between Eureka (96.8 cm) and Point St. George (169.7 cm) is 72.9 cm, although the two sites are only one degree of latitude apart. Precipitation decreases as one goes further south.

Westerly winds prevail along the California coast. Cooper (1967) mentioned five factors that control the California coast's wind regime: (1) prevailing westerly wind favoring onshore winds, (2) the north Pacific high pressure center, in summer at ca. 40°N and in winter 10° southward, (3) sea-land breezes, (4) cyclonic disturbances, and (5) direction parallelism with the coast due to barriers such as mountains or hills. These features add more variations to the wind regime in the California coast. The California

coast also has more northerly winds than the Oregon coast and the annual wind speed decreases as it moves southward.

Figure 3.19. Map of the California Coast: D.F. means dune field

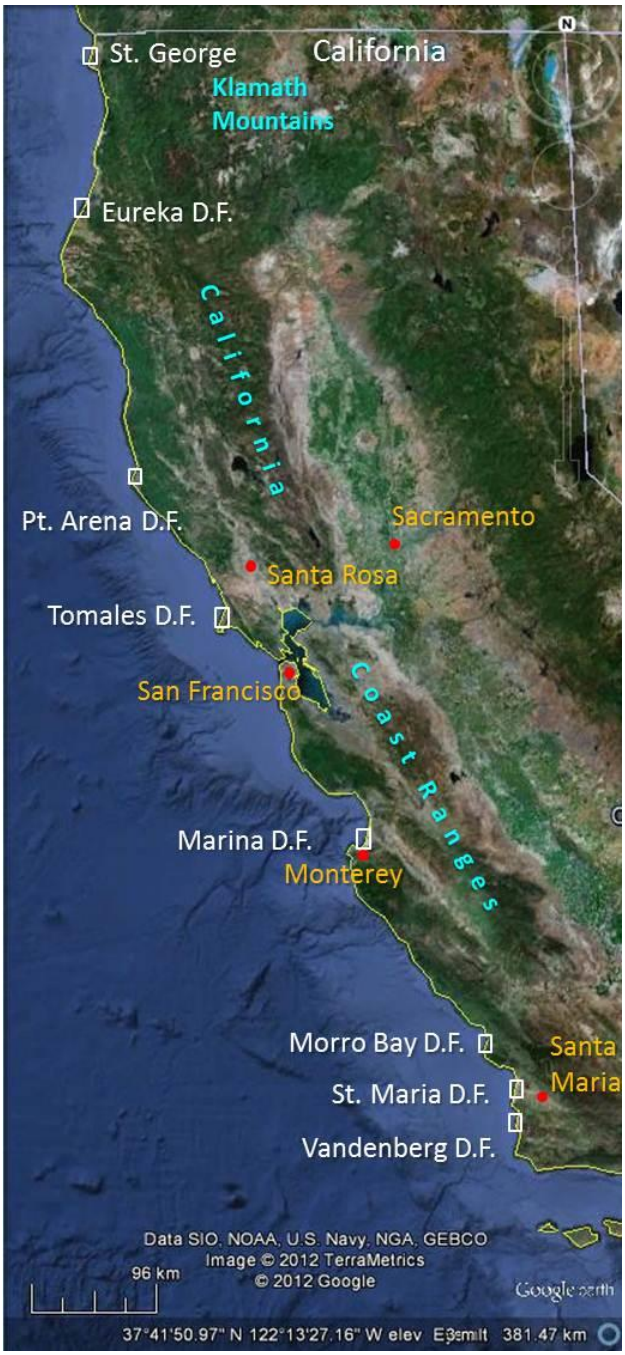

3.2.1 Point St. George

The Point St. George dune field is located at 41°53'N and 124°12'W, two miles north of Crescent City, and it is about 18 km long and is widest at 9 km. The dune field extends south-southwestward from the mouth of the Smith River to Point St. George (Figure 3.23). This dune field can be divided into two parts near Lake Tolowa. The northern half of the dune field was chosen for this study and extends 5.5 km south from the Smith River mouth. The southern half was not considered in this study because there is evidence of human influence such as roads and parking lots. Coastal development has been minimal since the 1960s (Savoy et al. 1985).

The inner dune field is older and stabilized by mostly Sitka spruce (*Picea sitchensis* (Bong.) Carr.) and lodgepole pine (Pinus contorta Douglas). Younger dune development is in a narrow belt along the shoreline, 0.5 – 0.7 m wide, whose dominant species are burweed (*Franseria chamissonis* Less.), beach morning glory (*Convolvulus soldanella* L.), yellow sand verbena (*Abroina latifolia* Escchs.), and marram grass (*Ammophila arenaria*) (Cooper 1967).

This dune field has a series of old parabolic dunes covered with vegetation on the southern half. Except for the coastal roads, the foredune is well vegetated with small sand patches. Effective wind is apparently northwest and a pyramid point on the north and the Smith River are the main sand sources for the dune field (Cooper 1967).

The annual average temperature in Point St. George is 52.1°F (11°C) and the temperature range is 11.9°F (6.5°C), which is slightly less than those in Oregon (Table 3.1). The annual total precipitation is 66.8 inches (169.7 cm). The annual average wind

speed is 5.3 m/s. Winds are faster in summer. The annual range of wind speed is 1.5 m/s. The annual average wind direction is southwest (234°) (Figure 3.22), but the wind directions vary dramatically in different months. Winds blow northwest in January and February, changes to southwest in April, south in June, east in September, northeast in October, and returns to the northwest in December (Figure 3.21).

Figure 3.20. Average monthly precipitation and temperature in St. George, CA (1979-2008)

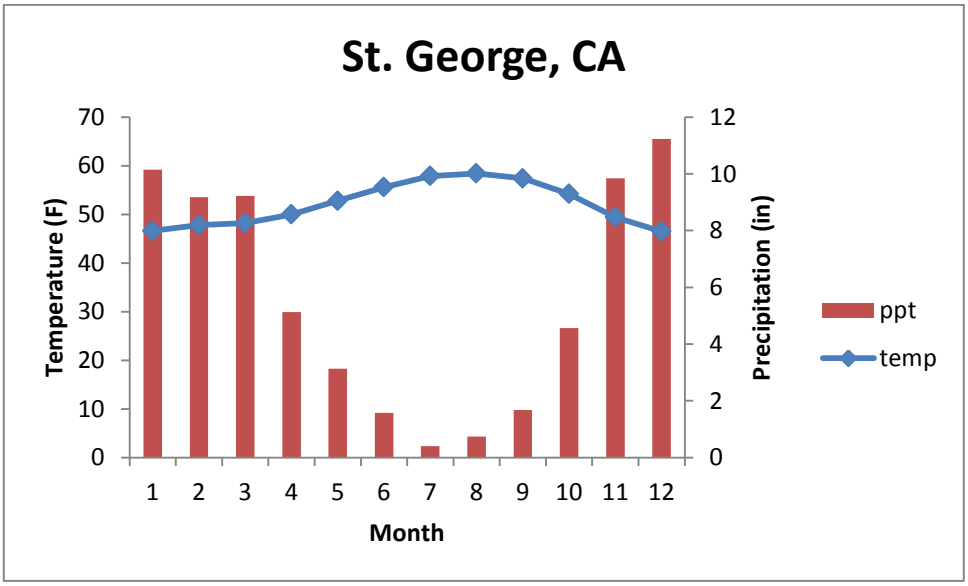

Figure 3.21. Average monthly wind speed and direction in St. George, CA (1979-2008)

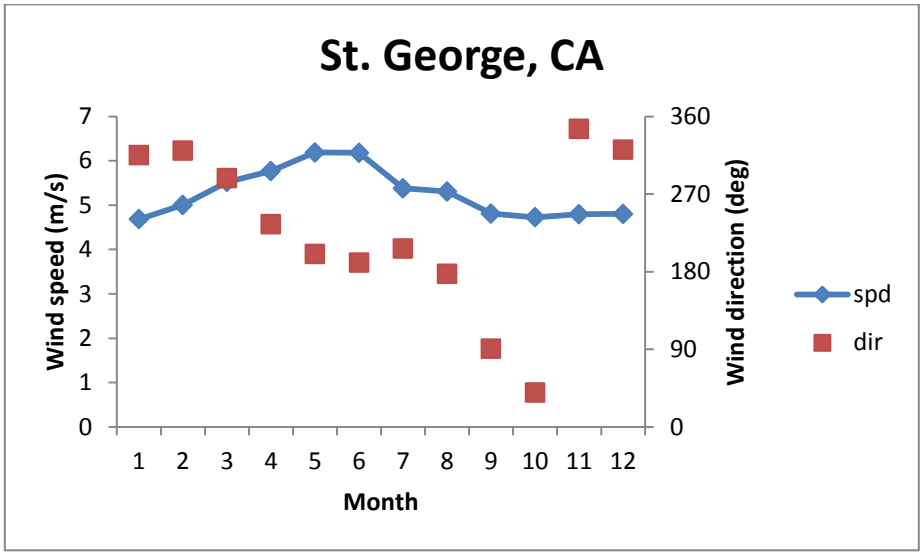

Figure 3.22. Wind rose in St. George, CA (1979-2008)

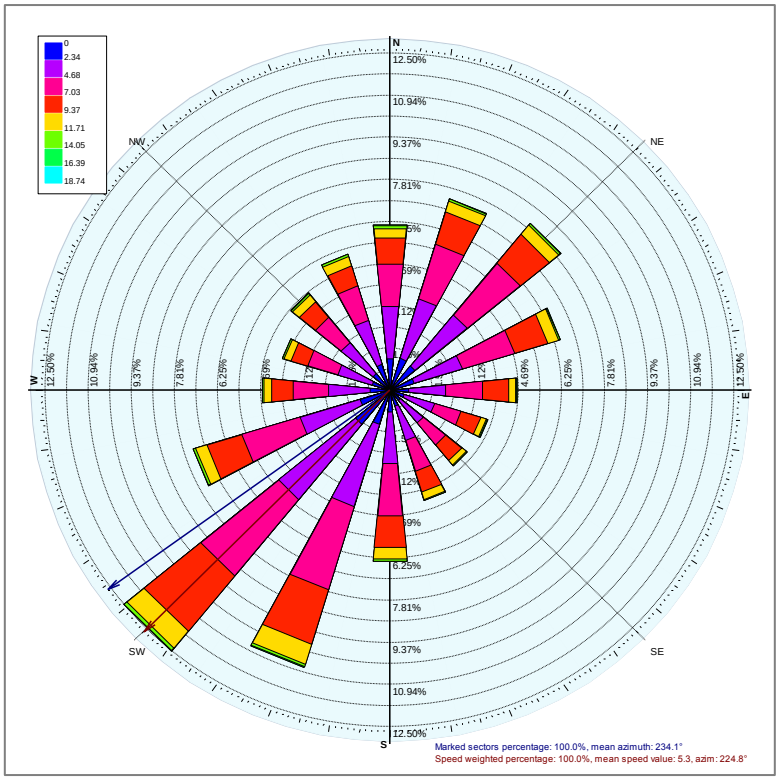

Figure 3.23. Map of Point St. George dune field. Note that foredune area (ca. 0.53 km^2) is in red box.

3.2.2 Eureka

The Eureka dune field is between Trinidad Head and the mouth of Humboldt Bay, and is located at 40°52'N and 124°09'W, two miles north of the city of Eureka (Figure 3.24). The length of the dune field is about 40 km, but for this study, about 7 km of the middle area was chosen extending from the mouth of the Mad River to the New Navy Base Road at the city of Samoa. This is because the northernmost dune field between the Little River and the Mad River is a narrow strip and the southern part near the city of Samoa is developed. American dunegrass (*Elymus mollis* Trin.), European searocket (*Cakile maritime* Scop.), European beachgrass (*Ammophila arenaria*), and thicket tribisee (*lasiacis ligulata* Hitchc. & Chase) are abundant on the dune field (Barbour, de Jong, and Johnson 1976).

Two major rivers, one flowing north (Mad River) and one flowing south (Eel River) of the dune field, created wide alluvial fans backed by the two bays and provide a good sand source for the dune field (Savoy et al. 1985). Cooper (1967) mentioned two episodes of dune ridges. The older dune ridges are inland and are parabolic dunes stabilized by spruces and pines. The younger dunes are seaward and continuous from the Mad River to Samoa. The inner edges of the younger dunes are lobate and parabolic, and extend southeast, indicating the prevailing wind direction, northwest. Except for several roads, most of the foredune areas are not developed.

The annual average temperature in Eureka is 52.9°F (11.5°C) and the temperature range is 10.8°F (5.9°C) (Table 3.1). The annual total precipitation is 38.1 inches (96.8 cm). The annual average wind speed is 6 m/s. Winds are faster in winter

and the annual range of the wind speed is 2 m/s. The annual average wind direction is northwest (307°) (Figure 3.28). Winds are southerly in January, become northerly in summer, and then return to southerly in December (Figure 3.27).

Figure 3.24. Map of Eureka dune field, CA. Note that foredune area (ca. 0.67 km^2) is in red box.

Figure 3.25. Average monthly precipitation and temperature in Eureka, CA (1979-2008)

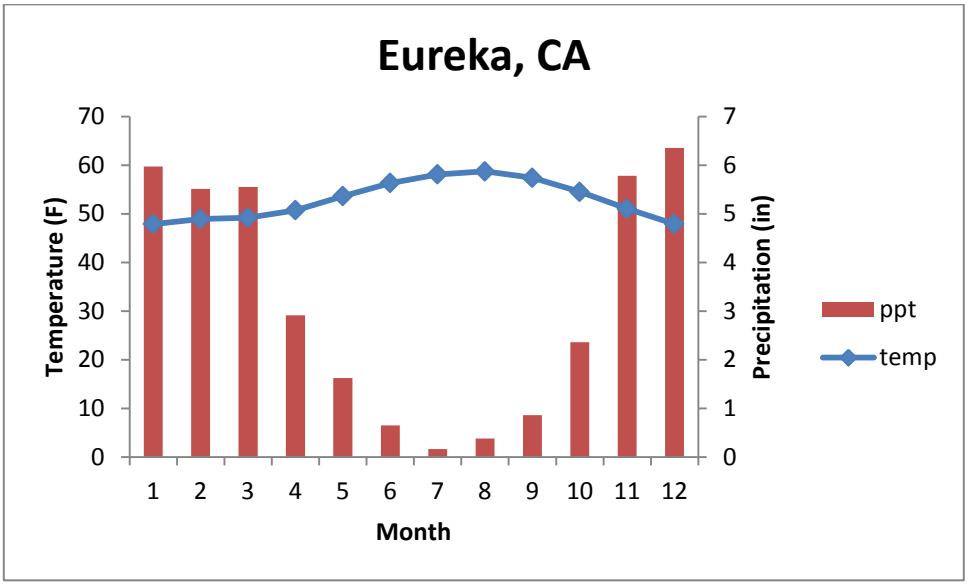

Figure 3.26. Average monthly wind speed and direction in Eureka, CA (1979-2008)

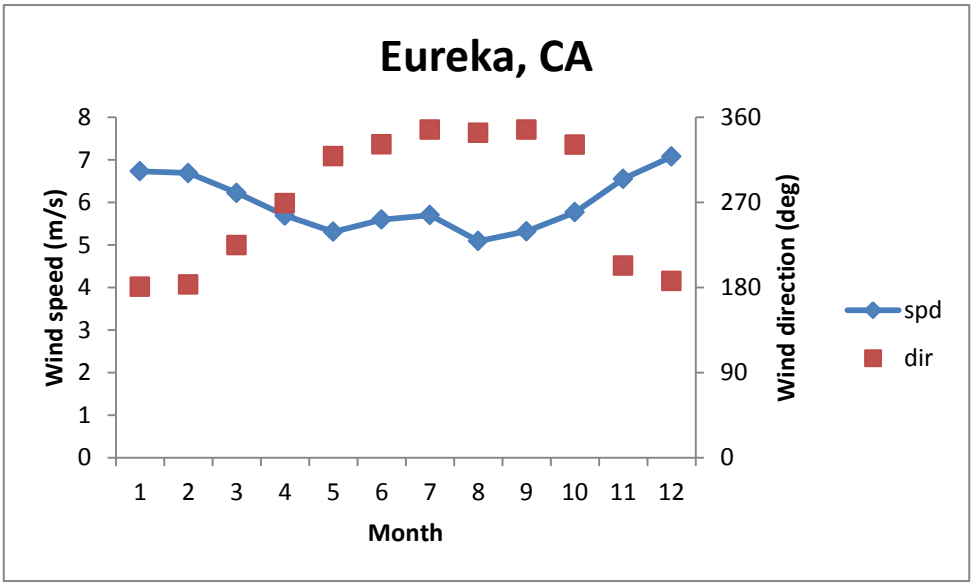

Figure 3.27. Wind rose in Eureka, CA (1979-2008)

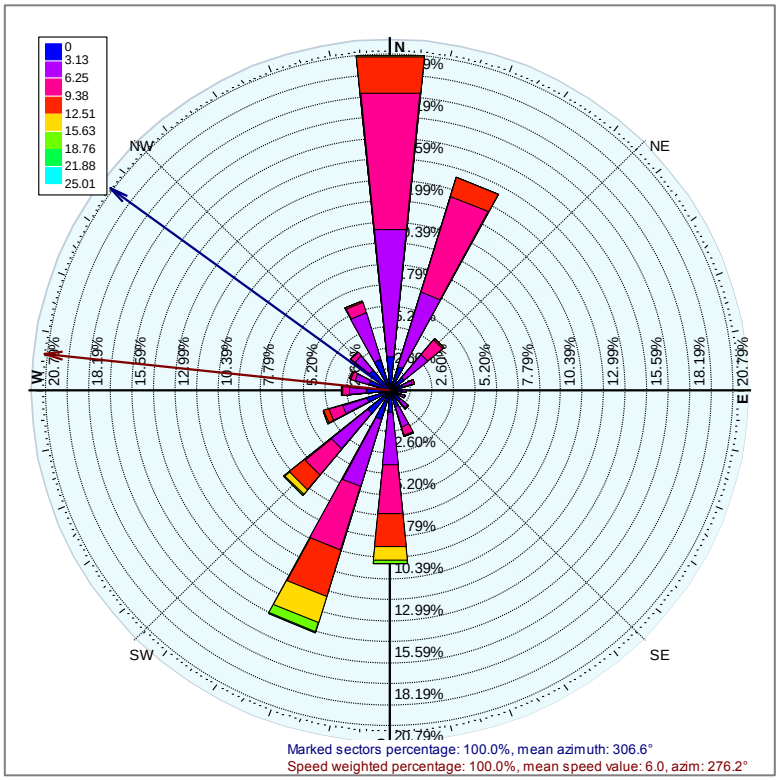

3.2.3 Point Arena

The Point Arena dune field is located at 38°57'N and 123°42'W, on a wide marine terrace. It is aligned northeast-southwest and is about 3 km long and 1 km wide. This dune field is backed by a flood plain associated with the Garcia River (Figure 3.28). The elevations of dunes increase gradually inland and deflation areas occur on the southern part of the dune field covered by wet-ground vegetation (Cooper 1967). There are active dunes in the middle of the dune field and old parabolic dunes inland.

The foredune line is very distinct, particularly on the northern half of the dune field. This can be seen clearly in aerial photographs taken by the California Coastal

Records Project (www.californiacoastline.org) and it is probably the result of dune erosion during storms. The foredunes are well vegetated with scattered small sand patches. Except for roads, human interference is minimal.

The annual average temperature in Point Arena is 53.1°F (11.6°C) and the temperature range is 11.2°F (6.2°C) (Table 3.1). The annual total precipitation is 41.9 inches (106.3 cm). The average wind speed is 7 m/s, faster than any other site, probably because of the projecting angle of the coast. Winds are faster in summer (May ~ July) (Figure 3.30) and the annual range of wind speed is 2 m/s. The annual average wind direction is west (260°) (Figure 3.31). Winds are south-southwest in May through August, changing to westerly and then northwesterly fall through winter.

Figure 3.28. Map of Point Arena dune field, CA. Note that foredune area (ca. 0.28 km^2) is in red box

Figure 3.29. Average monthly precipitation and temperature in Pt. Arena, CA (1979-2008)

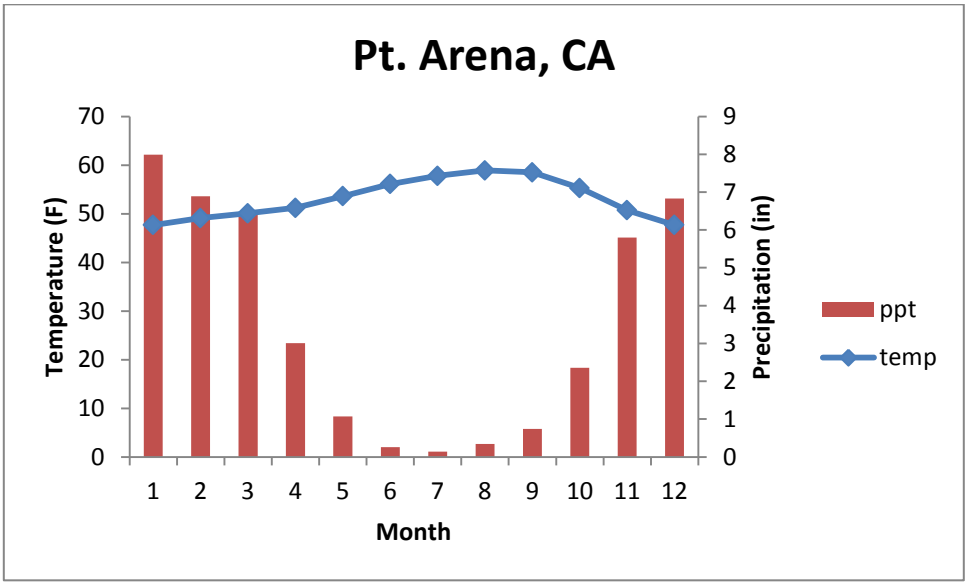

Figure 3.30. Average monthly wind speed and direction in Pt. Arena, CA (1979-2008)

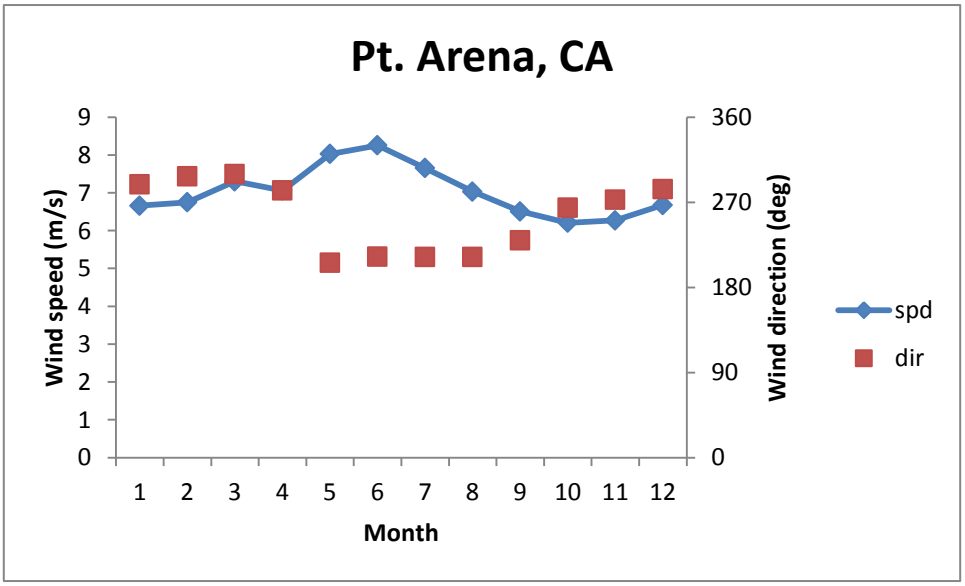

Figure 3.31. Wind rose in Pt. Arena, CA (1997-2008)

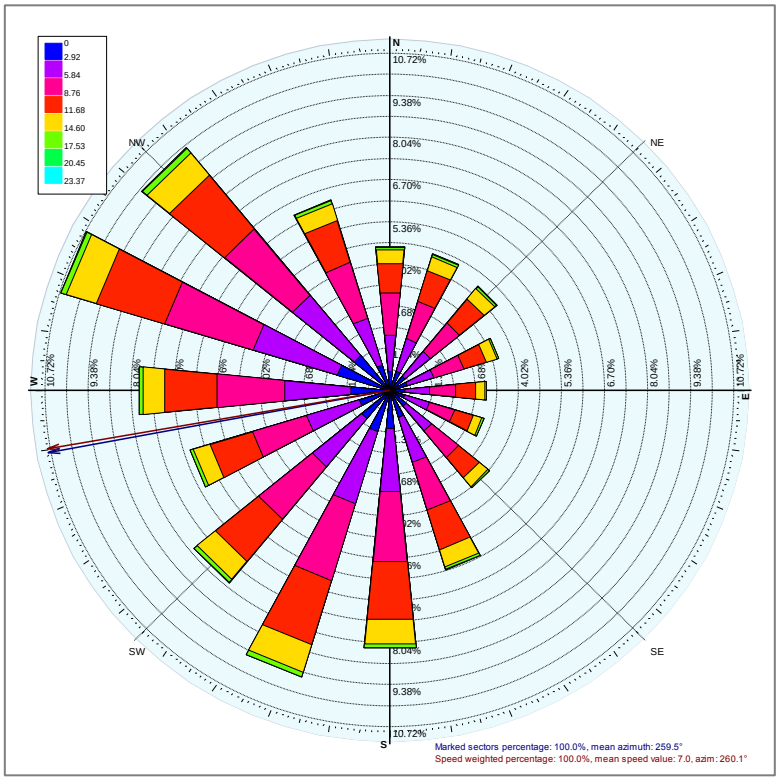

3.2.4 Tomales

The Tomales dune field is located at 38°5'N and 122°57'W, is about 18 km long reaching from Kehoe Beach to Point Reyes (Figure 3.32), and is 0.2 – 1.0 km in width. Two main sand sources for the dunes are Tomales Point and the granitic cliffs south of Tomales Point. These sands are transported by the southward longshore currents (Cooper 1967). The San Andreas Fault line passes east of the Tomales peninsula. Dune scarps are present from the middle of the dune field southward and the elevation between the dunes and the beaches changes abruptly (5 – 10 m). This can be seen in Google Earth™ or at the website of the California Coast Project

(www.californiacoastline.org). The foredunes are stabilized with marram grass and other native species (Cooper 1967). The Tomales dune field is characterized by lobate and stabilized parabolic dunes superimposed by younger active dunes. The parabolic dunes tend southward representing prevailing wind direction. Because the dune field is protected within Point Reyes National Seashore, human interference is minimal.

The average temperature in Tomales is 59°F (14.9°C) and the temperature range is 19.2°F (10.6°C) (Table 3.1). The temperature in Tomales is the highest among all sites on the west coast in the U.S (Figure 3.33). The annual total precipitation is 34.3 inches (87.1 cm). Point Reyes is one of the foggiest area on the California Coast during the driest months (Pitts and Barbour 1979). The annual average wind speed is 5.6 m/s. Winds are faster in spring (March ~ June) and slow down in summer (July ~ September) (Figure 3.35). The annual range of wind speed is 2.2 m/s. The annual average wind direction is predominantly northwest (316°) (Figure 3.36) and is consistent throughout the year (Figure 3.35).

Figure 3.32. Map of Tomales dune field, CA. Note that foredune area (ca. 0.72 km^2) is in red box.

Figure 3.33. Annual average temperature of all sites. Note that Tomales' temperature is the highest among all sites in California

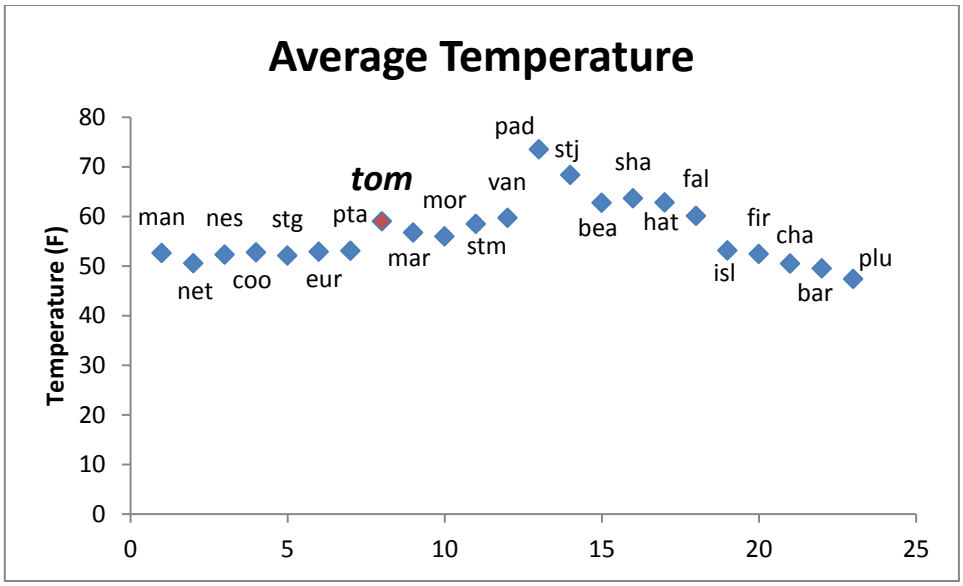

Figure 3.34. Average monthly precipitation and temperature in Tomales, CA (1979-2008)

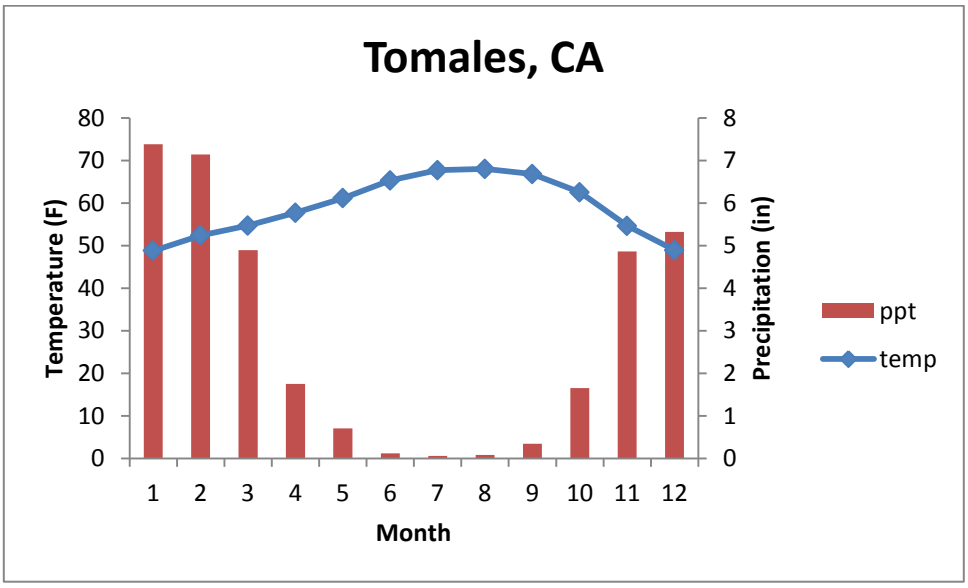

Figure 3.35. Average monthly wind speed and direction in Tomales, CA (1979-2008)

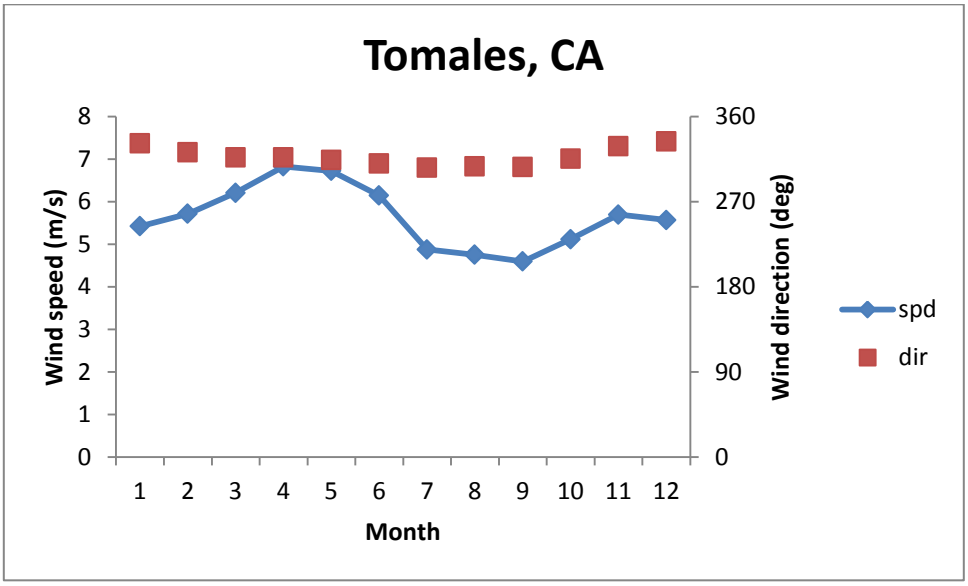

Figure 3.36. Wind rose in Tomales, CA (1979-2008)

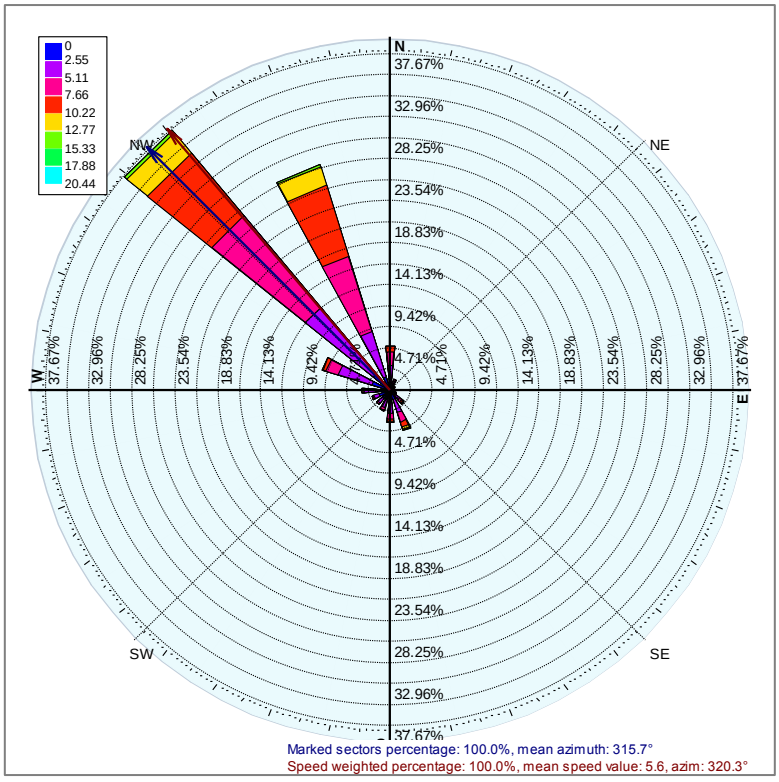

3.2.5 Marina

The Marina dune field system occurs along the coast from Santa Cruz Point south to the Monterey Peninsula and is 48 km long (Figure 3.37). The largest dune field within the system lies on the lower flood plain between the Salinas River on the north and the foot of the Monterey Peninsula on the south and at its widest part extends up to 13 km (Cooper 1967). The site chosen for this study extends from the mouth of the Salinas River to the south 2 km. Cliff erosion to the north and rivers – the Salinas and Pajaro and the streams that flow into Elkhorn Slough – are major sediment sources for the dune field (Cooper 1967). The longshore current is southward.

The elevation of the dune field increases gradually inland and the foredunes are 5 – 8 m in height. The foredune lines are broken by multiple rows of trough blowouts, but on the south end the foredunes are scarped due to storm-wave erosion. Parabolic dunes, either stabilized or still active, tending west-southwest, the prevailing wind direction, lie over pre-Flandrian sand dunes inland (Cooper 1967). The crests of the active parabolic dunes are about 33 m in height. There are several low spots in this area, vegetated by shrubs and wet plants. Except for parking lots and beach roads, the selected area has little human interference. The southern end of the study site is developed for residential and recreational uses. According to McBride and Stone (1976), the foredunes are dominated mostly by marram grass (*Ammophila arenaria*) with shrubs and sedges toward inland and the older dunes are dominated by California live oak (*Quercus agrifolia*) and Monterey pine (*Pinus radiate* D. Don) and 89 % of the dune sands are medium sized (0.25-0.5 mm) and 18 % fine sand (0.1 – 0.25 mm). Ice plant

(*Carpobrotus edulis*), a succulent and perennial plant introduced in early 1900s from South Africa into coastal dune fields in Monterey, U.S. to stabilize dunes (D'Antonio 1993; Guinon and Allen 1990).

The annual average temperature in Marina is 56.7°F (13.6°C) and the temperature range is 10.8°F (5.9°C) (Table 3.1). The annual total precipitation is 20.4 inches (51.7 cm), which is about 14 inches (35 cm) less than at Tomales. The annual average wind speed is 3.5 m/s. This is the slowest among all 22 sites. Winds are faster in spring (March ~ June), but they are consistent throughout the year with an annual wind speed range of 0.8 m/s (Figure 3.39). The annual average wind direction is west (274°) (Figure 3.41), but winds are north and northwest between May and October, but shift abruptly to southerly in November and continue until February (Figure 3.39). The wind pattern in Marina is different from other dune fields in southern California; they are slower and have a spreading wind direction (Figure 3.39, and Figure 3.40). This is probably because the site is in a large concave bay and winds diffuse over the bay (Figure 3.19 and Figure 3.37) (Cooper 1967).

Figure 3.37. Map of Marina dune field, CA. Note that foredune area (ca. 0.19 km^2) is in red box.

Figure 3.38. Average monthly precipitation and temperature in Marina, CA (1979-2008)

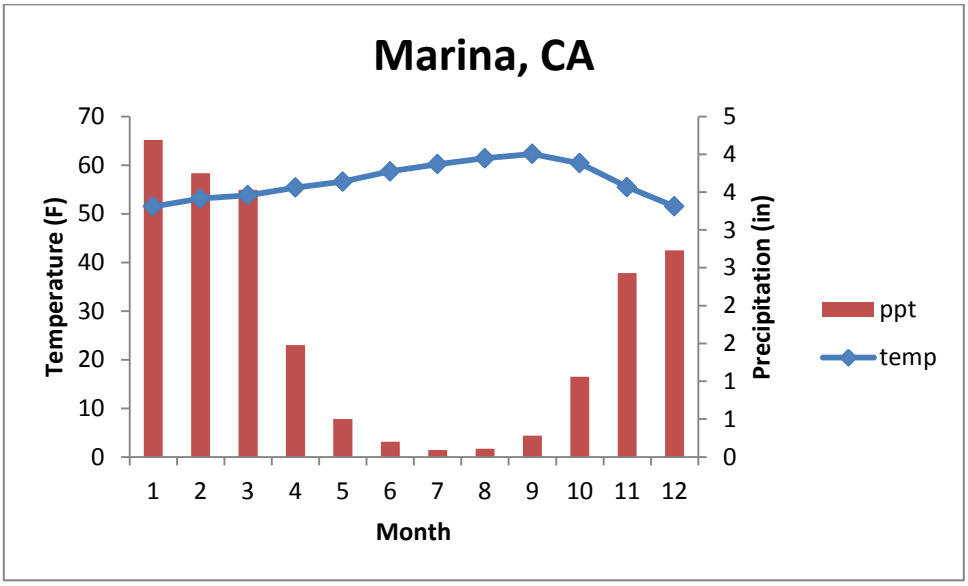

Figure 3.39. Average monthly wind speed and direction in Marina, CA (1979-2008)

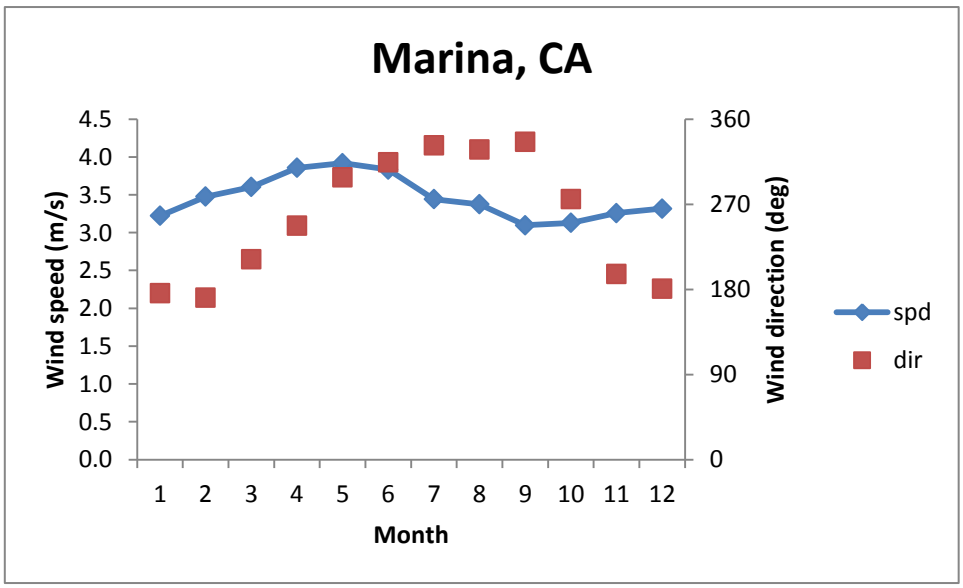

Figure 3.40. Annual average wind speed of all sites. Note that Marina has the lowest wind speed among all sites.

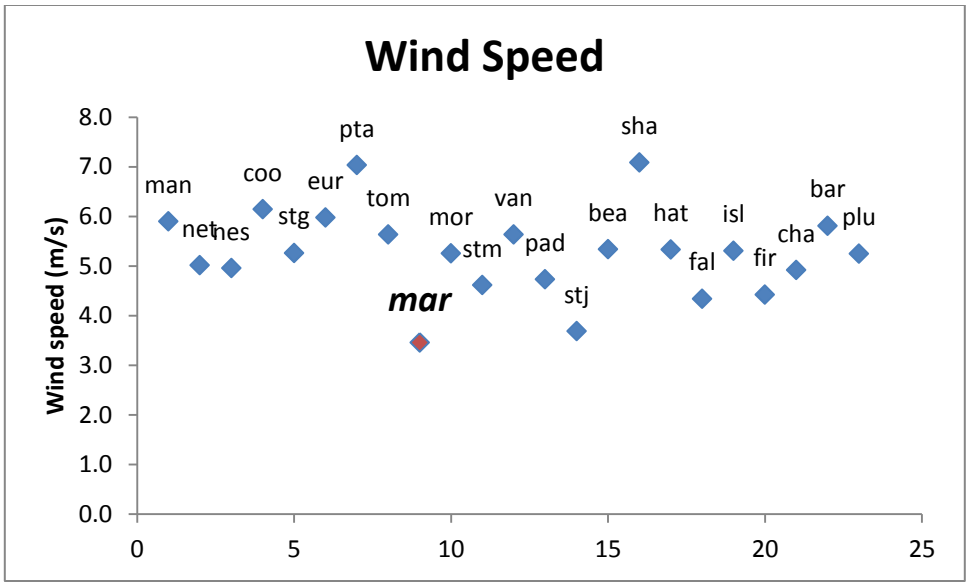

Figure 3.41. Wind rose in Marina, CA

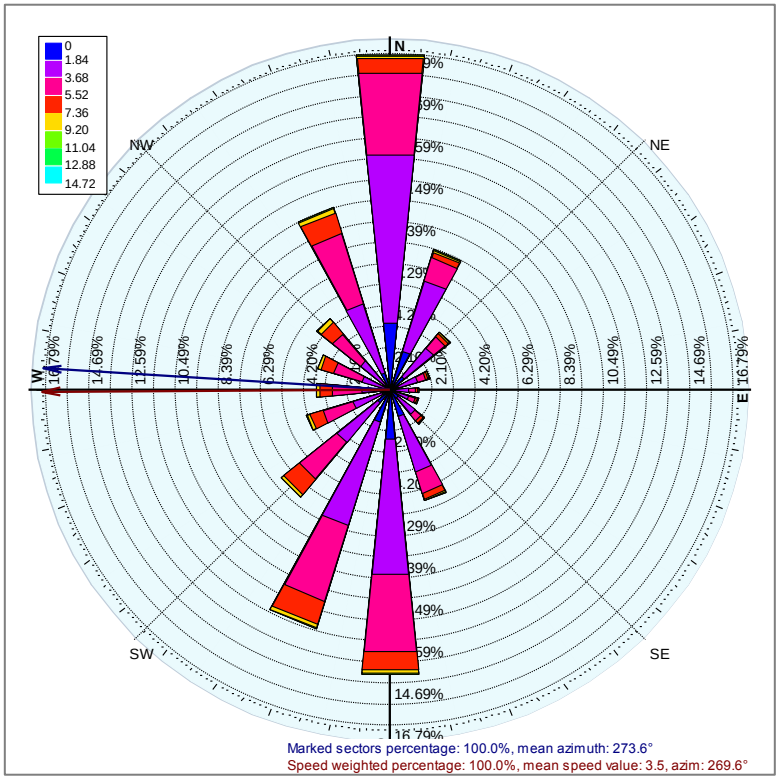

3.2.6 Morro Bay

The Morro Bay dune field is on a spit extending northward in front of Morro Bay and is located at 35° 20’ N and 120° 51’ W (Figure 3.42). The spit is about 9 km long and 0.3 – 0.65 km wide. Morro Bay is an estuary that was closed during the Holocene transgression. It is backed by intertidal mud flats and marshes (Orme 2005). The foredunes are dominated by European searocket (*Cakile maritime*) and red sand verbena (*Abronia maritima*) and a number of active blowouts and parabolic dunes have penetrated to the inland (Williams and Potter 1972), and the lobate margins of the active parabolic dunes extend across the spit to the bay and tidal mud flats (Cooper 1967). The area chosen for this study is 6 km long.

The annual average temperature in Morro Bay is 55.9°F (13.2°C) and the temperature range is 8.2°F (4.5°C) (Table 3.1). The annual total precipitation is 17.6 inches (44.7 cm). The annual average wind speed is 5.3 m/s and is relatively consistent throughout the year (4.7~6.2 m/s) (Figure 3.44). The annual average direction (298°) and prevailing wind direction are west-northwest (Figure 3.45). Wind direction is north in winter and shifts to the west in summer (Figure 3.44).

Figure 3.42. Map of Morro Bay dune field, CA. Note that foredune area (ca. 0.60 km^2) is in red box.

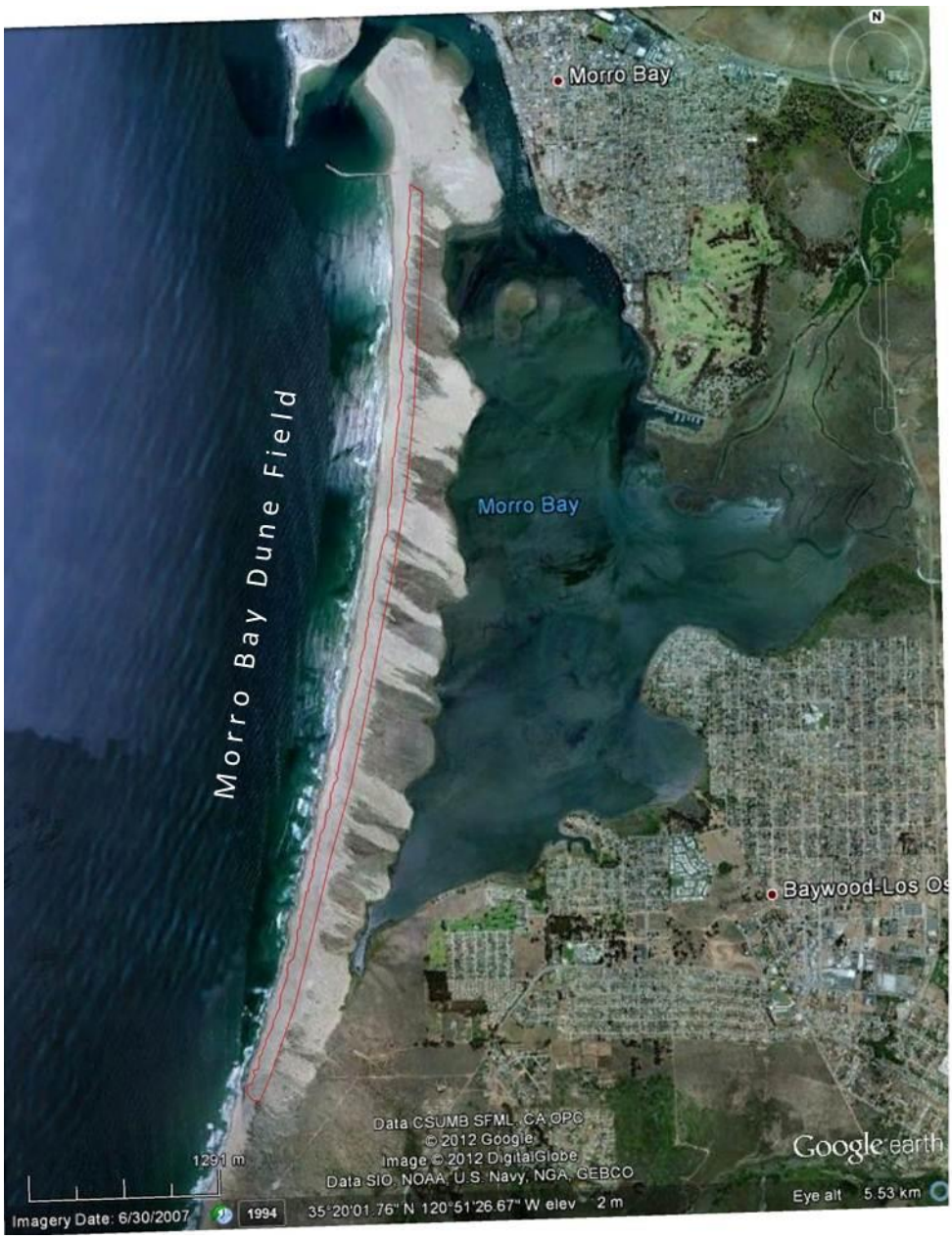

Figure 3.43. Average monthly precipitation and temperature in Morro Bay, CA (1979-2008)

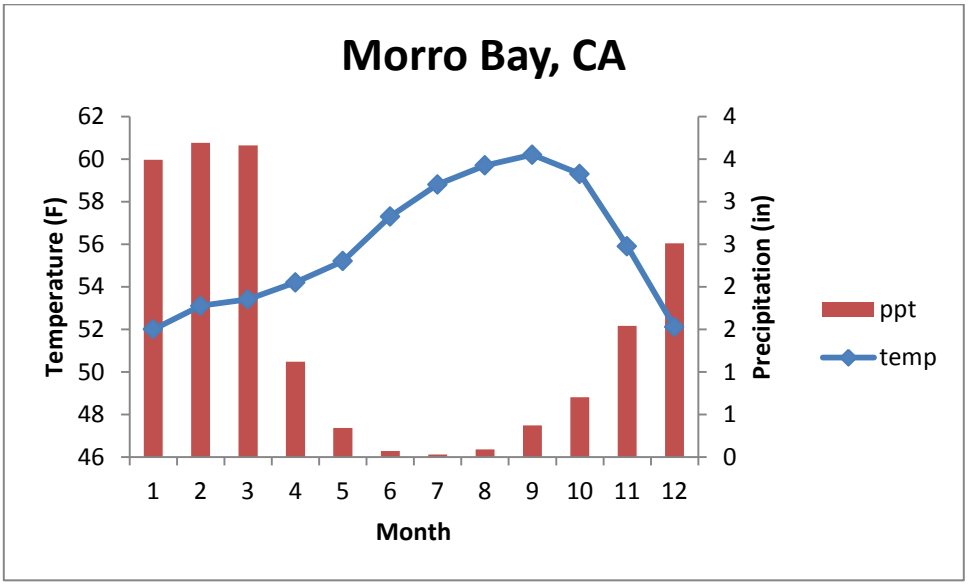

Figure 3.44. Average monthly wind speed and direction in Morro Bay, CA (1979-2008)

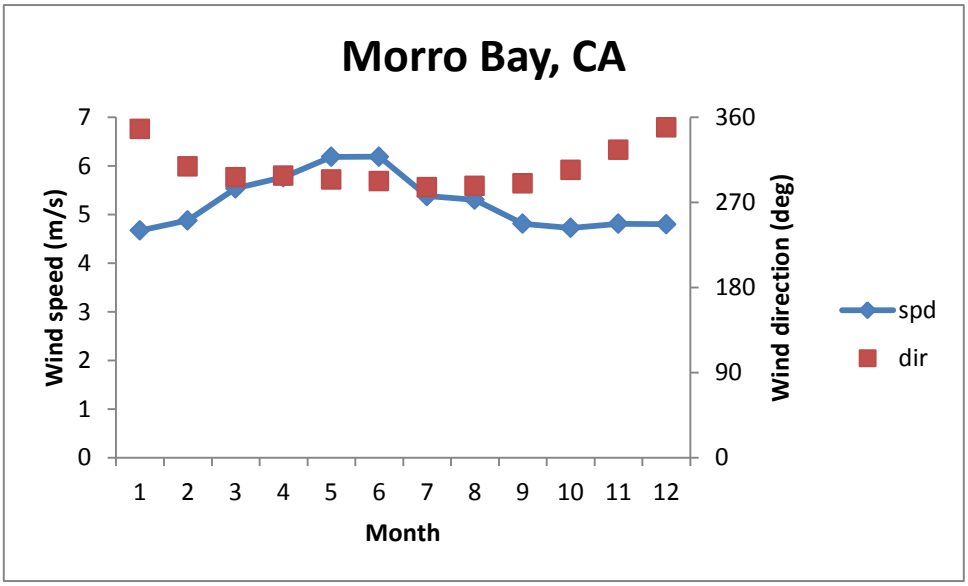

Figure 3.45. Wind rose in Morro Bay, CA (1979-2008)

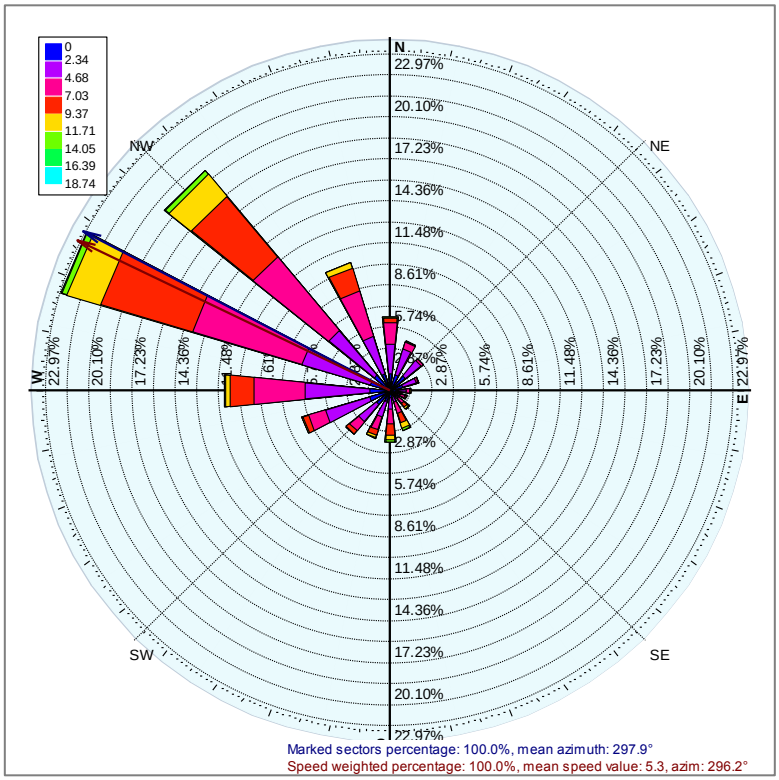

3.2.7 Santa Maria

The Santa Maria dune field system is on the shoreline between Pismo Beach on the north and Point Sal on the south (Table 3.1). There are three large sand dune complexes within this system. The north field is called the Callender Dune Complex according to Cooper (1967), which is now the Pismo Dunes Natural Reserve. This complex is located between Arroyo Grande Creek and Oso Flako Lake, at approximately 35° 03’ N and 120° 36’ W. This field consists of almost bare sand sheets with transverse dunes extending up to 3 km inland. The entire dune field is about 7.5 km long and up to 19 km wide.

The south complex, Mussel Rock Dune Complex (Cooper 1967), is the smallest among the three and is located between the Santa Maria River and Point Sal, at approximately 34° 56' N and 120° 38' W. The shoreline is curved, facing north-northwest. The dune field is about 7 km long and 8 km wide and includes established dunes extending back to Corralitos Canyon. This field is composed of extensive sand sheets like the Callender Dune Complex and several stabilized parabolic dunes. The transverse dunes in this complex are trending southeast, more oblique to its shoreline than in the other two fields.

The middle complex, the Guadalupe Dune Complex (Cooper 1967), is located at approximately 34° 59' N and 120° 37' W and was chosen for this study (Figure 3.46). This dune complex has more vegetation cover than the other two. The descriptions of geology are based on Cooper (Cooper 1967) except as otherwise noted. No pre-Flandrian dunes are found in this field. The dune field lies on an extensive flood plain of the Santa Maria River and is extensively invaded inland.

In the foredune areas, there are numerous elongated blowout openings between vegetated hillocks and ridges and they develop into active parabolic dunes inland. The reason why the middle complex was chosen for this study is that it is the least disturbed by human activity. Little human interference is found in the foredune areas while there are many roads, parking lots and oil rigs inland.

The annual average temperature in St. Maria is 58.5°F (14.6°C) and the temperature range is 9.5°F (5.2°C) (Table 3.1). The annual total precipitation is 17.8 inches (45.2 cm). The pattern of temperature and precipitation in St. Maria is similar to

that of Morro Bay (Figure 3.47). The annual average wind speed is 4.6 m/s and the range of the wind speed is 1.8 m/s. The annual average wind direction is northwest (316°) (Figure 3.49) and is very consistent throughout the year (Figure 3.48).

Figure 3.46. Map of St. Maria, CA. Note that foredune area (ca. 0.66 km2) is in red box.

Figure 3.47. Average monthly precipitation and temperature in St. Marina, CA (1979-2008)

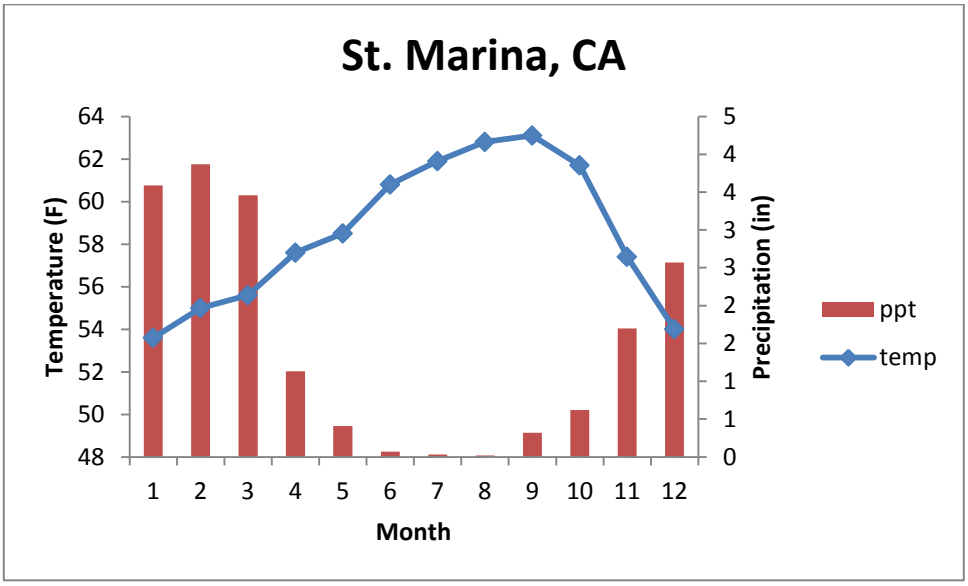

Figure 3.48. Average monthly wind speed and direction in St. Marina, CA (1979-2008)

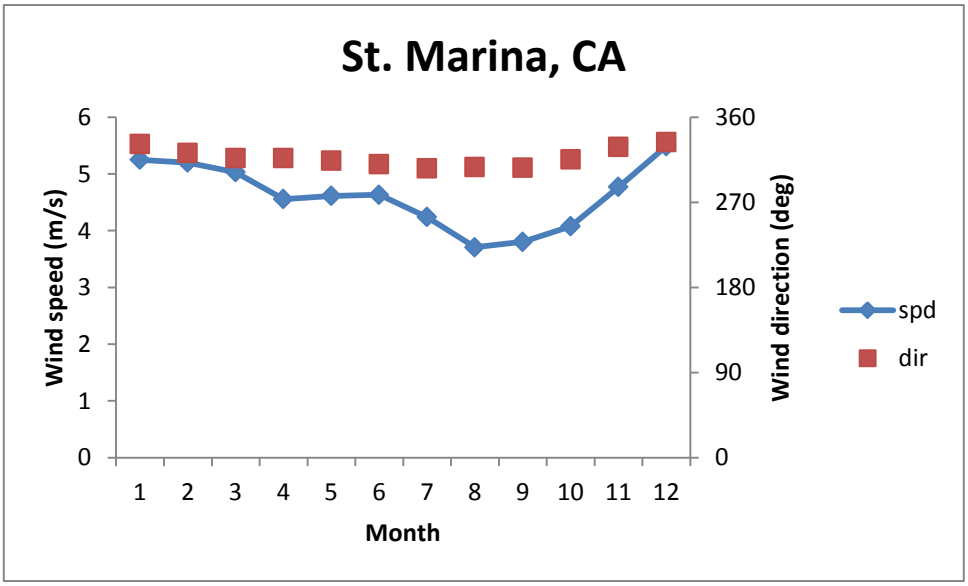

Figure 3.49. Wind rose in St. Maria, CA (1979-2008)

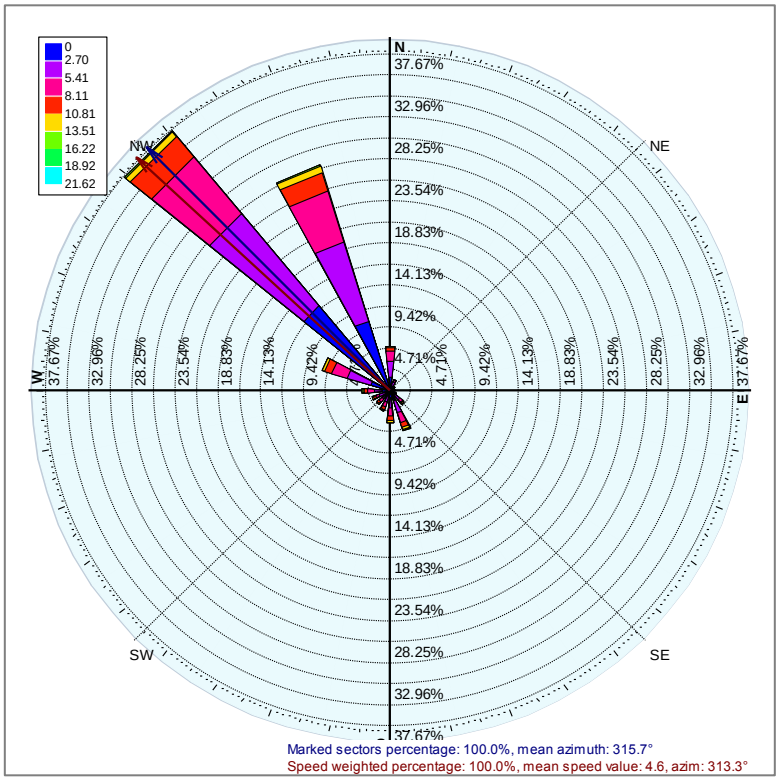

3.2.8 Vandenberg

The Vandenberg dune field is the southernmost dune field selected for this study along the U.S. west coast. Vandenberg is located at approximately 34° 50’ N and 120° 36’ W (Table 3.1). The dune field is between the Casmalia Hills and Purisima Point, and is 12 km long and up to 15 km wide. San Antonio Creek cuts the dune field into two parts, north and south. Only the northern part, which extends about 7 km, was considered for this study.

Descriptions of geology in this area are based on Cooper (1967) except as otherwise noted. The Vandenberg dune field lies in a very wide and triangular lowland

considered to be a marine terrace surface. In the foredune areas, a series of narrow and straight blowout openings developed into active parabolic dunes, tending southeastward, representing the prevailing northwesterly wind. Sediment sources are meager, mostly from cliff erosion at Point Sal on the north, resulting in thinner sand sheets than those in the St. Maria dune field. Little evidence of human interference is found on the foredunes, but roads, parking lots, and buildings are found inland.

The annual average temperature at Vandenberg is 59.7°F (15.2°C) and the temperature range is 12.2°F (6.7°C). The annual total precipitation is 15.9 inches (40.3 cm). The precipitation at Vandenberg is the lowest among all the sites but the temperature is the highest among sites on the west coast (Table 3.1). The annual average wind speed is 5.6 m/s and the range of wind speed is 2.2 m/s. The annual average wind direction is west-northwest (299°) (Figure 3.53) and it is very consistent throughout the year, fluctuating between north-northwest and west-northwest (Figure 3.52).

Figure 3.50. Map of Vandenberg, CA. Note that foredune area (ca. 0.44 km2) is in red box.

Figure 3.51. Average monthly precipitation and temperature in Vandenberg, CA (1979-2008)

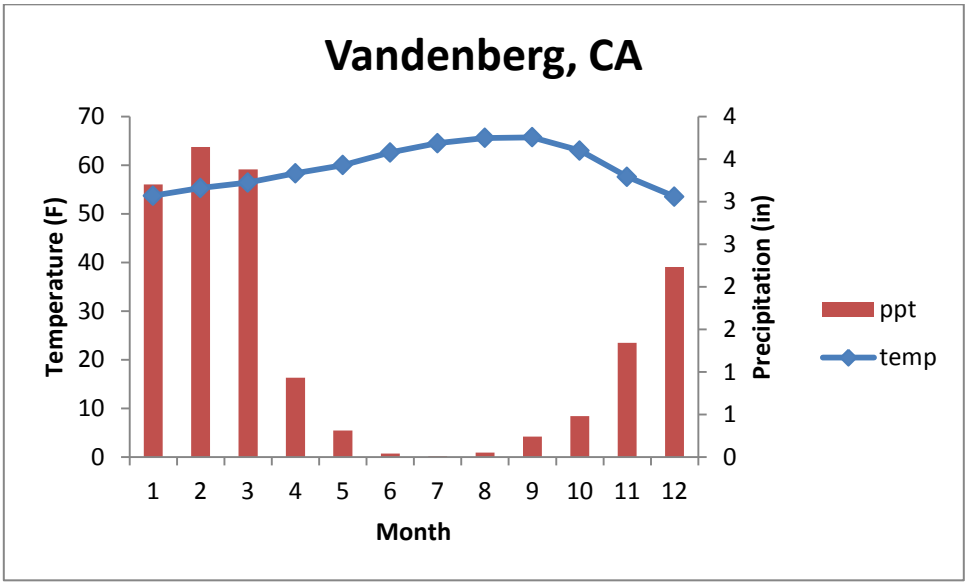

Figure 3.52. Average monthly wind speed and direction in Vandenberg, CA (1979-2008)

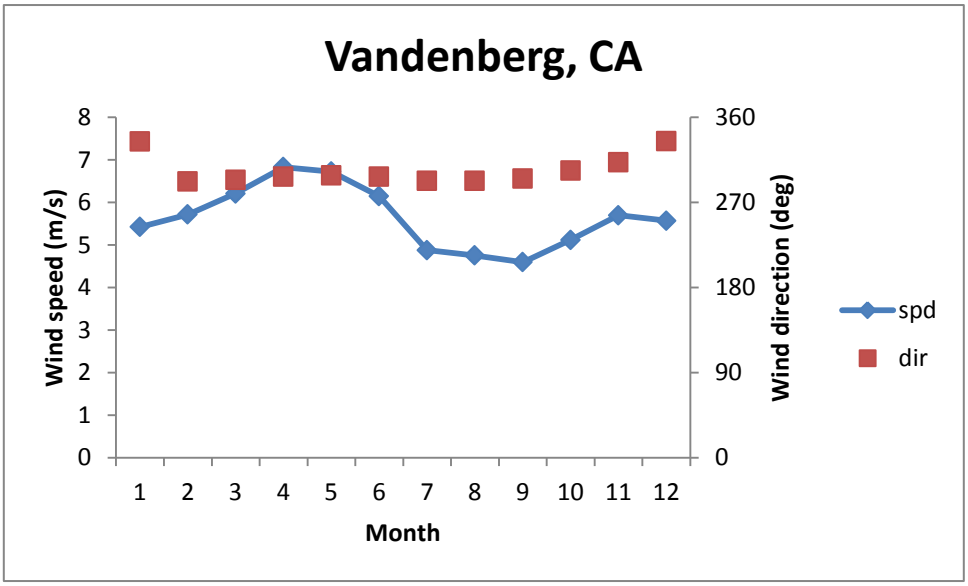

Figure 3.53. Wind rose in Vandenberg, CA (1979-2008)

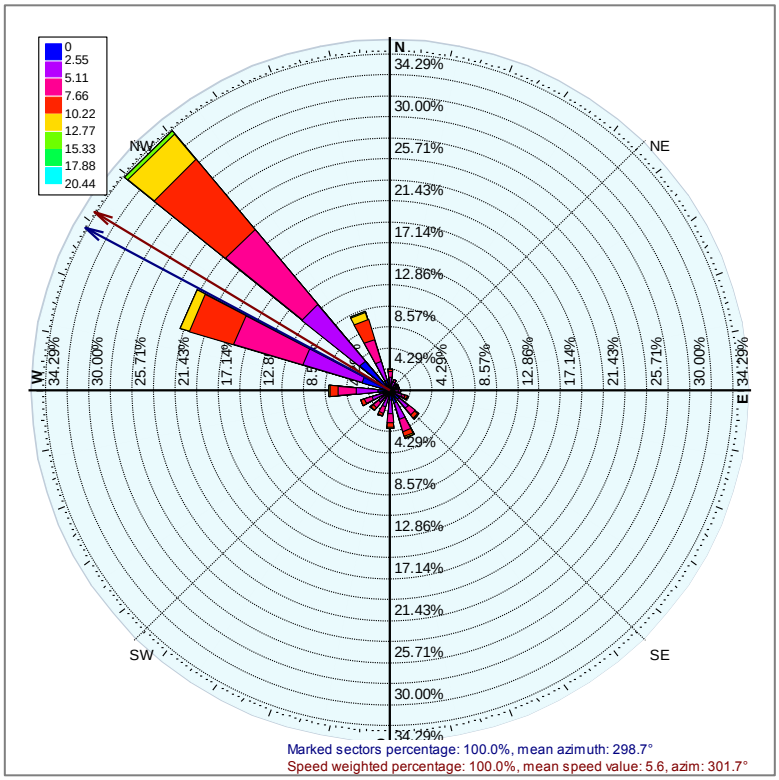

3.3 Gulf of Mexico

Parts of Padre Island, Texas, and the Saint Joseph barrier island, Florida, were chosen for this study (Figure 3.1). The small dune fields in Louisiana, Mississippi, and Alabama were not considered for this study because of their size and because they are extensively developed for human usage. The undeveloped dune fields in these states are not large enough to form established dunes. Examples are the barrier islands on the Mississippi coast, and Cat Island, Horn Island, or Dauphin Island on the Alabama coast (Figure 3.54). This is partly due to a lack of sediment sources, especially from the

Mississippi Delta due to westward sediment transport (Bird and Schwartz 1985), and the chronic erosion of their barriers.

The Louisiana coast is characterized by a deltaic system and the Atchafalaya and the Balize are still building delta complexes seaward (Mendelssohn et al. 1991). Most dune fields on the Louisiana coast are formed on barrier islands, but they are not big enough to have secondary dunes. Barrier islands in Louisiana are formed by eroded and reworked sediments from abandoned deltas and the existing barriers are being used as a sediment source for the further development of other barriers (Bird and Schwartz 1985; Mendelssohn et al. 1991).

The descriptions of the Texas coast are based on Bird and Schwartz (1985) except as otherwise noted. The entire Texas coastline is about 590 km long. A littoral drift convergence zone occurs at about 27° N with westward drift on the north and north/northeastward on the south from the convergence zone. Rainfall decreases and temperature increases southward. Hurricanes have played a major role in the Texas coast morphology and sediment regime; the hurricane-generated storm surges create washovers, move sand inland, and accrete and erode beaches and dunes. Sediments of the Texas coastline are fine to very fine and there is well-sorted sand on dunes and beaches.

The descriptions of the Florida coast are based on Davis (1997) except as otherwise noted. The Florida coast around the Saint Joseph barrier island is wave-dominated and the rates of the sediment influx are the highest on the Florida coast. The primary sediment source is from the Apalachicola Delta. The barriers around

Apalachicola Bay were formed by the reworked sediment transported by waves and extensive northward littoral drift. Consequently, the northern end of St. Joseph Island is prograding, resulting in the growth of many beach ridges.

Figure 3.54. Map of the Louisiana, Mississippi and Alabama coasts

3.3.1 Padre Island

Padre Island is the longest barrier island in the United States, ranging for more than 180 km from southeast of Corpus Christi to the border of the U.S. and Mexico (Figure 3.55). The northern island is protected within the Padre Island National Seashore. The shoreline is concave seaward. Padre Island is relatively young and was formed 3,000 – 5,000 years ago. It is separated from the Texas mainland by Laguna Madre and was formed and developed from an offshore submerged sandbar, by spit accretion by longshore drift (Wise and White 1980). In addition, tropical storms and hurricanes strike

South Padre Island about every six years and the average return period for all hurricanes on North Padre Island is 14 years (Muller and Stone 2001). Dominant vegetation species are *Heterotheca subaxillaris* and *Chamaecrista fasciculate* on the primary dunes and *P. monostachyum*, *S. scoparium*, and *Indigofera miniata* on the secondary dunes (Carls, Lonard, and Fenn 1991). Sediments are comprised of fine sand and shell fragments and the average grain sizes of the beaches are about 0.12 mm on North Padre Island and 0.17 mm on South Padre Island (Bible 1962; Carls, Lonard, and Fenn 1990; Mazzullo and Kennedy 1985).

The northern part of the Padre National Sea Shore, specifically from the south of the visitor center to 13 km southward was chosen for this study because it is little disturbed and is protected within Padre Island National Seashore (Figure 3.55). It is located at approximately 27° 23' N and 97° 18' W. Some blowouts are found on foredunes, but the secondary dunes are well vegetated except for oval blowouts and parabolic dunes with bare sand. Stabilized parabolic dunes are further inland backed by marshes and an extensive lagoon, Laguna Madre. Little evidence of human activity is found except roads, but off-road vehicles and pedestrian traffic can be seen from place to place (McAtee and Drawe 1980).

The annual average temperature on Padre Island, TX is 73.5°F (22.8°C), the highest among all sites and the temperature range of 27.9°F (15.3°C) is also the greatest (Table 3.1). The annual total precipitation is 33.4 inches (84.9 cm) and it is humid throughout the year (Figure 3.56). This site falls in the Cfa category (Humid Subtropical Hot-Summer Climate) according to Köppen's climate classification system. The annual

average wind speed is 4.7 m/s and the wind speed range is 1.2 m/s. The annual average wind direction is west-southwest (257°) (Figure 3.58). Wind direction changes dramatically from northwest to south. Offshore, northwesterly winds prevail from May to October, and onshore, southerly winds for the rest of year (Figure 3.57).

Figure 3.55. Map of Padre Island dune field, TX. Note that foredune area (ca. 1.13 km^2) is in red box.

Figure 3.56. Average monthly precipitation and temperature in Padre Island, TX (1979-2008)

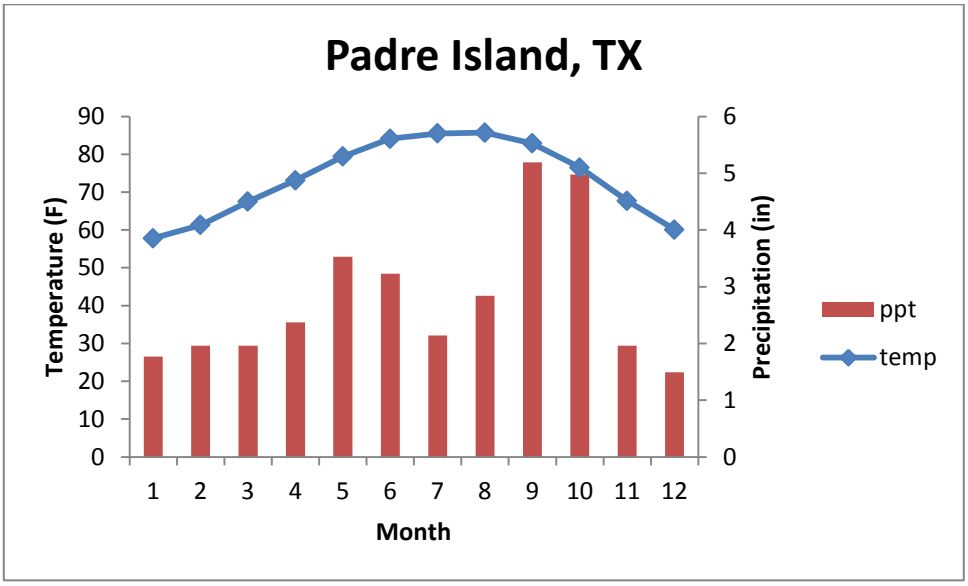

Figure 3.57. Average monthly wind speed and direction in Padre Island, TX (1979-2008)

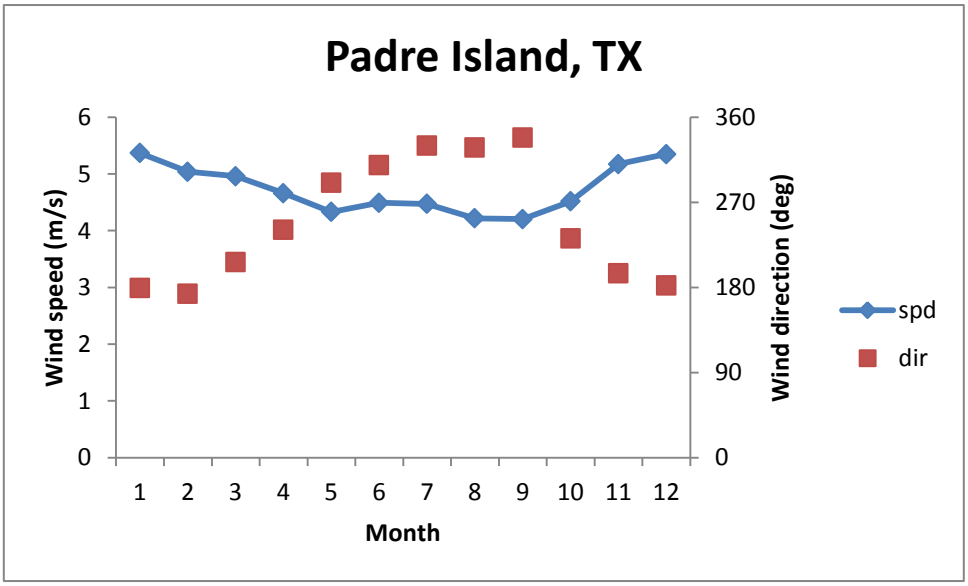

Figure 3.58. Wind rose in Padre Island, TX (1979-2008)

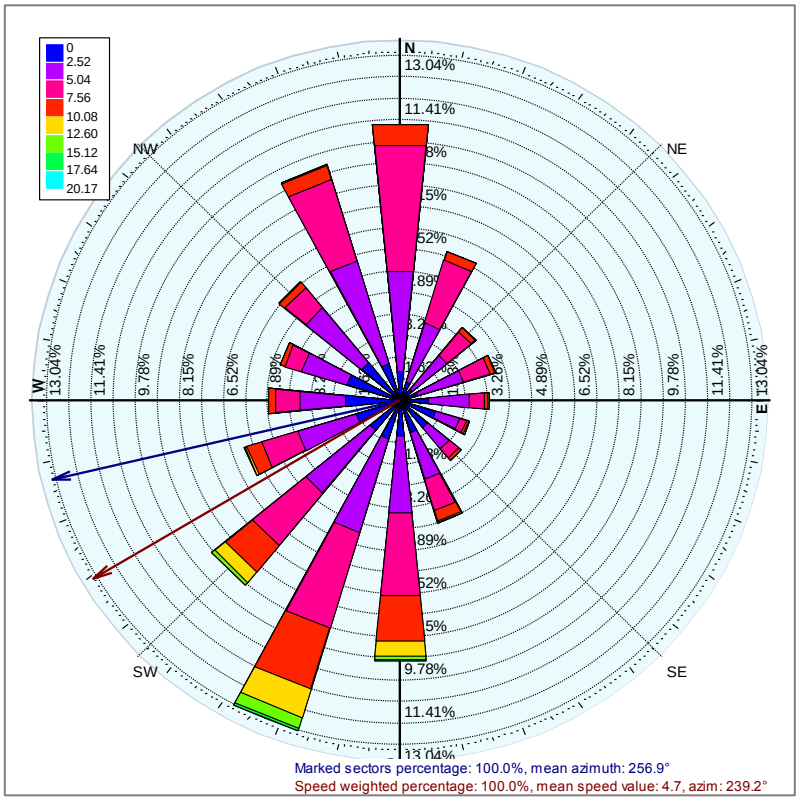

3.3.2 Saint Joseph

The Saint Joseph dune field is in the St. Joseph Peninsula State Park (29° 50’ N, 85° 24’ W) and is backed by the St. Joseph Bay (Figure 3.59). The peninsula is a spit, extending northwestward and is about 26 km long from Cape San Blas on the south to its northern end, and it is 0.1 – 1.5 km wide. Major sand supplies are from the Apalachicola River and the deposits of the coastal plain, transported northward by the longshore current to form the spit (Stewart and Gorsline 1962). This results in the presence of many dune ridges on the northern part of the St. Joseph spit. The spit has been affected by tropical storms and hurricanes, at an annual probability of 7 % (Bush et al. 2001) and

100-year flood levels are estimated at 9.5 to 12.5 feet above mean sea level (Doyle et al. 1984).

The sediment in this area is predominantly quartz sand and fragmented shells (Stauble and Warnke 1974). The dominant vegetation species on the dunes is *Uniola paniculata* and ground-clinging plants such as *Cnidoscolus stimulosus* and *Croton punctatus* (beach tea) are common (Carlton 1977). Foredune areas have blowouts, either individual or merged, causing complicated sand patches. The site chosen for this study is about 10 km long, starting north of Eagle Harbor to the northern end of the peninsula. There are several roads parallel to the shoreline and some access roads to the beach. The secondary dunes are well vegetated, but small sand patches occur along beach ridges.

The annual average temperature in St. Joseph is 68.3°F (20°C) and the temperature range is 29.2°F (16.1°C) (Table 3.1). The annual total precipitation is 56.5 inches (143.5 cm) and it is humid throughout the year (Figure 3.60). This site falls in the Cfa category (Humid Subtropical Hot-Summer Climate) according to Köppen's climate classification system. The annual average wind speed is relatively low, 3.7 m/s and the wind speed range is 1.5 m/s. The prevailing wind direction is northwest (321°) (Figure 3.62). Wind directions vary throughout the year; northwesterly wind between April and October and southeasterly for the rest of year (Figure 3.61).

Figure 3.59. Map of St. Joseph dune field. Note that foredune area (ca. 1.04 km^2) is in red box.

Figure 3.60. Average monthly precipitation and temperature in St. Joseph, FL (1979-2008)

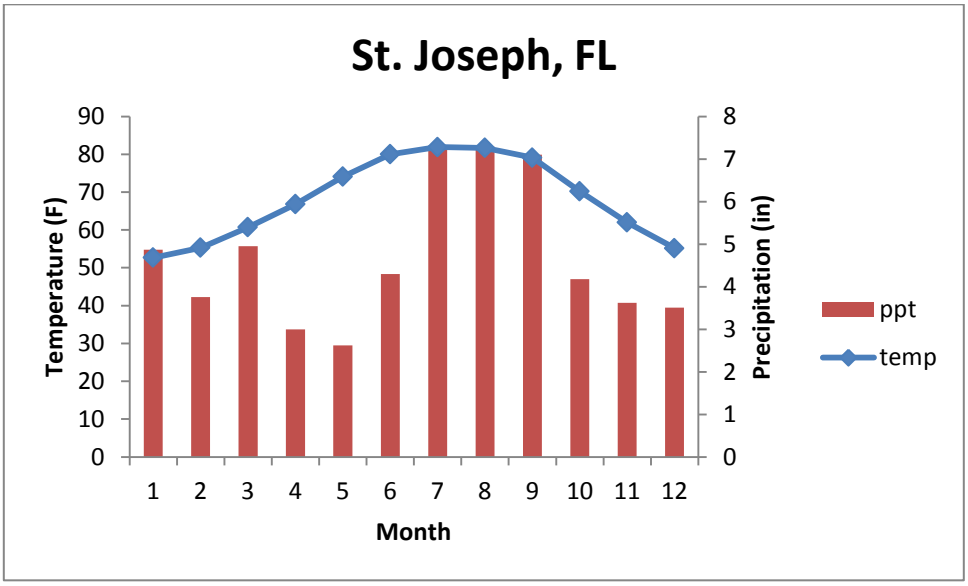

Figure 3.61. Average monthly wind speed and direction in St. Joseph, FL (1979-2008)

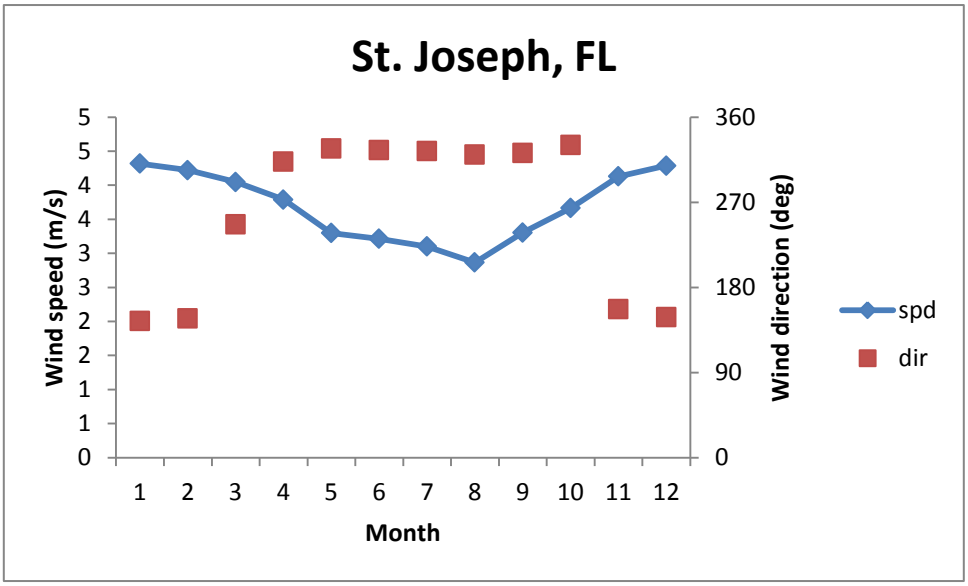

Figure 3.62. Wind rose in St. Joseph, FL (1979-2008)

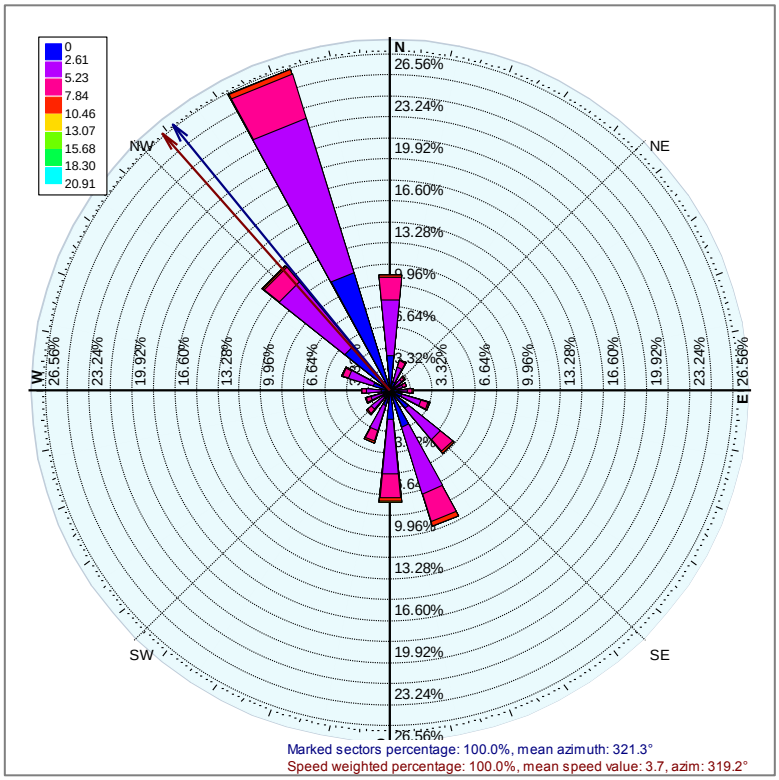

3.4 The Outer Banks

Three dune fields were chosen for this study on or near the Outer Banks barrier island system off the shore of North Carolina: Bear Island dune field, in North Carolina, Hatteras, North Carolina, and False Cape, in Virginia (Figure 3.63). Bear Island is not in the Outer Banks. It is about 50 km west of Cape Lookout, but is in a similar environment. The Outer Banks are 320 km long, extending north from Cape Henry to Cape Lookout. The Outer Banks are transgressive barrier islands with cuspate headlands and they are migrating inland under the combination of waves, currents, and sea-level rise. They

formed 3,000 to 5,000 years ago, are covered with maritime forests of pine and oak, and the sediments are predominantly fine to coarse sand and shells (Inman and Dolan 1989).

Brush fences were built on the barrier islands of the Outer Banks in the early 1930's by the Works Progress Administration – Civilian Conservation Corps (WPA – CCC) in order to encourage sand accumulation to stabilize the islands. This was followed by extensive dune stabilization by the National Park Service in the 1950's (Dolan 1972). The North Carolina coastline is characterized by wide coastal plains and gentle sloping continental shelves on trailing edges which are tectonically stable (Inman and Nordstrom 1971).

According to Bird and Schwartz (1985), the areas along the South Atlantic coast have abundant precipitation, frequent hurricanes at a rate of 3.5 storms per decade, and prevailing winds are offshore except during those storm events.

Figure 3.63. Map of the Outer Banks.

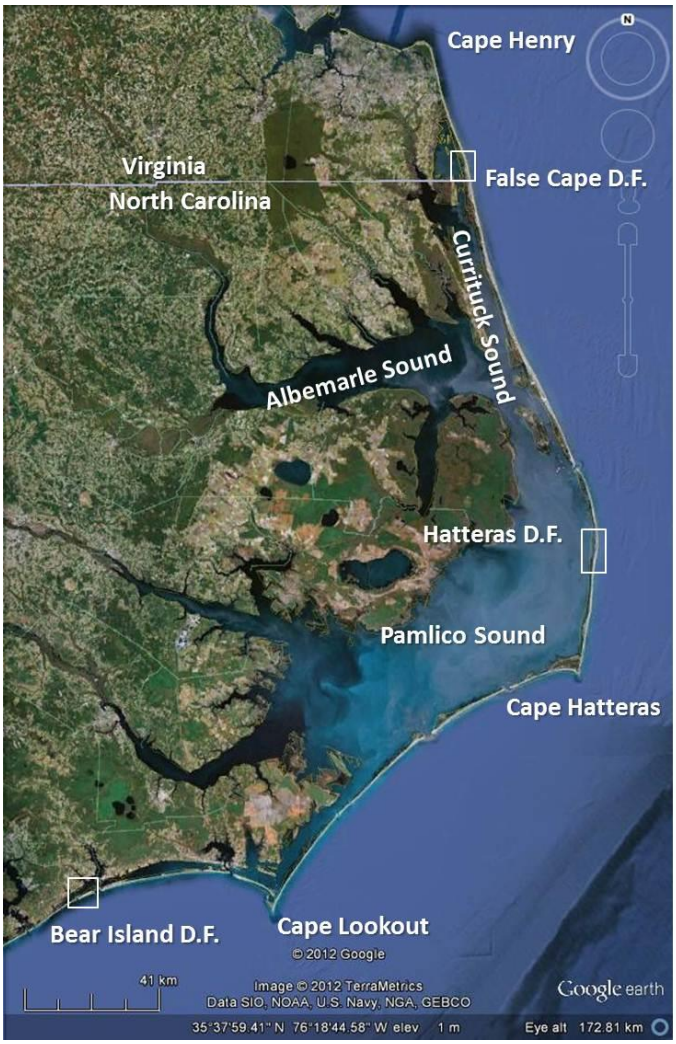

3.4.1 Bear Island

The Bear Island dune field is on a barrier island in North Carolina, located at 34° 38'N and 77° 08' W, on Onslow Bay (Figure 3.64). The island trends northeastward, influenced by a northeasterly gulf stream (Hofmann, Pietrafesa, and Atkinson 1981) and is about 6 km long and 0.4 – 0.6 km wide. Active dunes are 4 – 5 m in height and

stabilized dunes are up to 10 m in height. On the back of the island is a tidal flat and marshes. Bear Island is a thin "perched" barrier that overlays older geologic units and this feature is common in other barrier islands of the southeast coastline of North Carolina (Hofmann, Pietrafesa, and Atkinson 1981; Riggs, Cleary, and Snyder 1995). The dune field is protected within Hammocks Beach State Park, but had been used as a military reservation for target practice during World War II (www.ncparks.gov) and large bare sand hollows can be seen on the stabilized dune (Pilkey et al. 1980; Parks). The entire shoreline was used in this study. The dune field, whether on foredunes or inland, has a number of large sand patches and their shapes are irregular and very complicated.

The annual average temperature is 62.7°F (16.9°C) and the temperature range is 35.5°F (19.5°C) (Table 3.1). The annual total precipitation is 54.1 inches (137.3 cm). The precipitation is consistent throughout the year with slightly more precipitation in July – September (Figure 3.65). This site falls under the Cfa category (Humid Subtropical Hot-Summer Climate) according to Köppen's climate classification system. The annual average wind speed is 5.3 m/s. Winds are faster in winter and the annual range is only 2.6 m/s. Although the annual average wind direction is west-southwest (239°) (Figure 3.67), wind directions vary throughout the year (Figure 3.66). Most winds are offshore, but northwesterly and westerly winds are stronger in the winter. Winds start northwesterly in January, changes to southerly in May, and returns to northerly in winter.

Figure 3.64. Map of Bear Island, NC dune field. Note that foredune area (ca. 0.41 km^2) is in red box.

Figure 3.65. Average monthly precipitation and temperature in Bear Island, NC (1979-2008)

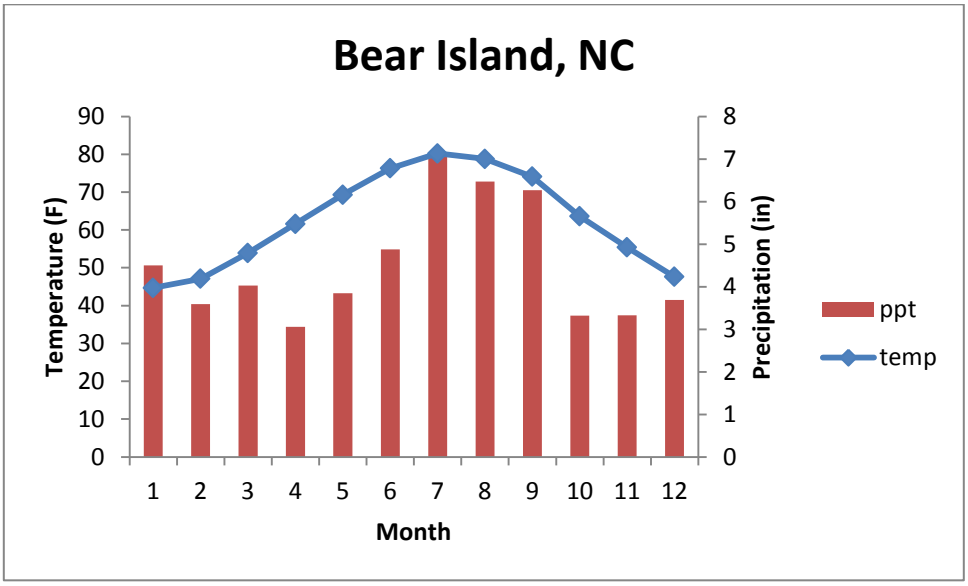

Figure 3.66. Average monthly wind speed and direction in Bear Island, NC (1979-2008)

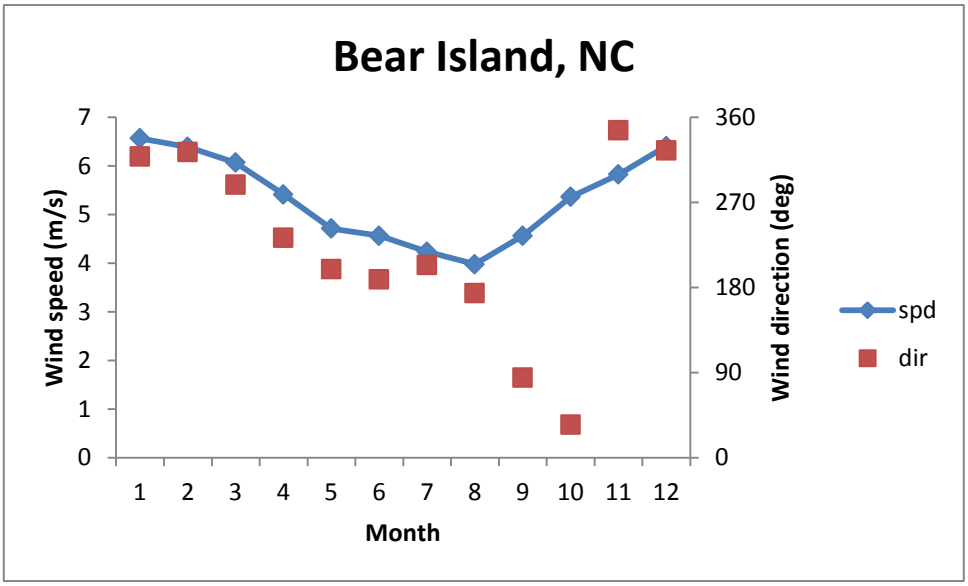

Figure 3.67. Wind rose in Bear Island dune field, NC (1979-2008)

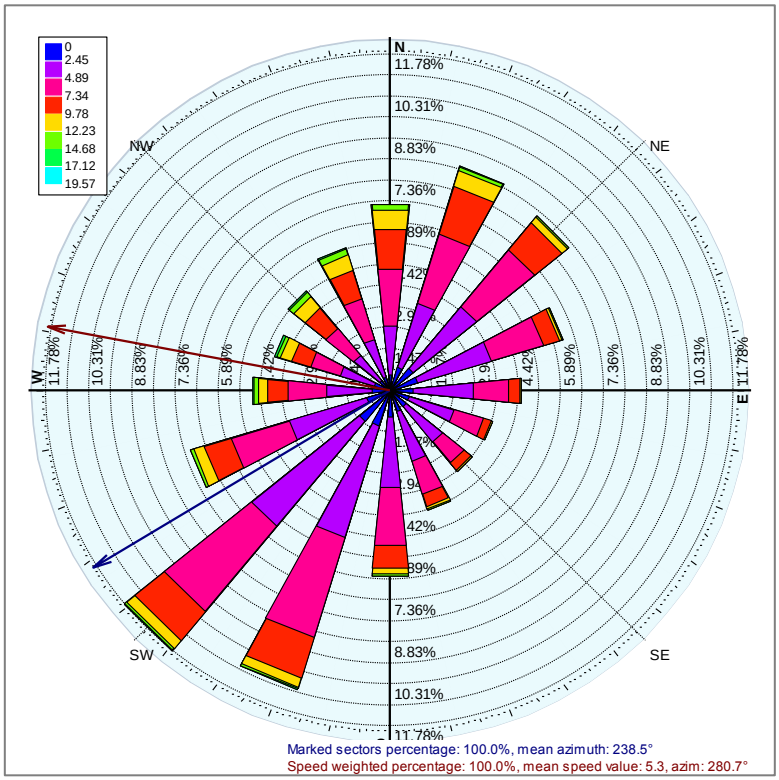

3.4.2 Hatteras

The Hatteras dune field is a portion of the Outer Banks barrier system, protected within Cape Hatteras National Seashore. The site chosen for this study is located at 35° 39'N and 75° 29'W, between Liza Lumps on the south and Cat Island on the north at the northern end of Hatteras Island (Figure 3.68). The shoreline of the study site is straight and northward. The Outer Banks were formed during the Holocene on a "trailing edge" coast, a stable plate margin away from the tectonically active plate, characterized by gentle sloping and broad continental shelves (Inman and Dolan 1989; Inman and Nordstrom 1971). The combination of waves, tidal currents and littoral drift with sea-

level rise formed barrier islands such as Cape Hatteras (Inman and Dolan 1989). Man-made stabilization has been employed on the dunes that were in danger of thinning because of high wave energy and sea-level rise (Dolan, Godfrey, and Odum 1973; Pilkey 1998). American beach grass (*Ammophila breviligulata*) and sea oats (*Uniola paniculata*) are dominant on the foredunes, S*partina patens*, golden rod (*solidago*) on flat areas such as washovers, and *Juniperus virginana* and *Quercus virginiana* on the inland areas (Dolan, Godfrey, and Odum 1973). The grain size is between 0.2 and 0.3 mm (Inman and Dolan 1989).

The total length of the Hatteras Island is approximately 60 km from the Oregon inlet to Hatteras Bight. This barrier island is relatively narrow and most of it is less than 1 km in width. The dune field used in this study is 5.3 km long, extending from Liza Lumps to Cat Island. The foredune areas have many different sizes of sand patches, most of which are small to medium and are of a complex shape. In the middle of the dune field there is a road (No. 12) parallel to the shoreline and there are several boardwalks for access to the beach.

The annual average temperature is 62.8°F (16.9°C) and the temperature range is 33.1°F (18.2°C) (Table 3.1). The annual total precipitation is 57.8 inches (146.7 cm). Precipitation is consistent throughout the year (Figure 3.69) and this site falls under the Cfa category (Humid Subtropical Hot-Summer Climate) according to Köppen's climate classification system. The annual average wind speed is 5.3 m/s but the range is 2.9 m/s. Winds are faster in winter and the annual average wind direction is west (261°) (Figure 3.71). Winds are northwesterly in January, change to southwesterly in summer, and end

up westerly in October (Figure 3.70). Throughout the year, offshore winds are predominant.

Figure 3.68. Map of Hatteras dune field. Note that foredune area (ca. 0.54 km2) is in red box.

Figure 3.69. Average monthly precipitation and temperature in Hatteras, NC (1979-2008)

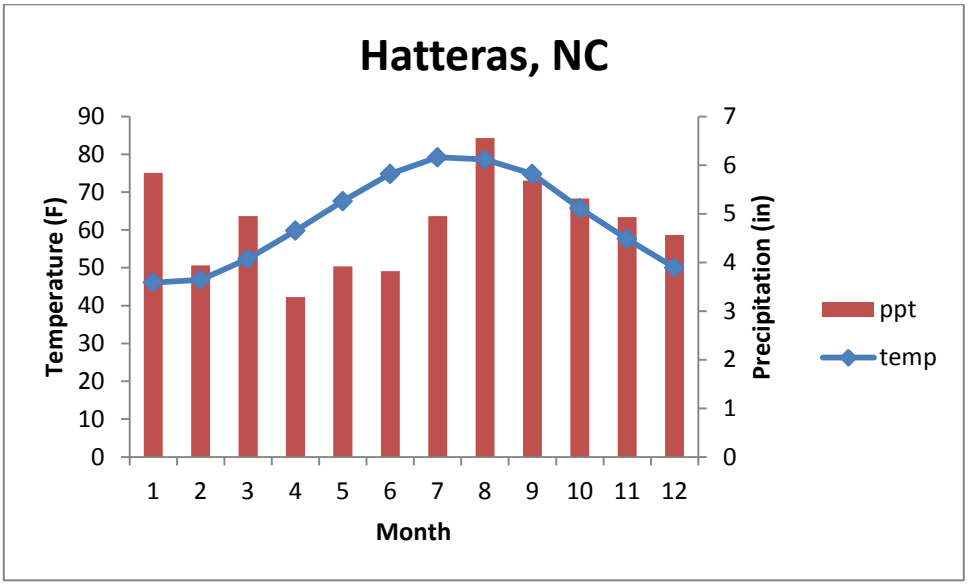

Figure 3.70. Average monthly wind speed and direction in Hatteras, NC (1979-2008)

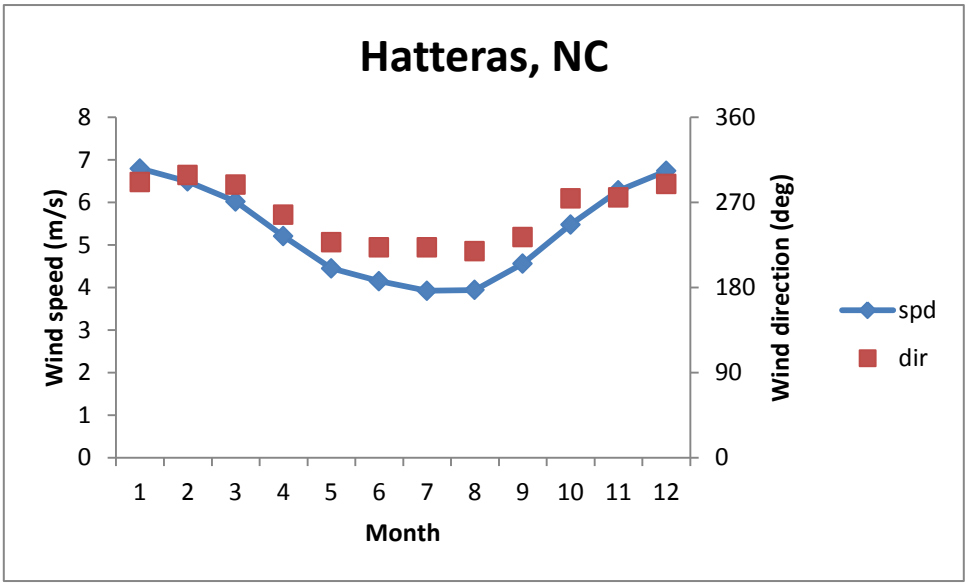

Figure 3.71. Wind rose in Hatteras dune field, NC (1979-2008)

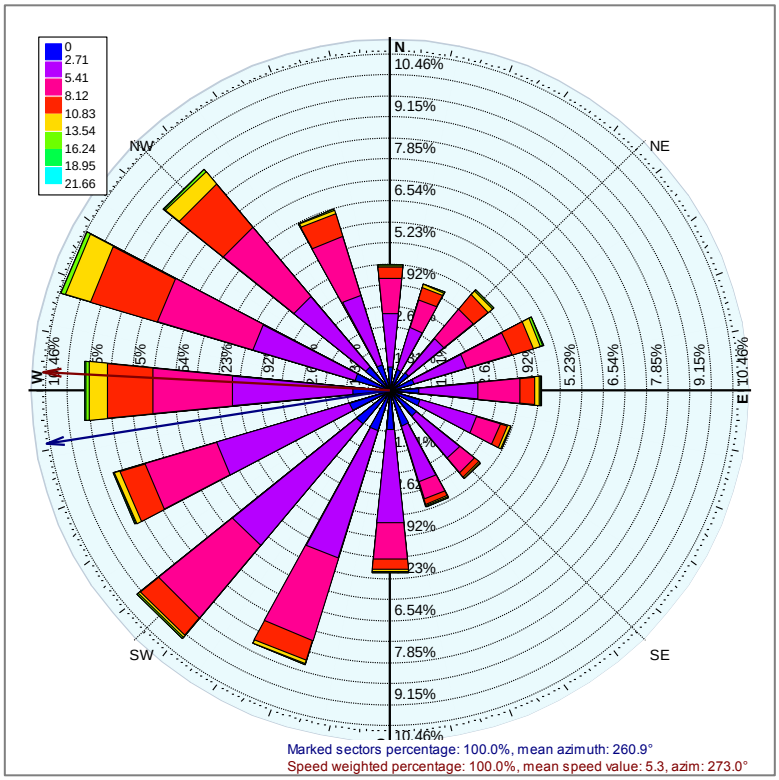

3.4.3 False Cape

The False Cape dune field is on a barrier spit, part of Virginia's Outer Banks and protected within False Cape State Park. The barrier spit is about 20 km long from the northern end to the Virginia/North Carolina border on the south and it is backed by the Back Bay of the Currituck Sound. The dune field chosen for this study is 6 km long, extending from the North Carolina and Virginia border to the north. It is 1.0 - 3.0 km wide and the shoreline is straight, trending northwestward (Figure 3.72). According to Hennigar (1977), a sand fencing project was initiated in this area in the 1930's and continued until 1972. Many homes were built along the shoreline just behind the

foredune in the 1940's and 1950's, but during the 1960's the Commonwealth of Virginia began purchasing the land to build a state park and expand the sand fencing project. Prior to the introduction of sand fences, the False Cape dune field was covered by a sand sheet. Sand hills, or "medoñas," that were formed due to extensive sand fencing and the seaward expansion of the maritime forest later developed into large parabolic dunes.

The foredune area has many sand patches associated with blowouts and parabolic dunes. The parabolic dunes are stabilized by forest and are elongated to the south, parallel to the shoreline. Those sand patches associated with the parabolic dunes are connected and merge with one another so that the sand patches appear very complicated. Except for some buildings along the bay shore and roads in the middle of the dune field, other human disturbances are not found. According to the state park (www.dcr.virginia.gov), vehicular access is prohibited, because the south end of the park is a wildlife refuge.

The annual average temperature is 60.1°F (15.5°C) and the temperature range is 37.7°F (20.7°C) (Table 3.1). The annual total precipitation is 46 inches (116.8 cm). Precipitation is consistent throughout the year (Figure 3.73) and this site falls under the Cfa category (Humid Subtropical Hot-Summer Climate) according to Köppen's climate classification system. The annual average wind speed is 4.3 m/s and the range is 1.7 m/s. Winds are faster in winter (Figure 3.74). Average wind direction is north-northwest (341°) (Figure 3.75). All monthly average wind directions are offshore. Winds are south-southeasterly in winter and becomes northwesterly or northerly in summer.

Figure 3.72. Map of False Cape, VA. Note that foredune area (ca. 0.64 km^2) is in red box.

Figure 3.73. Average monthly precipitation and temperature in False Cape, VA (1979-2008)

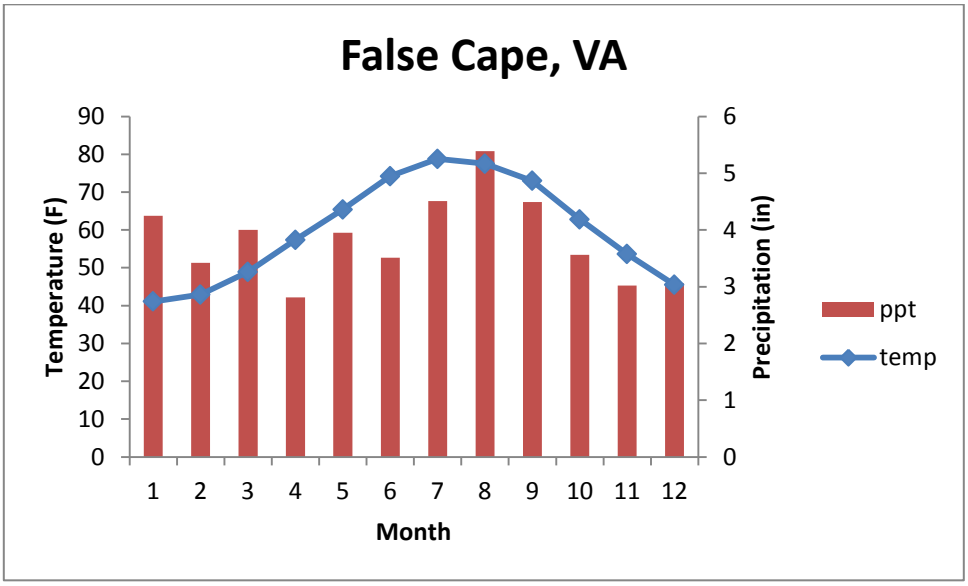

Figure 3.74. Average monthly wind speed and direction in False Cape, VA (1979-2008)

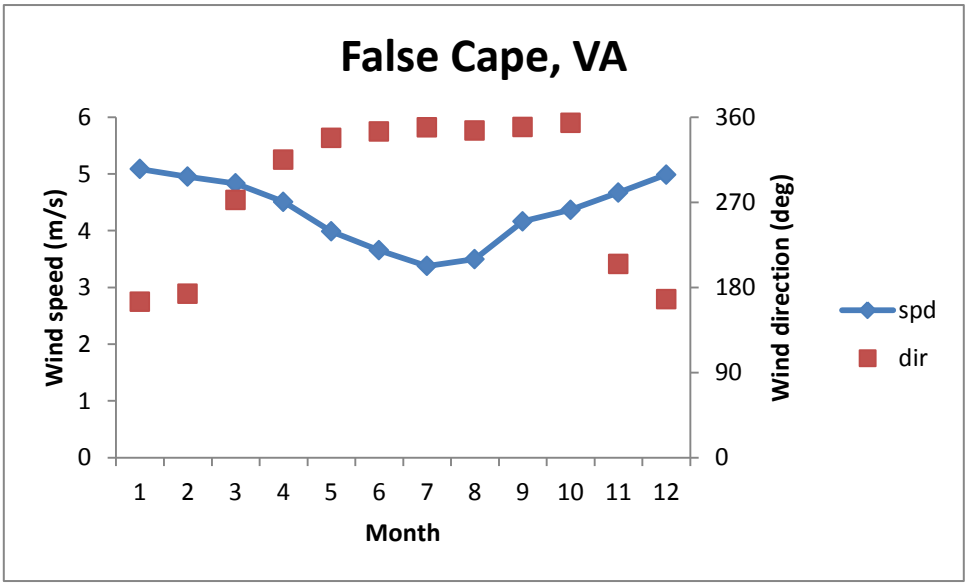

Figure 3.75. Wind rose in False Cape, VA (1979-2008)

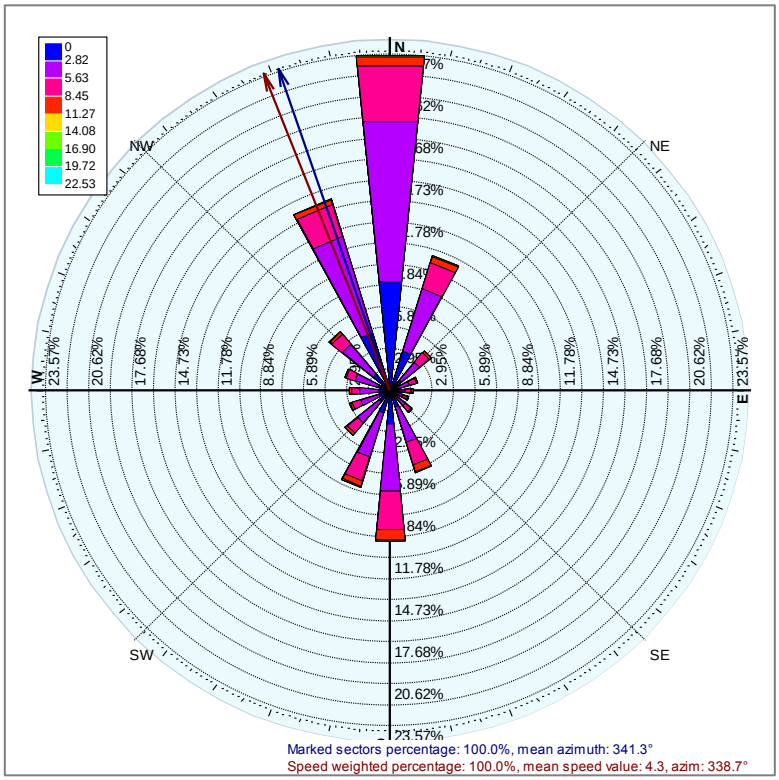

3.5 The Northeastern Atlantic coast

Five dune fields were chosen from the Northeastern Atlantic Coast: Island Beach in New Jersey, Fire Island, New York, Chappaquiddick, Massachusetts, Barnstable, Massachusetts, and Plum Island, Massachusetts (Figure 3.76). The coastline in this region lies on a wide coastal plain/continental shelf and is transgressing rapidly. The shoreline features Holocene deposits such as barrier islands, bays or lagoons, and estuaries. The barrier islands along the coastline are wave-dominated and micro-tidal and the tidal range is 1 m along Fire Island to 3 m along Cape Cod (Bird and Schwartz 1985).

The coast line development is related to the final retreat of the glaciers of the Wisconsinan Stage during which the maximum extent of the ice sheet reached southern Long Island (Fitzgerald and Van Heteren 1999). The New Jersey coast was considered to be in a similar condition to Long Island because of its proximity to the southernmost extension of the ice sheet (Bird and Schwartz 1985). When the glaciers retreated, vast amounts of water were released and sediment was transported to the sea, resulting in sediment deposition because isostatic rebound exceeded eustatic sea-level rise (Jones and Cameron 1977; Fitzgerald and Van Heteren 1999; Roman et al. 2000).

Ammophila breviligulata is the dominant vegetation in the dunes (Godfrey 1977). Precipitation is abundant throughout the year and southeasterly offshore winds are predominant in summer, but northeasterly winds with higher velocity occur during storms in winter, resulting in southward littoral drift. Northeasterly storm winds occur about five to six times a year and hurricanes once every 16 years (Bird and Schwartz 1985).

Figure 3.76 Map of North Atlantic Coast

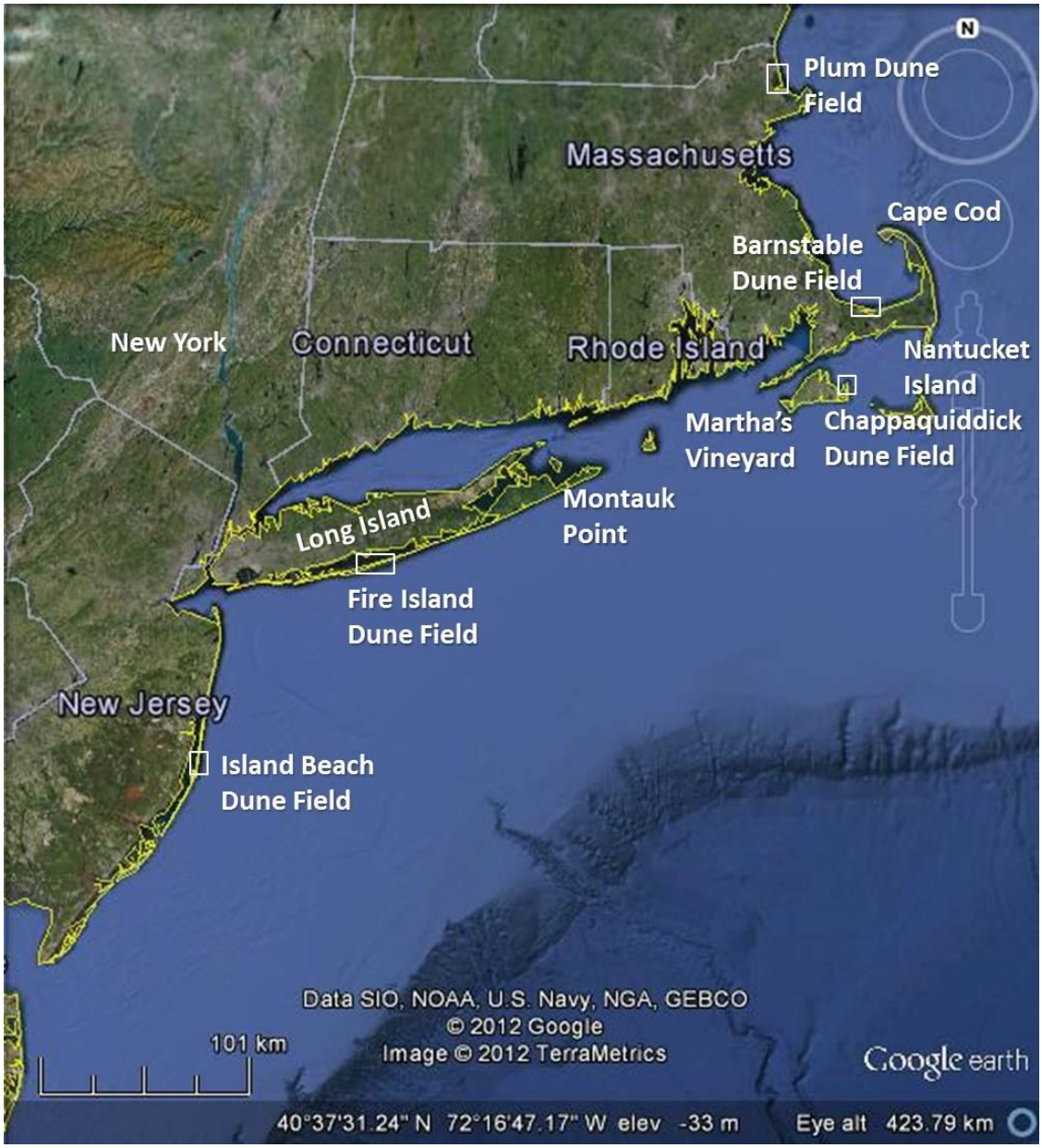

3.5.1 Island Beach

The Island Beach dune field is on a barrier spit and is part of the Island Beach State Park in New Jersey, which extends 15 km from the northern border of the park to

Barnegat Inlet on the south (Figure 3.77). The park was disturbed by human usage such as resorts, walkways, etc., but after the state obtained the land, the dunes were protected and stabilized by sand fences and vegetation planting which was conducted between 1962 and 1977 (Gares 1992; Gares and Nordstrom 1995; Nordstrom et al. 1986).

The site chosen for this study is located at about 39° 49'N and 74° 05'W, and is 3.5 km long, starting from south of the parking lot on the north to the south and is 0.3 – 1.0 km wide (Figure 3.77). The barrier island is thin and low, and it is 4 – 5 m in height. The shoreline is straight and trends southward. A main road (Central Avenue) runs parallel to the shoreline and several parking lots are on the dune field. There are numerous blowouts through which pathways were made, trending southwestward. At the back of the barrier island are marshes and Barnegat Bay. Dominant species are American beachgrass (*Ammophila breviligulata*) on the foredunes, beachheather (*Hudsonia tomemtosa*) on low, protected dunes in the primary and secondary backdune areas, and Reedgrass (*Phragmites communis*) on sandy ridges bordered by the bay shore (Martin 1959). Mean grain size of the undeveloped beach is 0.375 mm (Gares 1987).

The annual average temperature is 53.1°F (11.6°C) and the temperature range is 43.8°F (24.1°C) (Table 3.1). The annual total precipitation is 48.8 inches (124 cm). Precipitation is consistent throughout the year (Figure 3.78). According to Köppen's climate classification system, this site falls under the Dfa category (Humid Continental Hot-Summer Climate), where there is at least one month with a temperature below zero, and it is in January. The annual average wind speed is 5.3 m/s and its range is 2.5 m/s. Winds are faster in winter (Figure 3.79) and the annual average wind direction is west-

southwest (256°) (Figure 3.80). The wind direction varies throughout the year. In November winds are northwesterly, become westerly, and end up northwesterly. Most winds are offshore (easterly or northeasterly) except in September and October, but onshore winds are stronger and associated with storms.

Figure 3.77. Map of Island Beach dune field. Note that foredune area (ca. 0.36 km^2) is in red box.

Figure 3.78. Average monthly precipitation and temperature in Island Beach, NJ (1979-2008)

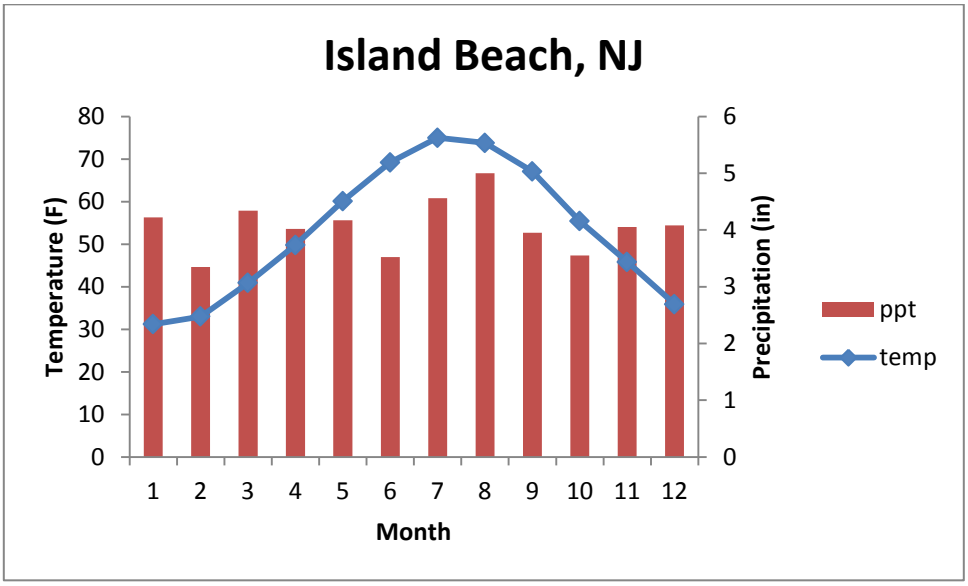

Figure 3.79. Average monthly wind speed and direction in Island Beach, NJ (1979-2008)

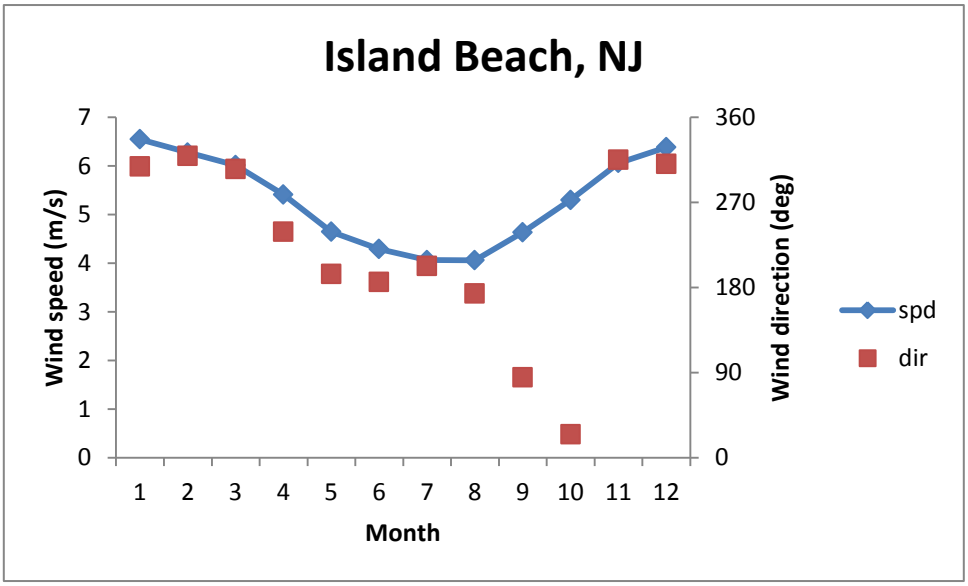

Figure 3.80. Wind rose in Island Beach, NJ (1979-2008)

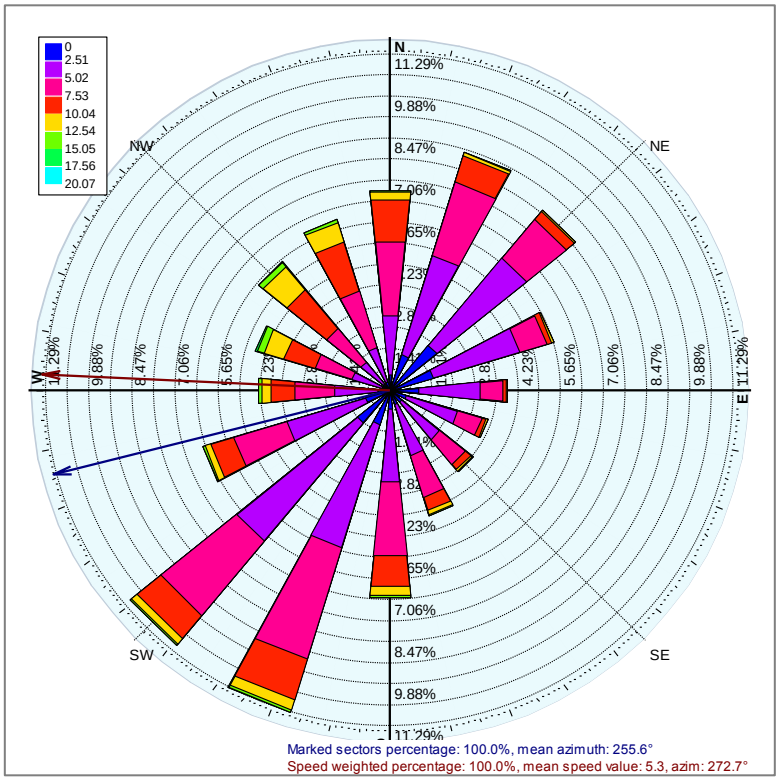

3.5.2 Fire Island

The Fire Island dune field is located at approximately 40° 42'N and 72° 56'W and is in a protected area within on the Fire Island National Seashore (Figure 3.81). The Fire Island National Seashore extends from Fire Island Inlet on the west to Shinnecock Inlet on the east and is about 50 km long. The site chosen for this study is 3.7 km long. The shoreline extends from east to west and is straight. Sediment sources are primarily from westward transport of sediments eroded from an eastern headland (Montauk Point) and from reworked shoreface and inlet scouring. Dune sediment is fine-grained with no shells or pebbles (Leatherman 1985). The average tidal range at Fire Island Inlet is 1.3 m

(Leatherman 1985). Prevailing winds are offshore (southwesterly), and onshore winds (easterly) are not frequent but are stronger with storms (Schwab et al. 2000). Hurricanes and extratropical storms affect this island one or two times per decade (Schwab et al. 2000).

Although Fire Island is a National Seashore, it is extensively developed for recreation. The area selected for this study is relatively undeveloped with no buildings or paved roads. A large road running parallel to the shoreline and many other access roads and pathways branching off from it are numerous on the dunes and such disturbances are probably associated with off-road vehicle activities.

The annual average temperature is 52.4°F (11.2°C) and the temperature range is 43.7°F (24.0°C) (Table 3.1). The annual total precipitation is 46.5 inches (118.2 cm). Precipitation is consistent throughout the year (Figure 3.82). This site falls in the category Dfa (Humid Continental Hot-Summer Climate) according to Köppen's climate classification system. The annual average wind speed is 4.4 m/s and its range is 1.8 m/s. Winds are faster in the winter and the annual average wind direction is west (262°) (Figure 3.84). The wind direction varies throughout the year and the pattern is almost the same as at Island Beach, New Jersey (Figure 3.83). Southeasterly onshore winds occur between May and August.

Figure 3.81. Map of Fire Island dune field. Note that foredune area (ca. 0.37 km^2) is in red box.

Figure 3.82. Average monthly precipitation and temperature in Fire Island, NY (1979-2008)

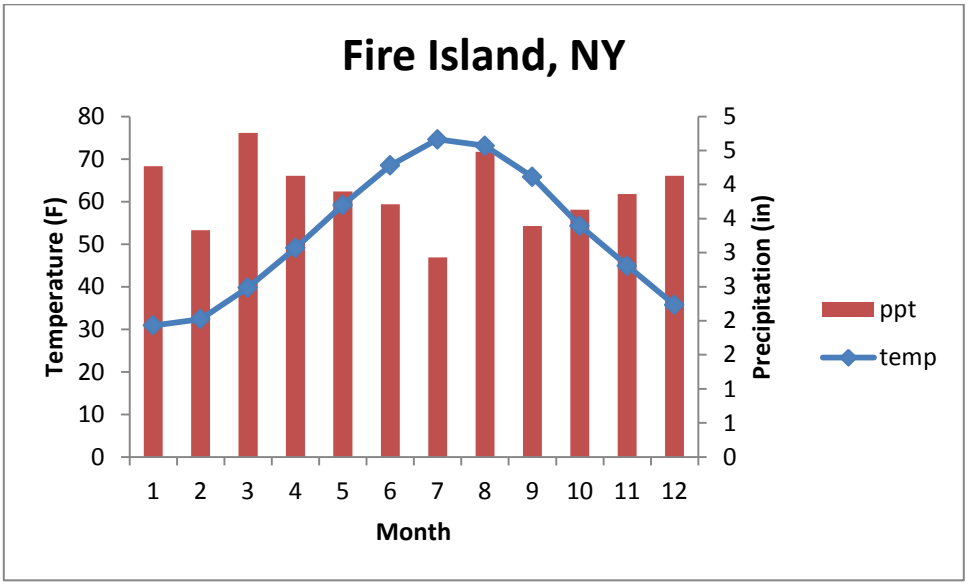

Figure 3.83. Average monthly wind speed and direction in Fire Island, NY (1979-2008)

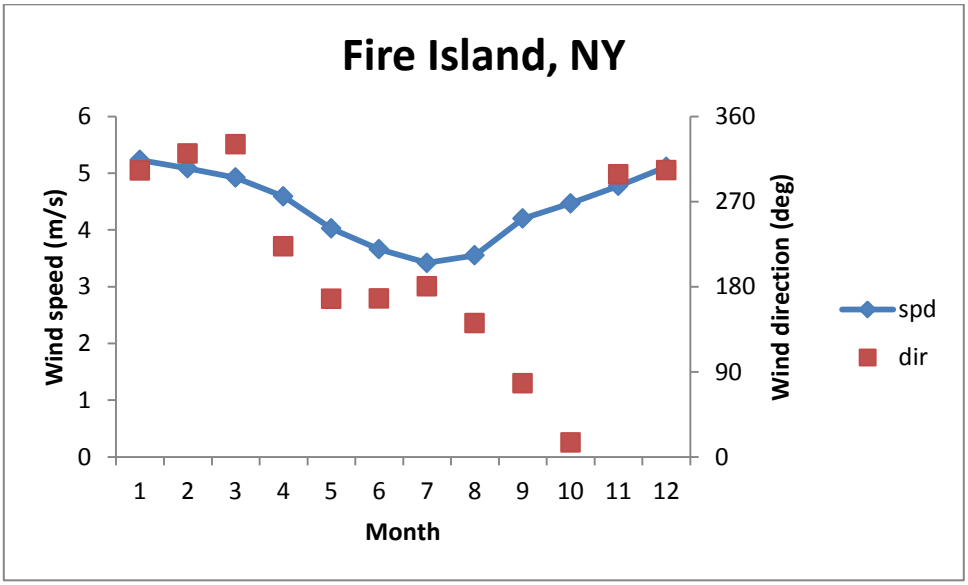

Figure 3.84. Wind rose in Fire Island, NY (1979-2008)

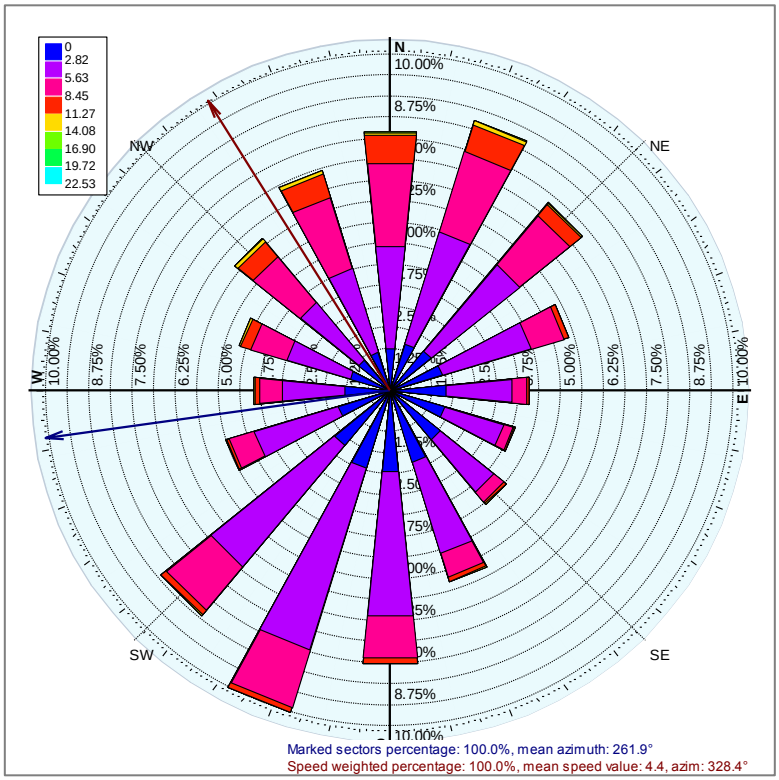

3.5.3 Chappaquiddick

The Chappaquiddick dune field is on a barrier spit of Chappaquiddick Island, part of the larger island of Martha's Vineyard. It is backed by Cape Poge Bay, and is located at approximately 41° 23'N and 70° 26'W (Figure 3.85). Historically this island was intensively utilized by humans. According to Capece (2001), this island had long been inhabited by native Americans (Wampanoag) prior to European settlement, and was affected by human disturbances such as mowing, clearing, grazing and burning. The Indians used this area for hunting and agriculture, mostly by burning, and European

settlers have used it for grazing livestock since the 1600's. Most of the Cape Poge Bay area was donated to the Trustee of Reservation by the mid-1900's.

The site chosen for this study is about 2.5 km long, extending from southeastern Cape Poge Bay to the north, and is 0.1 – 0.3 km wide. The shoreline is almost straight, facing east, formed by a southward longshore drift and developed from a terminal moraine of Wisconsin glaciation (Bird and Schwartz 1985). The average frequency of severe hurricanes is once every five years (Arpin 1970).

The study site is not within a protected area. Several of unpaved roads run along the shoreline and some access roads are on the dune field. Numerous irregular and complex sand patches connected with one another are on the foredune area.

The annual average temperature is 50.5°F (10.2°C) and the temperature range is 39.8°F (21.9°C) (Table 3.1). The annual total precipitation is 46.1 inches (117 cm). Precipitation is consistent throughout the year (Figure 3.866). This site falls in the Dfb category (Humid Continental Mild-Summer Climate) according to Köppen's climate classification system. The annual average wind speed is 4.9 m/s and its range is 2 m/s. Winds are faster in winter and the annual average wind direction is west (267°) (Figure 3.88), fluctuating between southwesterly in summer and northwesterly in winter (Figure 3.87).

Figure 3.85. Map of Chappaquiddick dune field. Note that foredune area (ca. 0.24 km^2) is in red box.

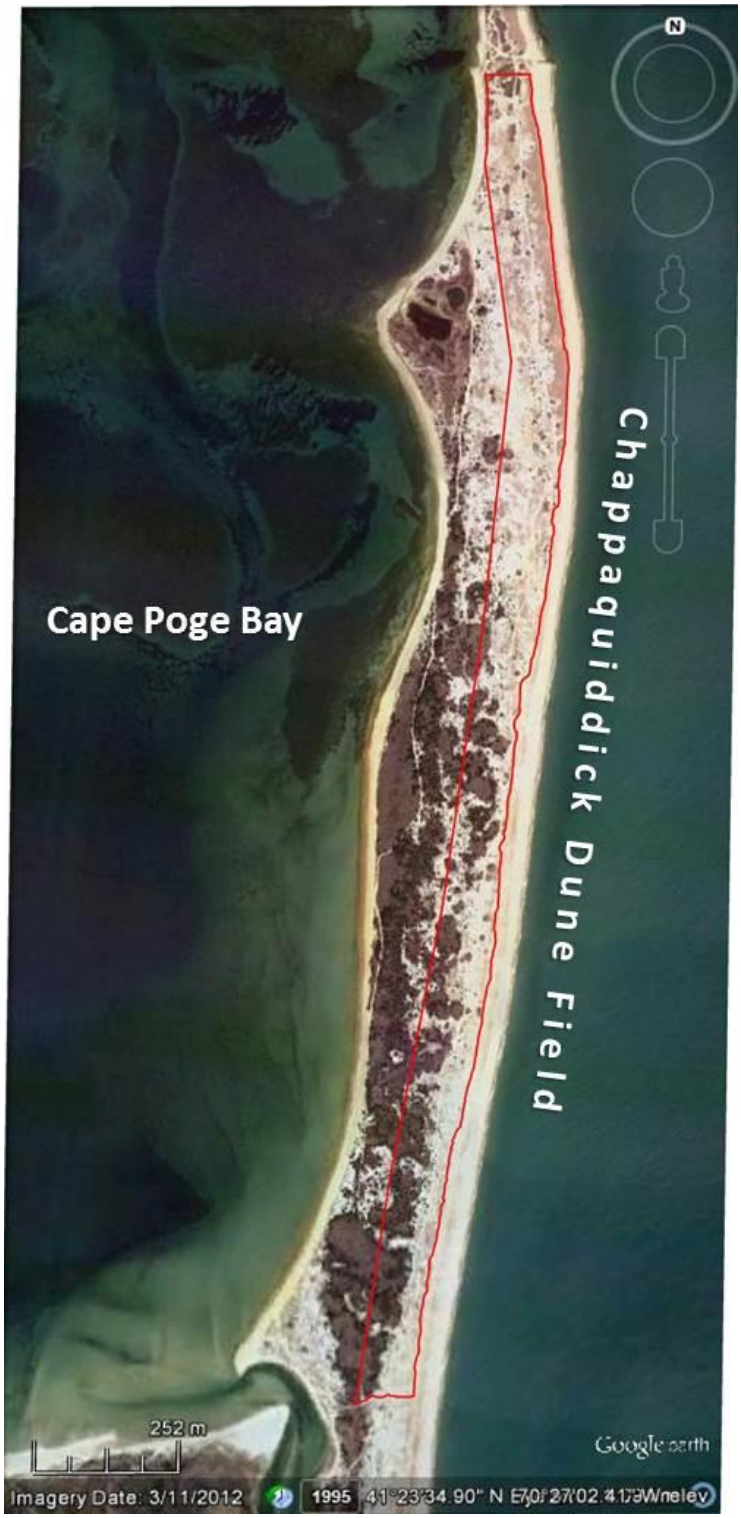

Figure 3.86. Average monthly precipitation and temperature in Chappaquiddick, MA (1979-2008)

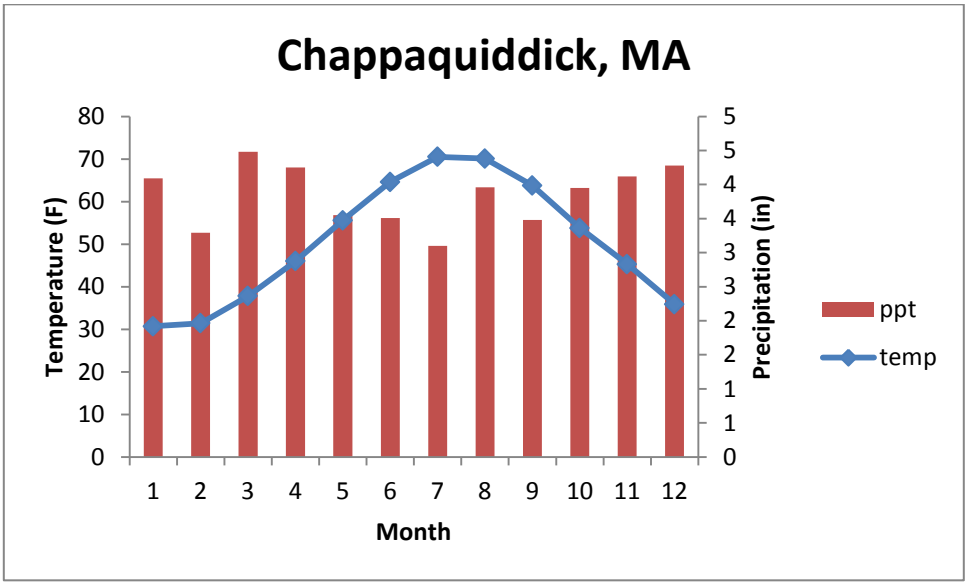

Figure 3.87. Average monthly wind speed and direction in Chappaquiddick, MA (1979-2008)

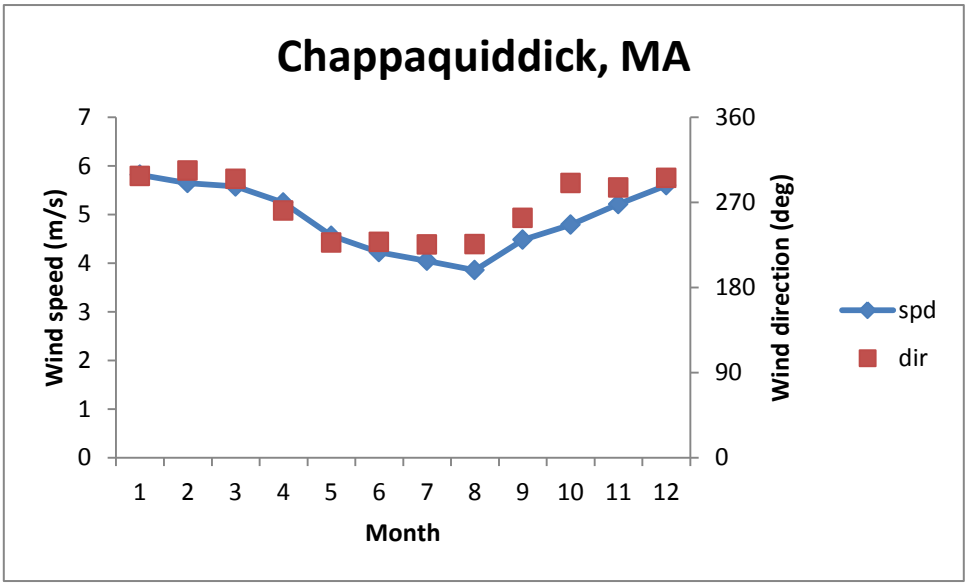

Figure 3.88. Wind rose in Chappaquiddick, MA (1979-2008)

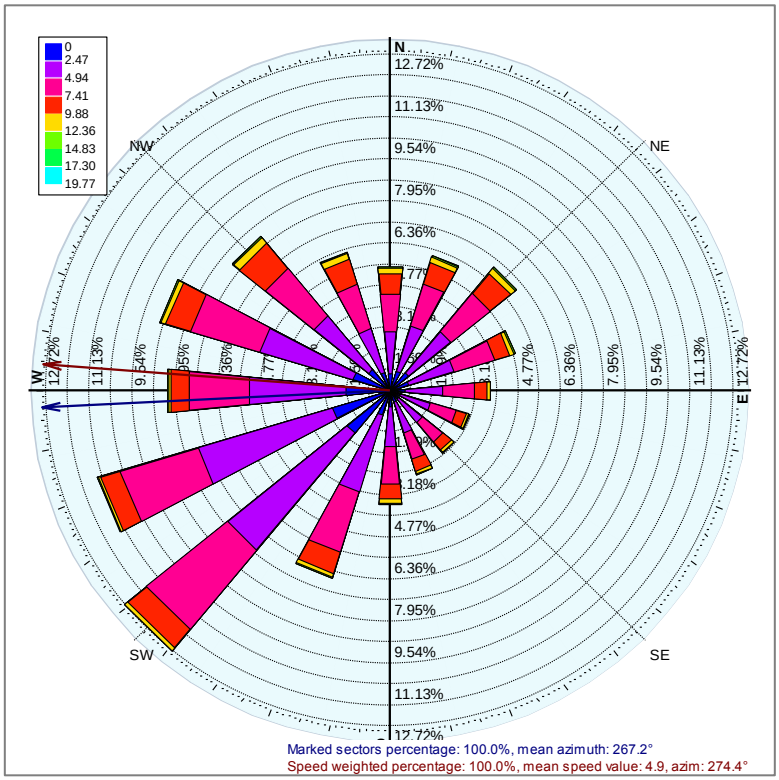

3.5.4 Barnstable

The Barnstable (Sandy Neck) dune field is on an eastward barrier spit (Figure 3.89), about 10 km long and 07 – 1.3 km wide, located at approximately 41° 44'N and 70° 21'W, and it is not within a protected area. This area is a meso-tidal (mean tidal range 2.9 m), mixed energy barrier spit, developed on the southern shore of Cape Cod, Massachusetts (Van Heteren and Van de Plassche 1997). Dominant vegetation species are American beachgrass (*Ammophila breviligulata)* on the foredune, maritime forest of pitch pine (*Pinus rigida)* inland, and the dune field has been strictly protected from off road vehicles, pedestrians, and sports fishermen since the early 1980's (Shumway 1996).

The site chosen for this study is about 7.5 km long, and excludes the easternmost margin of the spit. There is a main road and access roads running along the edge of the back dune. Off-road vehicles are allowed only on the beach. The entire dune field is covered by a bare sand area with vegetation clumps. Most bare sand areas consist of numerous blowouts and parabolic dunes, which tend toward the east or southeast.

The annual average temperature is 49.5°F (9.6°C) and the temperature range is 41.3°F (22.7°C) (Table 3.1). The annual total precipitation is 43 inches (109.3 cm). Precipitation is consistent throughout the year (Figure 3.90). This site falls in the Dfb category (Humid Continental Mild-Summer Climate) according to Köppen's climate classification system. The annual average wind speed is 5.8 m/s and its range is 2.8 m/s. Winds are faster in winter (Figure 3.91) and the annual average wind direction is west (262°) (Figure 3.92) with a seasonal pattern almost the same as Chappaquiddick, Massachusetts. Onshore winds occur only in summer.

Figure 3.89. Map of Barnstable dune field, MA. Note that foredune area (ca. 0.72 km^2) is in red box.

Figure 3.90. Average monthly precipitation and temperature in Barnstable, MA (1979-2008)

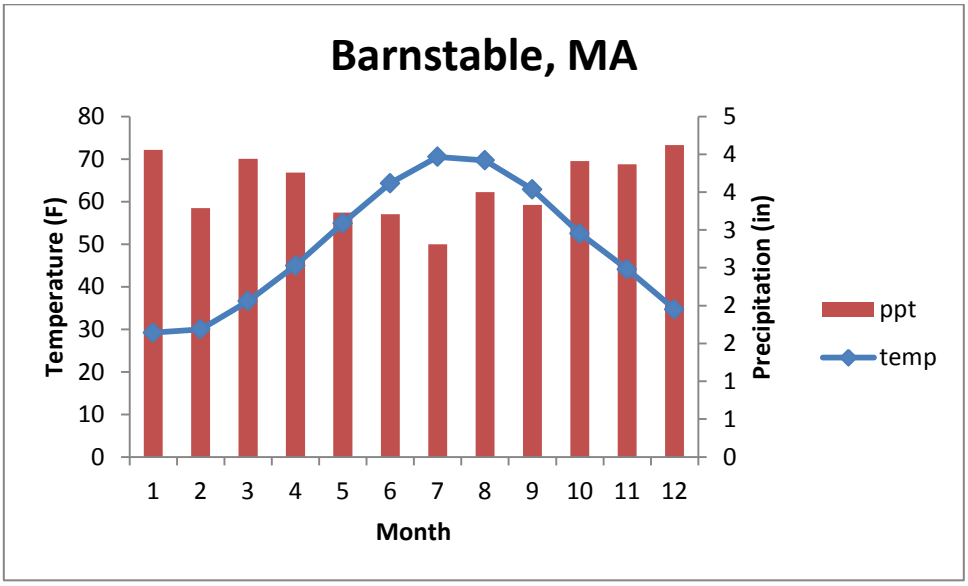

Figure 3.91. Average monthly wind speed and direction in Barnstable, MA (1979-2008)

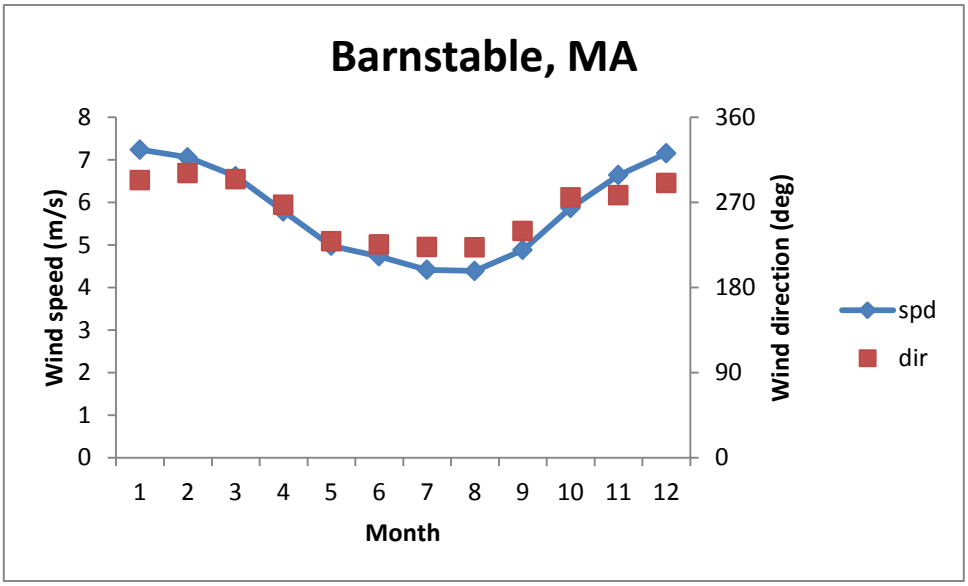

Figure 3.92. Sand rose of Barnstable, MA (1979-2008)

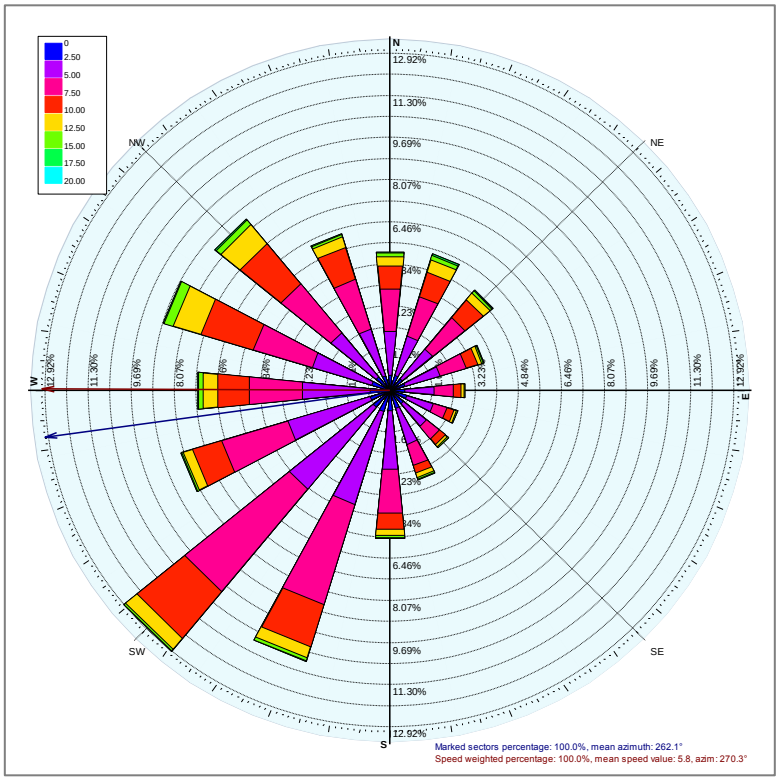

3.5.5 Plum

The Plum dune field is a barrier island trending southeastward, located at approximately 42° 44'N and 70° 47'W (Figure 3.93). It is about 13 km long and 0.3 – 1.5 km wide, and has a meso-tidal range of 2.9 m (Vallino and Hopkinson 1998). The island is protected within the Parker River National Wildlife Refuge, which was established in 1942 (www.fws.gov). Since the late 1960's vehicles have not been allowed on the dunes (McDonnell 1981). The island was developed by two primary sources of sediment: glacial deposits from the estuary and coastal plain, and reworked sediment from cliffed headlands, both of which were transported by predominantly

southward littoral drift (McIntire and Morgan 1962). The prevailing westerly wind direction is offshore, but southerly (including southeasterly) high velocity winds associated with storms caused by frequent low pressure cells result in extensive overwash and inland sediment transport make this dune field subject to erosion (Jones and Cameron 1977; McIntire and Morgan 1962).

The site chosen for this study is 9.6 km long, excluding a developed area in the north. A paved road runs along the edge of the back dune and there are some boardwalks for beach access and paths on the dunes. The foredune line is clearly visible due to the vegetation line, but there are many blowouts and bare sand areas on both the foredune and inland. Dominant vegetation species are American beachgrass (*Ammophila breviligulata*), beach pea (*Lathyrus japonicas*), and dusty miller (*Artemisia stellariana*) on the foredune area, and Woolly beachheather (*Hudsonia tomemtosa)* inland (McDonnell 1981). The mean grain size in this area is 0.49 mm (Jones and Cameron 1976).

The annual average temperature is 47.4°F (8.5°C) and the temperature range is 43.7°F (24°C) (Table 3.1). The annual total precipitation is 46.9 inches (119.1 cm). Precipitation is consistent throughout the year (Figure 3.94). This site falls in the Dfb category (Humid Continental Mild-Summer Climate) according to Köppen's climate classification system (Table 3.1). The average wind speed is 5.2 m/s and with a range of 1.3 m/s. Winds are slightly faster in winter, but are almost consistent throughout the year (Figure 3.95). September has the lowest velocity at 4.4 m/s. The annual average wind

direction is east-southeast (120°) (Figure 3.96), which is parallel to the shoreline, fluctuating between east and south.

Figure 3.93. Map of Plum dune field, MA. Note that foredune area (ca. 0.95 km^2) is in red box.

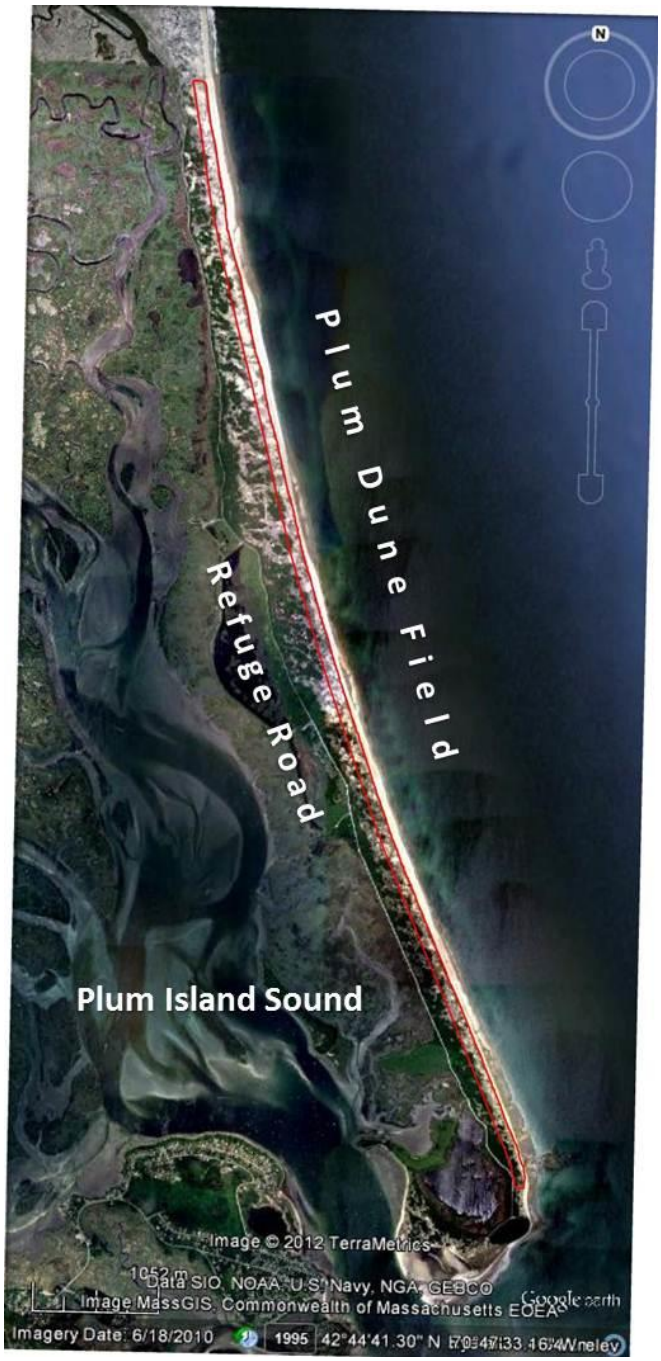

Figure 3.94. Average monthly precipitation and temperature in Plum, MA (1979-2008)

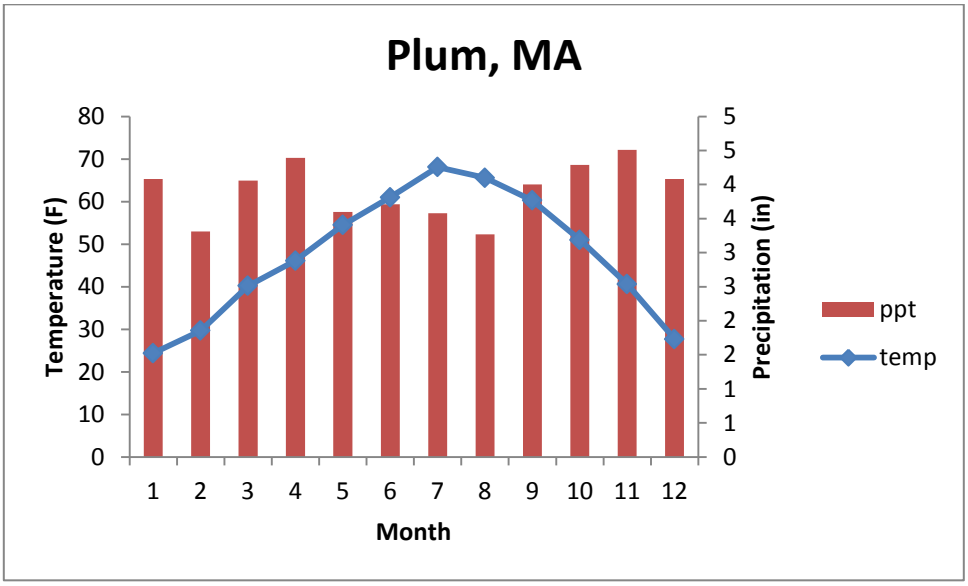

Figure 3.95. Average monthly wind speed and direction in Plum, MA (1979-2008)

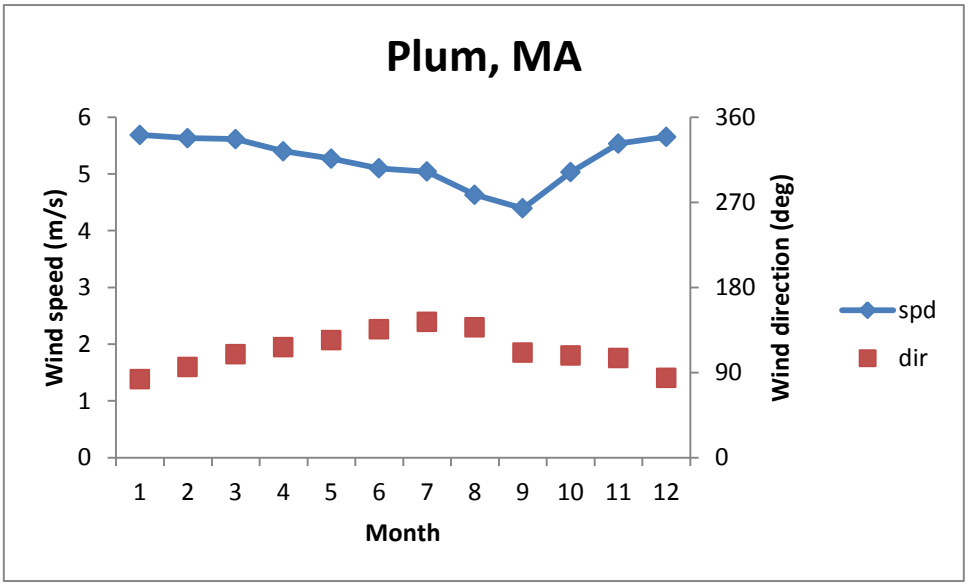

Figure 3.96. Wind rose in Plum, MA (1979-2008)

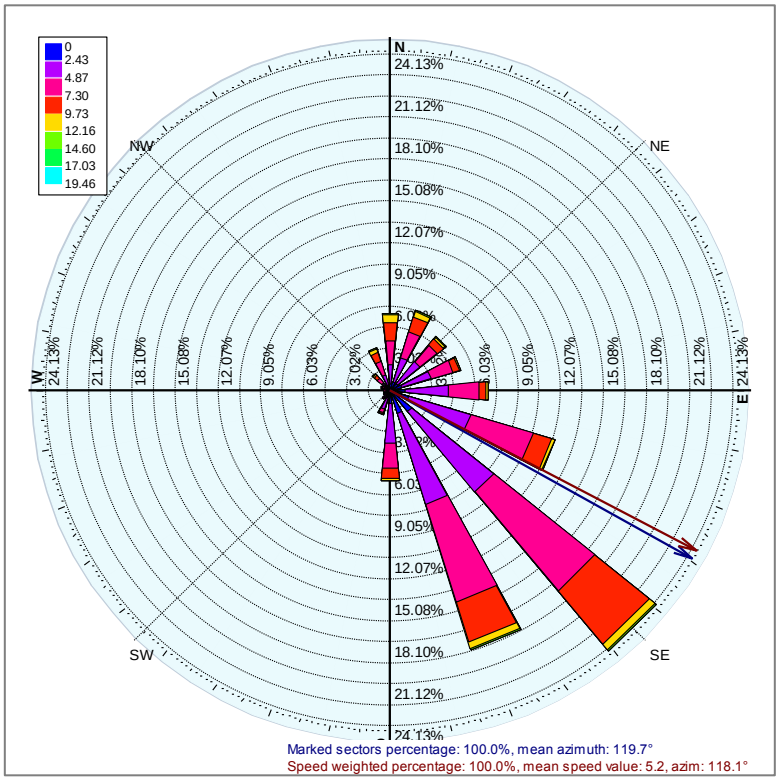

4 METHODOLOGY

4.1 Data sources

4.1.1 Aerial photographs

The aerial photographs used in this study were downloaded from the National Map Seamless Server (http://seamless.usgs.gov). The photographs are seamless orthoimages which are geospatially-accurate digital maps corrected by removing any of the distortions caused by the tilt of the camera or topography of the land. Two types of orthoimagery from the National Map Seamless Server were used for this study: Digital Orthophoto Quadrangles (DOQ) and U.S. Department of Agriculture (USDA) National Agriculture Imagery Program (NAIP). DOQs are produced by the U.S. Geological Survey (USGS) as gray-scale, natural color, or color-infrared images with a 1-meter ground resolution and cover an area measuring 3.75-minutes latitude by 3.75-minutes longitude or 7.5-minutes latitude by 7.5-minutes longitude. The NAIP acquires imagery during the agricultural peak growing seasons for the conterminous United States with a resolution ranging from 0.5 m to 1 m. This study uses either DOQ or NAIP images. The geographic coordinate system of both image types is UTM (Universal Transverse Mercator) in projection and NAD (North American Datum) 83 in horizontal datum.

Each study site isrepresented by two aerial photographs taken at different times so that the stability of the vegetation patterns through time could be assessed. This also reduces the chance of assessing a foredune system that is not in a characteristic configuration because of short-term conditions, such as severe foredune erosion caused

by storm waves. The years of the old image sets range from 1988 to 1999 and the new sets from 2005 to 2009. Details of the images for this study are in Table 4.1.

Table 4.1. Information on aerial photographs. B/W: black and white, N: Natural color, I: infrared color. The order of sites is from the northwest coast through the Gulf of Mexico to the northeast coast.

Site	Time (month/year)		Resolution (m)		Color	
	Old	New	Old	New	Old	New
Manzanita, OR	4/1998	6/2005	1.0	0.5	B/W	N
Netarts, OR	8/1994	6/2009	1.0	1.0	B/W	N
Nestucca, OR	5/1994	6/2005	1.0	0.5	B/W	N
Coos Bay, OR	5/1994	6/2005	1.0	0.5	B/W	N
St. George, CA	8/1988	6/2005	1.0	0.5	I	N
Eureka, CA	4/1989	6/2009	1.0	1.0	I	N
Pt. Arena, CA	9/1989	6/2009	1.0	1.0	B/W	N
Tomales, CA	7/1993	6/2009	1.0	1.0	B/W	N
Marina, CA	6/1993	6/2009	1.0	1.0	B/W	N
Morro, CA	5/1994	6/2009	1.0	1.0	B/W	N
St. Maria, CA	9/1994	6/2009	1.0	1.0	B/W	N
Vandenberg, CA	9/1994	7/2009	1.0	1.0	B/W	N
Padre Island, TX	1/1995	10/2008	1.0	1.0	N	N
St. Joseph, FL	1/1994	3/2006	1.0	1.0	I	N
Bear Island, NC	1/1998	5/2009	1.0	1.0	I	N
Hatteras, NC	2/1998	8/2009	1.0	1.0	I	N
False Cape, VA	3/1994	6/2009	1.0	1.0	I	N
Island Beach, NJ	3/1995	8/2008	1.0	1.0	I	N
Fire Island, NY	4/1994	5/2009	1.0	1.0	I	N
Barnstable, MA	3/1995	7/2008	1.0	1.0	B/W	I
Chappaquiddick, MA	3/1995	7/2008	1.0	0.5	B/W	N
Plum Island, MA	3/1995	7/2008	1.0	1.0	B/W	N

4.1.2 Climate data

Precipitation data and temperature data to calculate the potential evapotranspiration (PET) were downloaded from the PRISM (Parameter-elevation Regressions on Independent Slopes Model) climate mapping system, which is a model that incorporates point data, a digital elevation model, and expert knowledge of complex

climatic extremes, including rain shadows, coastal effects, and temperature inversions (http://www.prism.oregonstate.edu). The resolution of PRISM is 4 km (2.5 arc min). The datasets for the precipitation and temperature are monthly for 30 years (1979-2008). PRISM provides only mean maximum and mean minimum for temperature, so the mean monthly temperature was calculated by averaging the two min and max temperatures for each month.

Wind data (wind speed at 10 m above the surface and its direction) were obtained from the NCEP (National Centers for Environmental Prediction) and the NARR (North American Regional Reanalysis Archive: http://dss.ucar.edu/pub/narr/). The NARR model is NCEP's high resolution (32 km) combined model and assimilated dataset and covers the years 1979 to the near present. NARR data can be usable in spreadsheet programs after they are retrieved by using the GrADS (The Grid Analysis and Display System) program, which is downloadable from the website (http://www. Iges.org/grads/). GrADS is a useful tool for accessing, manipulating, and visualizing earth science data. Among many data file formats, GRIB (GRIdded Binary) data were used in this study. GrADS uses a 5-dimensional data environment: longitude, latitude, vertical level, time, and an optional 5^{th} dimension. The wind data used in this study are every three hours (8 sets on each day: 0-, 3-, 6-, 9-, 12-, 15-, 18-, 21-hour) for 30 years (1979-2008).

4.2 Image analysis

The purpose of the classification process is to categorize all pixels in a digital map into several land cover classes (themes) by classifying each individual pixel based

on spectral information. Two types of classifications are generally used in image processing: unsupervised and supervised classifications and both were used in this study.

Unsupervised classification arranges pixels into distinct clusters based on similar spectral characteristics. Unsupervised classification does not have user-defined classes. The two most commonly used algorithms for unsupervised classification are K-means and ISODATA. Both of these algorithms are interative procedures in which 1) an initial cluster vector is assigned; 2) each pixel is classified to the closest cluster; and 3) the new cluster mean-vectors are calculated based on all the pixels in one cluster (Center). The second and third steps are repeated until a given iteration number is reached. The ISODATA algorithm can be further refined by splitting and merging of clusters based on a certain threshold which can be given by users (Jensen 2000).

A supervised classification clusters pixels into classes corresponding to user-defined training areas, so the knowledge of an area of interest is desirable. Two commonly used algorithms are maximum likelihood and parallelepiped. A maximum likelihood classification calculates the probability of a given pixel belonging to a certain class and each pixel is assigned to a class of the highest probability. The parallelepiped classification defines dimensions based on a standard deviation threshold from the mean of each selected class. If a pixel value lies below the threshold, the pixel is assigned to the class. If two threshold values are set, a pixel between the high threshold and low threshold is assigned to the class. If the pixel value falls in more than one class, the pixel is assigned to the last class matched, and if the pixel does not fall within any classes, the pixel is unclassified (Solutions).

4.2.1 Unsupervised classification

If a site requires more than one image to cover the whole area, the images were mosaicked geographically using ENVI 4.7. Afterwards, a classification technique was used to extract bare sand from the images using ENVI 4.7. All black and white images, because single band images cannot be classified by supervised classification, and some of natural color and infrared color images were classified by unsupervised classification. The results of classification vary with the classification methods; ISODATA or K-means, and the number of classes and iterations (Figure 4.1). The method that showed better results was chosen for each site, after the images were examined.

The best result was selected after the classified image was examined with a different number of classes and iterations, and compared with images of Google Earth™ or those in websites related to the study site. A histogram enhancement technique (Figure 4.2) was also used for some images in order to compare an original image to the classified image to see if sand patches were well classified. The images that resulted from the histogram enhancement, however, were not directly used for classification.

Figure 4.1. Unsupervised classified images. Image (a) is classified by ISODATA with 3 iterations and image (b) is by K-means with 7 classes and 3 iterations.

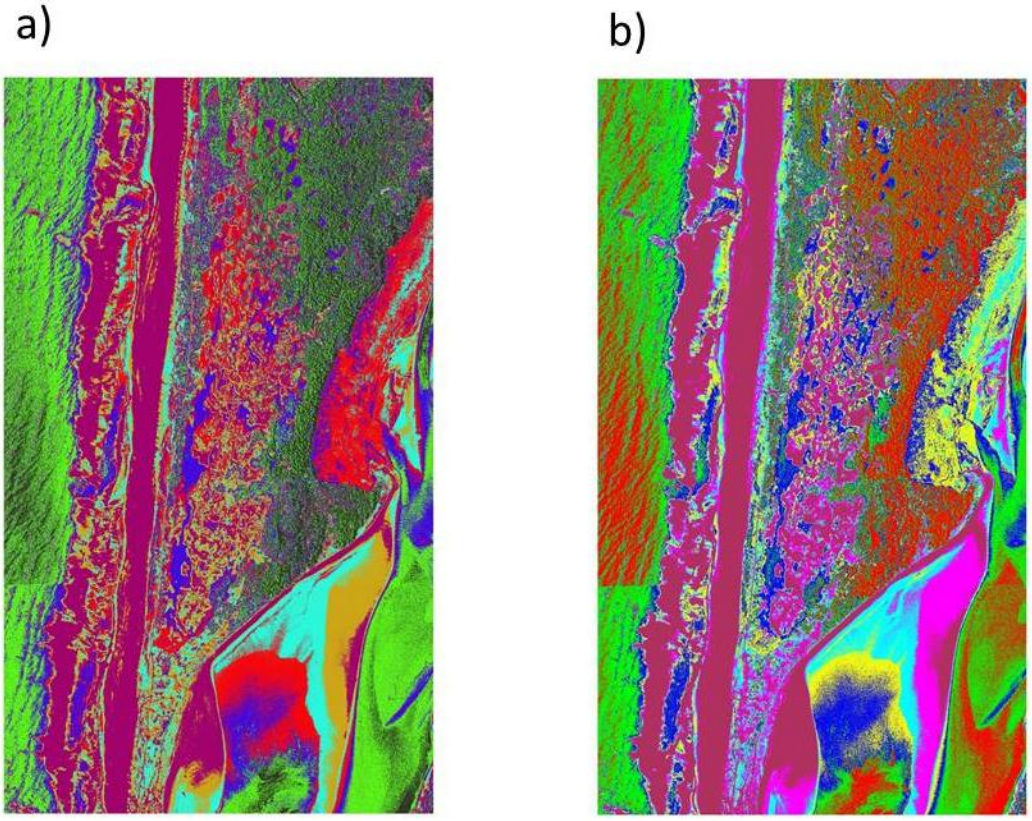

The classified images were converted into ArcView Raster (*.bil) in ENVI and then imported to ArcMap 9.3 (Figure 4.4 b). Because bare sand is the surface of interest in this study, a class (or classes) considered to be sand was reclassified in “sand” and assigned ‘1’ using the Spatial Analyst tools in ArcMap. All the other classes such as water, buildings, vegetation, etc. were reclassified as “others” and assigned ‘0’ (Figure 4.4 c). The reclassified images were converted into GRID in “Reclassify” in “Spatial Analyst” in ArcToolbox. The image in GRID can be used for the calculation of metrics in Fragstats, a computer program to calculate landscape metrics.

Figure 4.2. An example: interactive contrast stretching dialog for histogram enhancement in ENVI 4.7

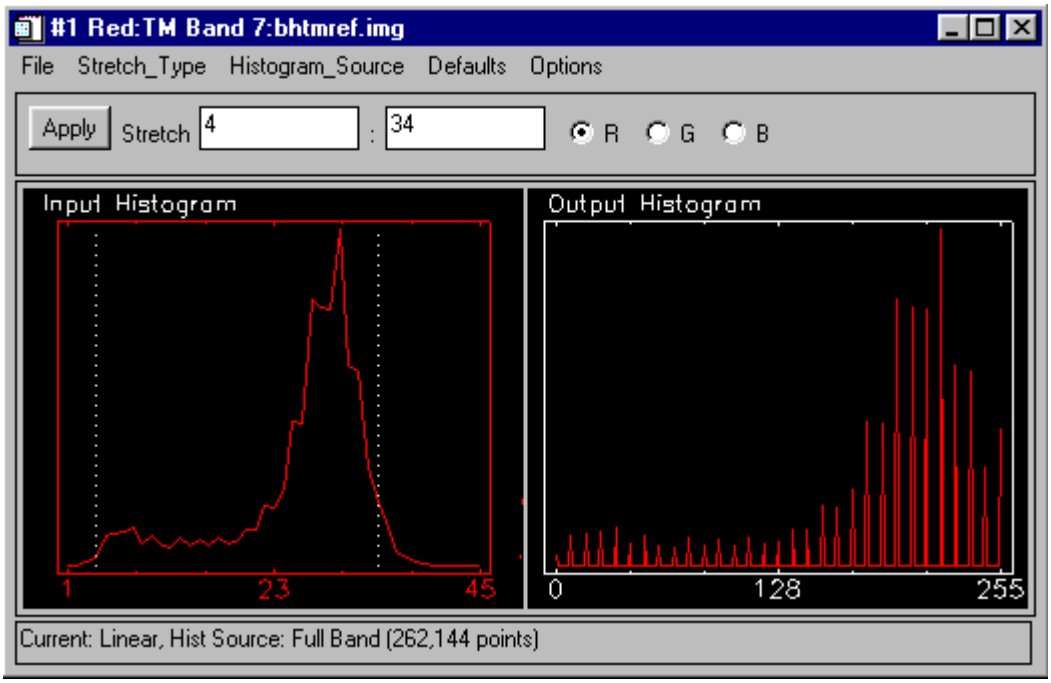

4.2.2 Supervised classification

Software such as ENVI lets you define Regions of Interest (ROIs) as training areas. In ENVI 4.7, I selected Tools > Region of Interest > ROI Tool, then the ROI Tool dialog box appeared. I named each class and drew polygons corresponding to those classes (Figure 4.3). Once I made ROIs, I selected Classification > Supervised > Maximum Likelihood (or Parallelpiped) with the ROIs. I first performed the maximum likelihood method, but if a classified image was not satisfying, I tried parallelpiped.

ROIs may be edited or more ROIs added to the original set until the classification was done correctly. Once a classified image was made, the image was saved as an ArcView raster (*.bil) in ENVI and then converted into GRID in ArcMap. The rest of

the procedures, such as image conversion, reclassifying, etc., were the same as described in the unsupervised classification section.

Figure 4.3. Region of Interest (ROIs) of an image (Neskowin, OR). Polygons in yellow are sand and those in green are others.

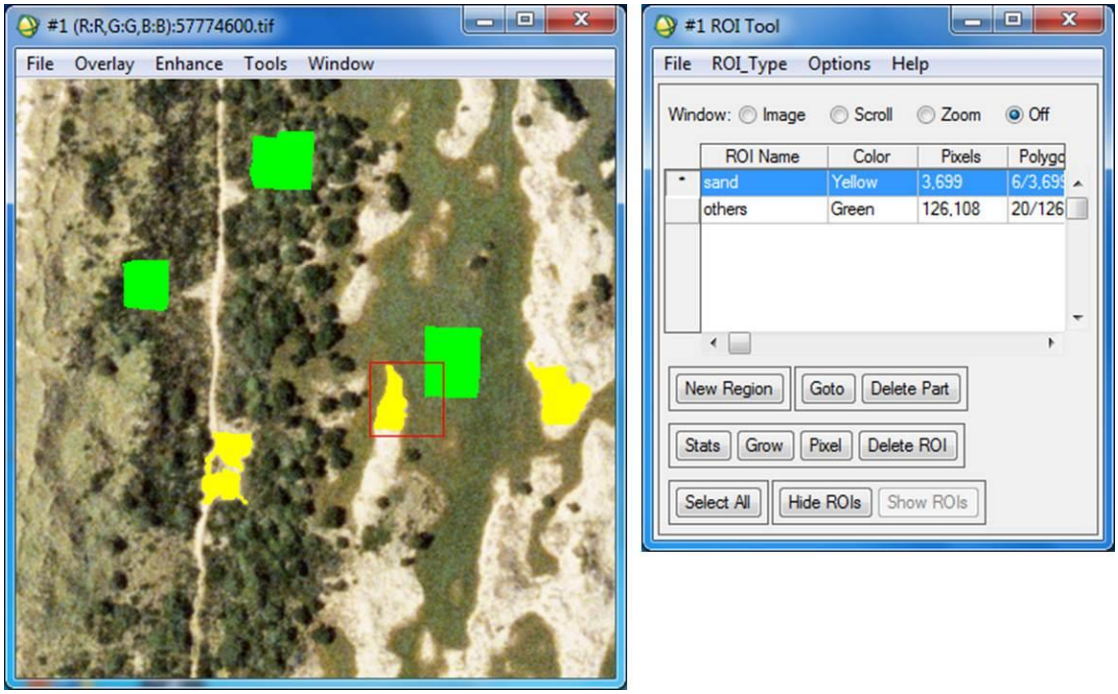

4.2.3 Removal of interfering human features

Some images include human features such as roads or parking spaces, which should be eliminated because in this study only the sand patterns caused by natural processes are considered. However, some of the features, especially in the dunes on the east coast (e.g. Island Beach dune field), were hard to attribute to either natural processes, human interference or both. Only features obviously considered human features (e.g. long, linear sand patches) were eliminated from the classified images.

The following process was used to remove unwanted features. First, I copied and pasted a reclassified image of interest into the ArcCatalog. In the toolbar of ArcMap, I opened "Customize" and checked "'Editor," "ArcScan," and "Raster Paining" in "Toolbars."" I also checked ArcScan in "Extensions" in "Customize" tool, so that I could use the toolbars I checked. In "'Editor," I clicked "Start Editing," and chose a raster image from which I wanted to remove features. Then, in the ArcScan toolbar, I chose the same raster as in "Editor," and then chose the "Raster Painting" toolbar in "Raster Cleanup" of the ArcScan toolbar. In the "Raster Painting" toolbar, I selected the type and size of brush, and toggled "Swaps BG/FG," and then removed the features. After the removal was done, I chose "Stop Cleanup," "Stop Editing" and then saved the editing by using "Save Editing."

4.2.4 Delineating study sites

In most dune fields, only a representative length of foredune area was analyzed. This was done for three reasons. First, if a foredune is on a barrier island, the ends of the barrier island are active and controlled by short-term changes, so I excluded both ends of the foredune area. Second, I excluded areas that were substantially modified, destroyed, or developed by humans. Third, if a scene comprised more than one image, and the images had different colors, it was sometimes too difficult to classify in the same color scale, so I chose only part of a dune field.

Within each dune field it was necessary to delineate an area of foredune environment for analysis because it is difficult to determine the landward extent of a foredune system using aerial photographs. I chose to delineate a representative width of

100 m perpendicular to a line along the seaward foredune toe. To do this, I made a new polygon shape file and drew a polygon. Once I finished drawing the polygon in a shape file, I masked the reclassified image with the polygon (Figure 4.4 e). The seaward end of a foredune polygon was drawn to represent the natural line where the foredune and the beach meet, but the landward end was drawn as a straight line (Figure 4.4 d).

Figure 4.4. Examples of image processing of Bear Island, NC: a) original image b) a classified image, c) a reclassified image assigned '1' as sand (yellow) and '0' as others (black), d) an original image with polygon shape file (red), and e) a reclassified image masked by a polygon shape file

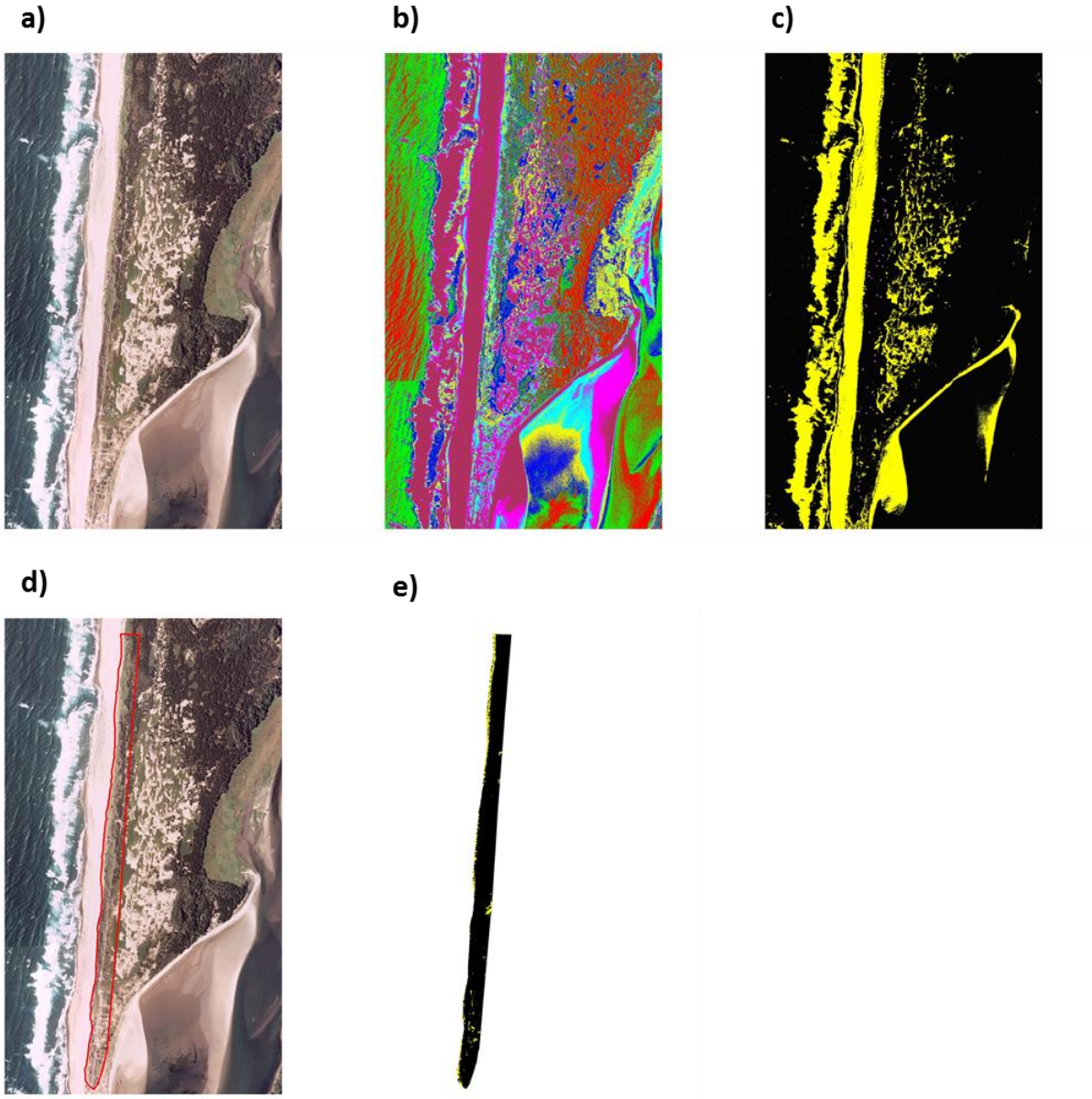

4.3 Calculation of metrics (indices) in Fragstats

In this study, because I was interested in the patterns of bare sand areas on dune fields as a whole, I chose the class level. In Fragstats 4.0 (Figure 4.5), to calculate

metrics for each site, I clicked "New" from the menu bar and added layers (ArcGIS GRID) by using the "Add layer" button. In the "Add layer" dialogue box, I selected data type, browsed and chose a dataset name, and inserted row and column numbers for each file, background value, and cell size. A batch file can be used to add several layers at once. Refer to McGarigal et al. (2012) for information on how to make a batch file.

A class properties file is necessary to run the Fragstats program. There are only two classes in my study: "sand" assigned "1" and "others" assigned "0." Refer to McGarigal et al. (2012) for instructions about how to make a class descriptor file. Once all the layers were inserted, I clicked the "Analysis parameters" tab to save the results and checked "Class metrics" only in the multi-level structure section.

Once all the information was typed in, in the right window, metrics can be chosen at each level and the quick results can be seen in the results option. Some metrics require putting in more information such as edge depth or threshold distance, but it was not necessary in my study because core area and contrast related metrics were not considered (see the next paragraph). Once all the metrics that I wanted to calculate were checked in, I clicked the "Run" button on the toolbar to allow Fragstats to calculate the metrics. After the calculation was completed, I opened the result files in an Excel 2010 spreadsheet.

The total number of metrics at class level available in Fragstats 4.0 is one hundred nine. I chose thirty three metrics that were commonly used and can be easily interpreted. Metrics in the category "core area" and "contrast" were not considered in this study. The two types of metrics are important in the study of ecosystem and ecology

because of "edge effects" – that the edges between patches can influence adjacent ecosystems in both or either abiotic or biotic environments (Murcia 1995). However, this study has only two patch types; "sand" and "others," so edge effects does not play a significant role. Thus, a core area, which is an area after removal of edge depth (distance between patches) and edge contrast between patches, was not considered. Although core areas and contrast metrics were not considered in this study, edge density (ED) was calculated.

In addition, I only considered mean (_MN), area-weighted mean (_AM), range (_RA), and coefficient of variance (_CV). Because mean is a robust average, median for average is redundant in this study, and CV is independent of unit. Further, I chose only metrics that are commonly used and simple and easy to interpret for the sand patch patterns.

After all the metrics for the old and new images for each site were calculated, each pair of metrics for both the old and new images of the same site was averaged because a single aerial photo cannot represent the general geomorphology of a dune field. A coastal zone is a very dynamic environment, so a single climatic event with a large magnitude such as a severe storm can alter a landform significantly, which can lead to a biased analysis if only a single image is considered. The averaged metrics of a pair of images taken at different times can decrease such risks and also provide more robust results.

Some metrics are strongly correlated to one another and are redundant (Riitters et al. 1995), so I eliminated them. I made a correlation coefficient matrix of the averaged

metrics in SPSS 16.0 GP, made a table of metrics groups that are correlated to each other by greater than either positive or negative 0.90 rounded after two decimal points, and then selected only one metric that represent each group.

Figure 4.5. Image capture showing the main window of Fragstats 4.0

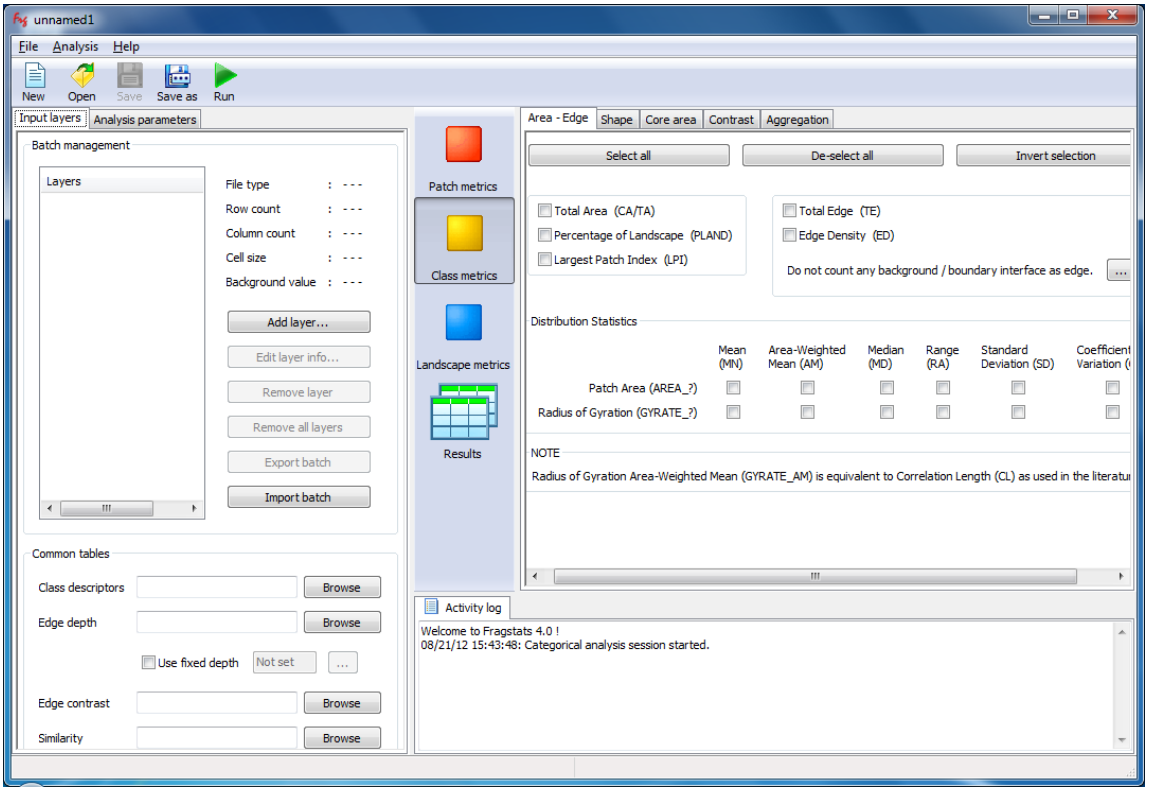

4.4 Calculation of climate variables

4.4.1 Precipitation

The dataset of PRISM is point data, but the sites are polygons. So the x, y coordinates of each site was roughly obtained from Google Earth ™ and then multiple precipitation point data within the polygons were obtained in ArcMap and averaged for

each site in Excel. The unit of the precipitation data in mm x 100 was then converted into mm.

Average annual precipitation (PPT) for each site was calculated by averaging the sum of each year's total precipitation for 30 years. Each year's standard deviation and coefficient of variance were calculated and then averaged to calculate the annual standard deviation (PPT_SD) and coefficient variance (PPT_CV) of each site for 30 years.

4.4.2 Potential evapotranspiration

PET was calculated using Thornthwaite's equation (Thornthwaite 1948);

$$PET = 16\left(\frac{L}{12}\right)\left(\frac{N}{30}\right)\left(\frac{10T_a}{I}\right)^{\alpha} \qquad (4.1)$$

where *PET* is the estimated potential evapotranspiration (mm/month), T_a is the average daily temperature in Celsius, *N* is the number of days in the month being calculated, and *L* is the average day length (hours) of the month. To calculate the mean possible duration of sunlight, $\left(\frac{L}{12}\right)\left(\frac{N}{30}\right)$, I referred to Table V in Thornthwaite (1948, p. 93).

I is a heat index, the sum of the heat index for each month and is calculated as follows:

$$I = \sum_{i=1}^{12}\left(\frac{T_a}{5}\right)^{1.514} \qquad (4.2)$$

Exponent α can be calculated as follows:

$$\alpha = (0.000000675)I^3 - (0.0000771)I^2 + (0.01792)I + 0.49239$$

Average annual potential evapotranspiration (PET) for each site was calculated by averaging the sum of each year's total potential evapotranspiration for 30 years. Each year's standard deviation and coefficient of variance were calculated and then averaged to calculate the annual standard deviation (PET_SD) and coefficient variance (PET_CV) of each site for 30 years.

4.4.3 Moisture index

The moisture index (MI) was calculated according to Thornthwaite and Mather (1955) and the equation is as follows:

$$MI = 100\left(\frac{PPT - PET}{PET}\right) \qquad (4.3)$$

$$= 100 \cdot (\frac{PPT}{PET} - 1)$$

where *MI* is moisture index, *PPT* is precipitation and *PET* is potential evapotranspiration. The original equation of this is as follows:

$$MI = 100\left[\frac{S - 0.6D}{PE}\right] \qquad (4.4)$$

where *S* is the moisture surplus, *D* is the moisture deficit. When the expression is integrated over the "average" year, $S \rightarrow \max[(P\text{-}E),0]$, where *E* is actual evapotranspiration, the moisture index (*MI*) becomes the first equation.

4.4.4 Wind data and drift potential

Wind that involves sediment movement should be above threshold velocity, which is 11.6 knots (ca. 5.975 m/s) according to Fryberger (1979). In this study, only wind speeds above 5.975 m/s were considered and winds below the threshold were discarded.

For the wind direction, only onshore winds were examined because offshore winds might not have played a significant role in creating sand patches in the foredune areas, although offshore winds could be involved in somehow moving sediment. In this study, onshore wind is defined as a wind that blows within between 0 and 180 degrees along the straight shoreline, representing the entire shoreline.

Fryberger (1979) proposed a sand migration model known as drift potential (DP), which is numerically expressed in vector units and the formula for DP is as follows:

$$Q \propto V^2(V - V_t) \cdot t \qquad (4.5)$$

where Q is a proportionate amount of sand drift, V is average wind velocity at a 10 m height, V_t is impact threshold wind velocity, and t is the time that the wind above the threshold velocity blew (%).

Fryberger derived this equation from Belly (1964), in which a sand surface of 0.30 mm average diameter quartz sand, the surface roughness factor (z') during sand driving was 0.3048 cm and the threshold wind velocity at height z' (V'_t) was 274 cm/s and V^*_t was 16 cm/s. Therefore, $V't$ may be extrapolated to a 10 m height using the equation below:

$$V_{(10m)} = 5.75V_t^* log\frac{Z}{Z'} + V_t' \qquad (4.6)$$

From this equation, a value of 11.613 (knots) is obtained for V_t. For this study, the value was converted into 5.757 m/s for calculations.

In this study, to obtain the onshore DP above the threshold wind velocity (OSDP), offshore winds and wind velocity (5.975 m/s) below the threshold were discarded. Based

on the monthly average DP and OSDP, the annual average, the annual standard deviation and coefficient variance of DP and OSDP were also calculated.

I calculated the annual average of resultant drift potential (RDP), which is the magnitude of the vector resultants of drift potentials from onshore directions, and the ratio of resultant drift potential to the drift potential, known as RDP/DP. The greater the directional variability of the effective winds at a station, the lower its associated RDP/DP will be. Annual average onshore RDP (OSRDP) and onshore RDP/DP (OSRDP/DP) were also calculated.

In addition, the ratio of onshore winds over all winds at a site (OS/ALL) and the ratio of winds above the threshold velocity over all winds at a site (Vt/ALL) were proposed in this study to see how the wind direction can affect the sand patterns. The number of all wind events was calculated as follows: 30 years × 365 (or 366) days × 8 of 3 hour events.

4.4.5 Mobility indices

Two mobility indices were calculated. Both indices were proposed for sand movement in inland deserts. Lancaster (1988) suggested that there are two main factors in sand movement in deserts: wind velocity and vegetation cover. Wind velocity is the driving force of sand mobility, while vegetation cover is a resistant force. The ratio of precipitation (P) and potential evapotranspiration (PE) is for the portion of vegetation cover and the percentage of the time the wind is blowing above threshold velocity (W; the same as Vt/ALL in this study) is for the portion of the wind. I calculated Lancaster's original mobility index (MB) and also the onshore mobility index (OSMB) by using

OS/ALL for W, instead of Vt/ALL. The equation for these two forces is suggested below:

$$MB = W/\left(\frac{P}{PE}\right) \tag{4.7}$$

He found critical values of *MB* for the Namib sand sea and the southwestern Kalahari; a value index of >200 for fully active dunes with a vegetation cover of <10%, of <50 for inactive dunes with a vegetation cover of >20%.

The second mobility index (MB_2) was proposed by Tsoar (2005). He thought that rainfall was not an important factor in dune mobilization because sand's permeability is much greater than soil composed of silt and clay. Therefore drift potential is a better index of sand mobility. So he proposed a sand mobility equation based on drift potential as shown below:

$$MB_2 = \frac{DP}{1000 - \left(750\frac{RDP}{DP}\right)} \tag{4.8}$$

I calculated the original MB_2 and also calculated the onshore MB_2 ($OSMB_2$) by using onshore DP (OSDP) and onshore RDP (OSRDP). Lancaster's (MB) and Tsoar's sand mobility (MB_2) indices were calculated and will be compared to see which one provides a better explanation for sand patch patterns in coastal areas.

Table 4.2. Climate variables calculated in this study

Climate variable	Description
PPT	Annual average precipitation
PET	Annual average evapotranspiration
MI	Moisture index
MI_SD	Standard deviation of MI
MI_CV	Coefficient of variance of MI
MB	Lancaster's sand mobility index
OSMB	Onshore winds above the threshold velocity of MB
OSALLMB	Onshore winds of all wind events of MB
OS/Vt	Onshore winds above the threshold velocity (%)
OS/ALL	Onshore winds of all wind events (%)
Vt/ALL	Wind above the threshold velocity (%)
DP	Drift potential
RDP	Resultant drift potential
RDP/DP	Resultant drift potential / drift potential
OSDP	Onshore portion of all DP
OSRDP	Onshore portion of all RDP
OSRDP/DP	OSRDP/OSDP
MB_2	Tsoar's sand mobility index
$OSMB_2$	MB_2 calculated with OSRDP and OSDP
PPT_SD	Standard deviation of PPT
PPT_CV	Coefficient of variance of PPT
PET_SD	Standard deviation of PET
PET_CV	Coefficient of variance of PET
P:PET	Ratio of PPT to PET

4.4.6 Cumulative averages

Using monthly averages of precipitation (PPT), potential evapotranspiration (PET) and drift potential (DP), cumulative averages were calculated for each variable set in order to see if the number of sand patches (PLAND) were related to the climate variables as time went on. The average of the first year was calculated first, starting from

the month of the previous year when an image was taken. For instance, if an image was taken in August 1998, the first yearly cumulative average was from August 1997 to July 1998. For the second average, the next previous yearly average was added to it and this procedure was repeated until the earliest year (1979) of the data. Cumulative averages were calculated for both old images and new images.

I also calculated the ratio of PPT to PET in order to compare the results obtained in this study with the results of Hugenholtz and Wolfe (2005b). All climate variables used in this study and their descriptions are shown in Table 4.2.

4.5 Cluster analysis

Hierarchical cluster analysis was conducted in SPSS 16.0 GP by using the twenty three metrics. For cluster analysis, four or five clusters would be an appropriate number because less than four clusters can have more than half the number of study sites in one cluster, and more than five clusters can have too few sites in one cluster, which would be harder to interpret. In addition, I used four or five metrics for cluster analysis because more than five metrics would not make better clusters and less than four clusters tend to make fewer and aggregated clusters, which would be against expectations. I mostly used Ward's method with Euclidean distance or squared Euclidean distance, but also tried other methods such as nearest neighbor or farthest neighbor. I sometimes standardized the values with z scores to have each variable contribute equally.

A metric, PLAND (percentage of bare sand area) is a very simple metric used to easily understand and interpret the sand patch patterns of sand dunes (Hugenholtz and Wolfe 2005a; Hugenholtz and Wolfe 2005b). I used PLAND as a pivotal metric and

added as many other variables from each metric category as I could. For instance, PLAND is in an area-edge category and I chose three or four other metrics from other categories and added them to PLAND. And I also tried almost all combinations of all metrics, no matter what categories the metrics belonged to. Cluster analysis was continued until the most reasonable result was found. The most reasonable result in this case would mean that clusters after cluster analysis would match visually with the classified images in terms of the patterns and textures of the bare sand area and possibly with their geographical locations too.

For hierarchical analysis, in SPSS I clicked "Analyze" from the toolbar, moved the metrics that I chose to analyze into the "Variable(s)" window, and checked "Dendrogram" in the Plots menu. In the "Method" menu, I chose a method from "Cluster Method." a measure from the "Interval" menu, and z scores for standardization from the "Transform Values" menu.

4.6 Clusters and climate comparison

Once clusters were made, the next step was to examine the relationship between climate variables and the metrics of clusters. To do this, I made a matrix scatter plot in SPSS 16.0 GP, with all climate variables that were calculated. The markers in the scatter plots were set in different colors by cluster numbers. If I found a graph that could separate more than or equal to one cluster from the rest of the other clusters, I recorded the two climate variables comprising the graph and made another matrix scatter plot without it. Once the second cluster was separated from the others, I recorded the climate variables and then made another matrix scatter plot without the second cluster to see

what climate variables separated the third cluster from the others. This procedure was repeated until all the clusters were separated from all the others as much as possible.

5 RESULTS

5.1 Processed images

All twenty-two study sites were classified by either an unsupervised or supervised method and were delineated by a narrow strip in the foredune area 100 m wide. Figure 5.1 shows all of the processed images masked by the 100 m wide narrow strips. Sand was classified as yellow and all other classes, such as vegetation, were in black. Images are presented geographically from the northwest coast through the south to the northeast coast, but have been rotated from their true orientation for presentation purposes only.

Figure 5.1. Twenty-two processed images (scale: 1:7,000). Sand is in yellow and other classes are in black. Dates when the original images were taken, are written in parentheses.

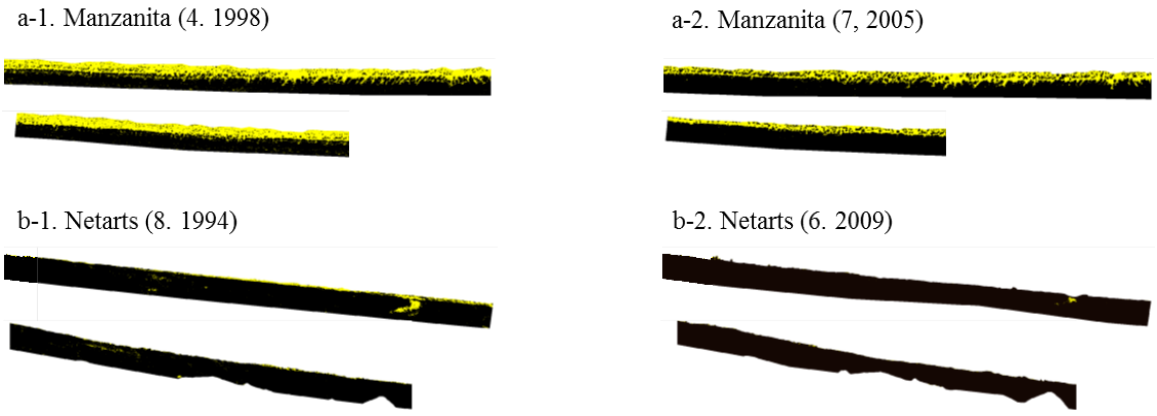

Figure 5.1 continued.

c-1. Nestucca (5. 1994)

c-2. Nestucca (7. 2005)

Figure 5.1 continued.

d-1.Coos Bay (5. 1994)

d-2. Coos Bay (7. 2008)

Figure 5.1 continued.

e-1. St. George (8. 1988)

e-2. St. George (7. 2005)

f-1. Eureka (4. 1989)

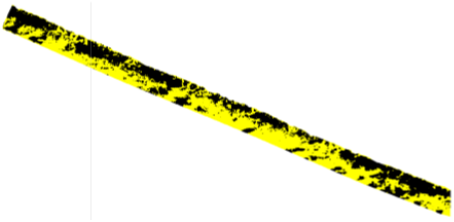

f-2. Eureka (6. 2009)

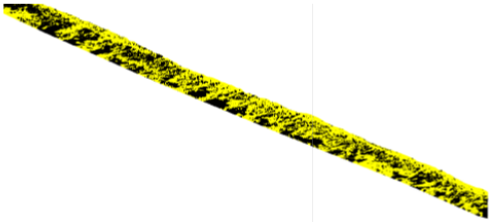

g-1. Pt. Arena (9.1998)

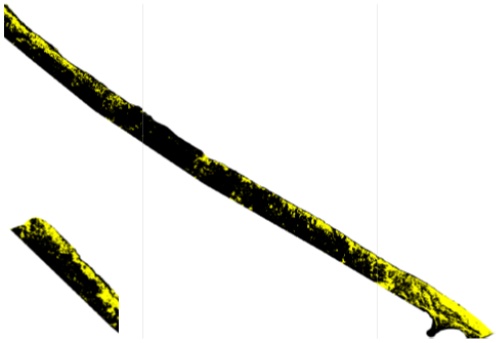

g-2. Pt. Arena (6. 2009)

Figure 5.1 continued.

h-1. Tomales (7. 1993)

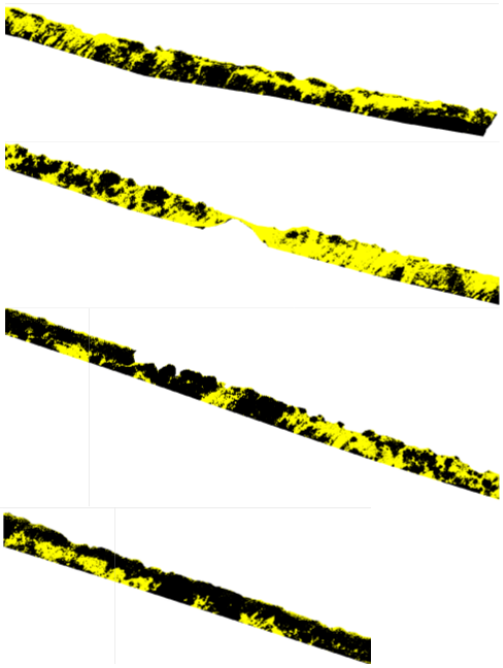

h-2. Tomales (6. 2009)

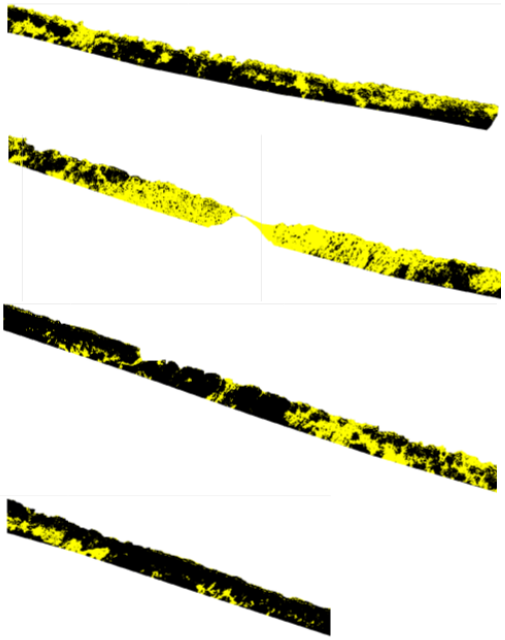

i-1. Marina (6. 1993)

i-2. Marina (6. 2009)

j-1. Morro Bay (5. 1994)

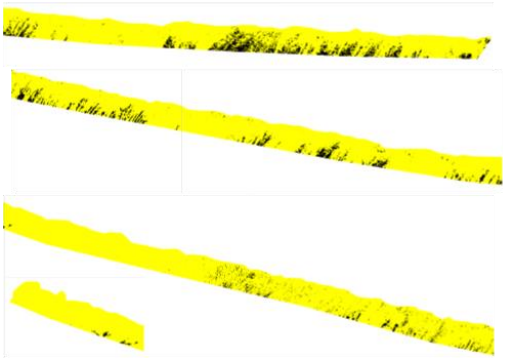

j-2. Morro Bay (6. 2009)

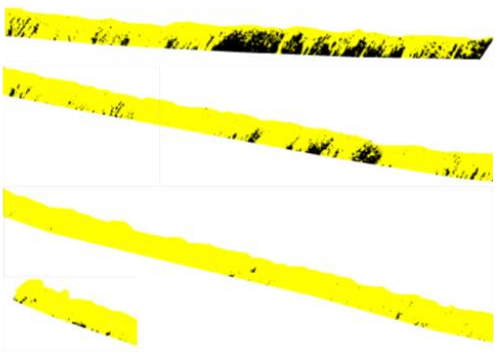

Figure 5.1 continued.

k-1. St. Maria (9. 1994)

k-2. St. Maria (6. 2009)

l-1. Vandenberg (9. 1994)

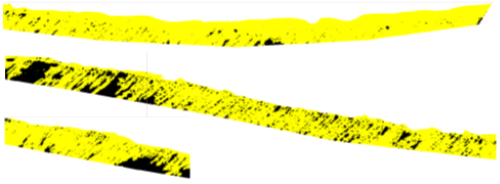

l-2. Vandenberg (7. 2009)

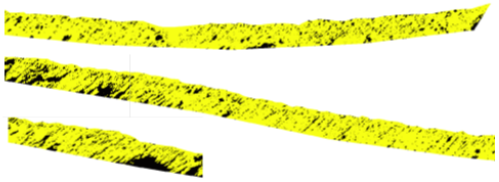

Figure 5.1 continued.

m-1. Padre Island (1. 1995)

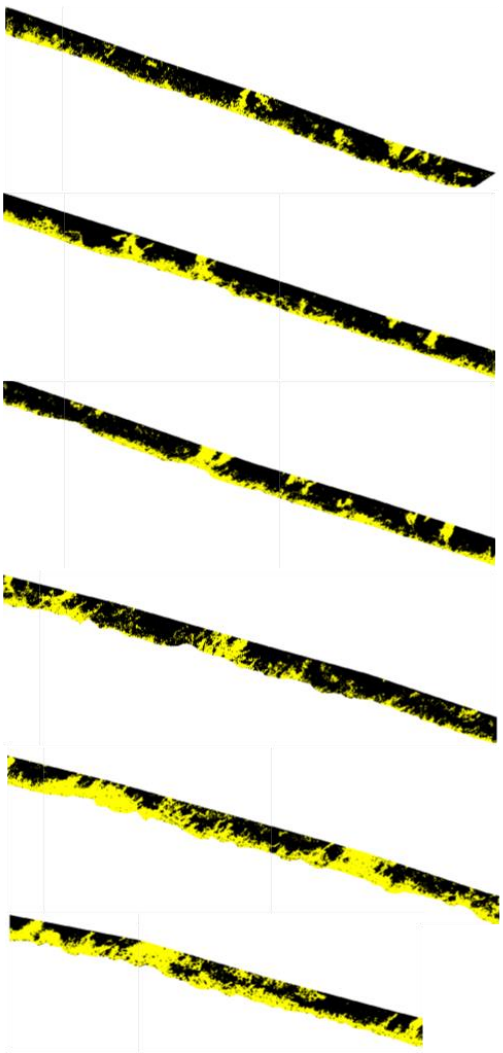

m-2. Padre Island (10. 2008)

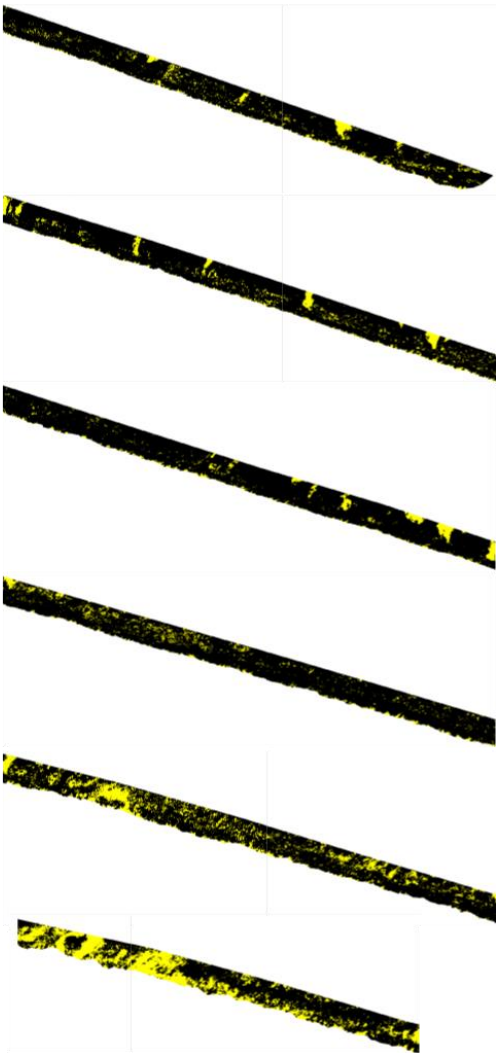

n-1. St. Joseph (1. 1994)

n-2. St. Joseph (3. 2006)

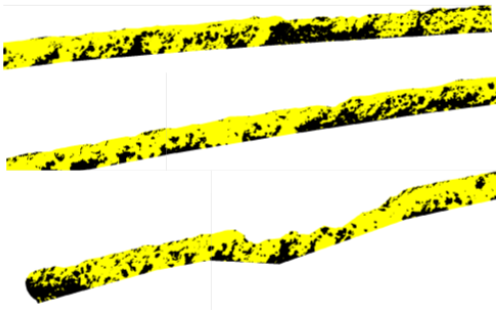

Figure 5.1 continued.

o-1. Bear Island (1. 1998)

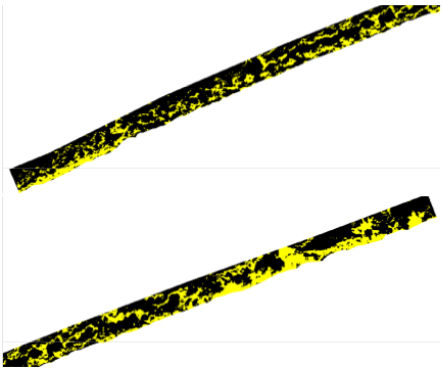

o-2. Bear Island (5. 2009)

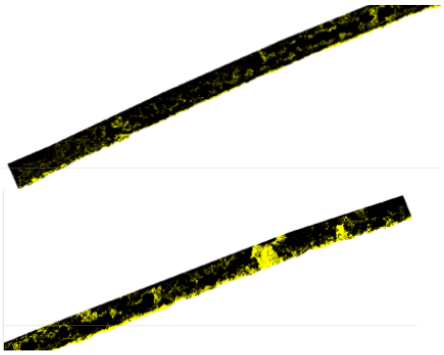

p-1. Hatteras (2. 1998)

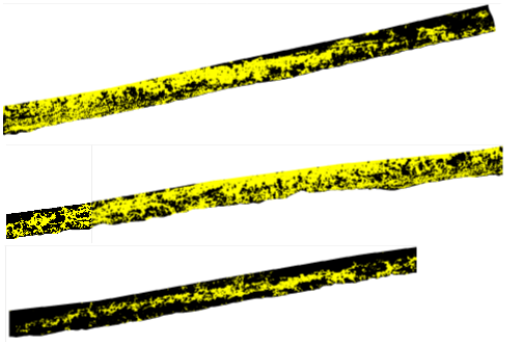

p-2. Hatteras (8. 2009)

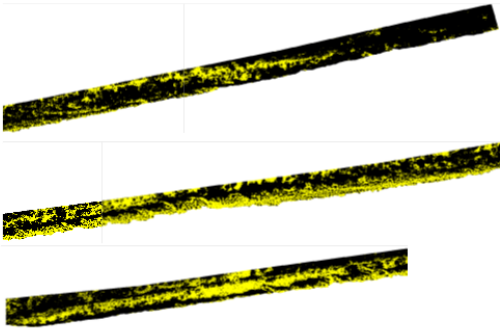

q-1. False Cape (3. 1994)

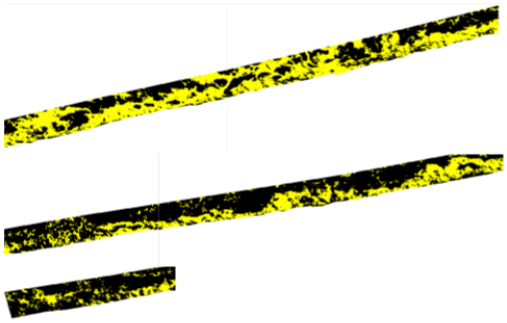

q-2. False Cape (6. 2009)

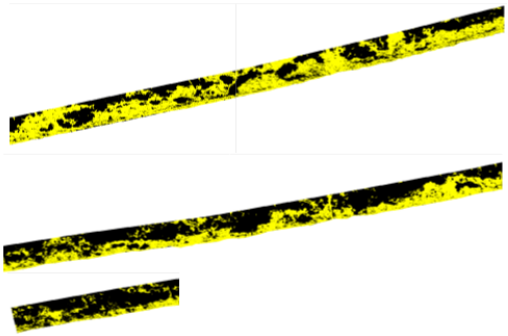

Figure 5.1 continued.

r-1. Island Beach (3. 1995)

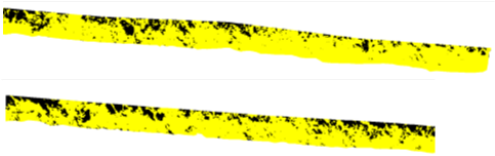

r-2. Island Beach (8. 2008)

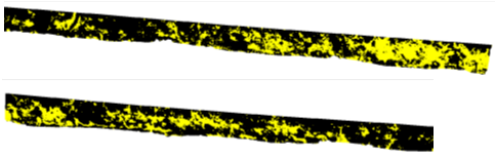

s-1. Fire Island (4. 1994)

s-2. Fire Island (5. 2009)

t-1. Chappaquiddick (3. 1995)

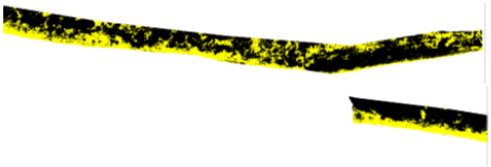

t-2. Chappaquiddick (7. 2008)

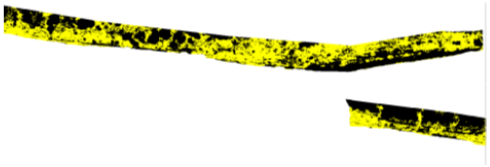

Figure 5.1 continued.

u-1. Barnstable (3.1995)

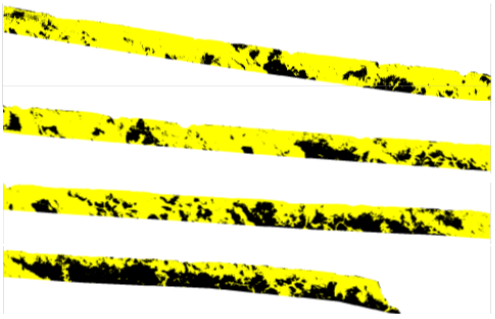

u-2. Barnstable (7.2008)

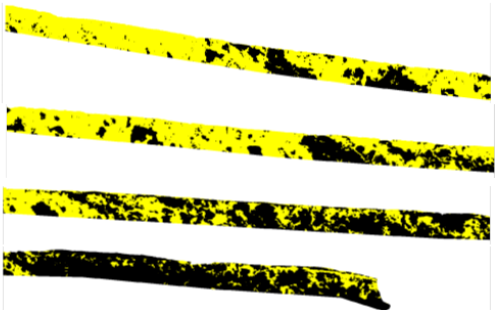

v-1. Plum Island (3. 1995)

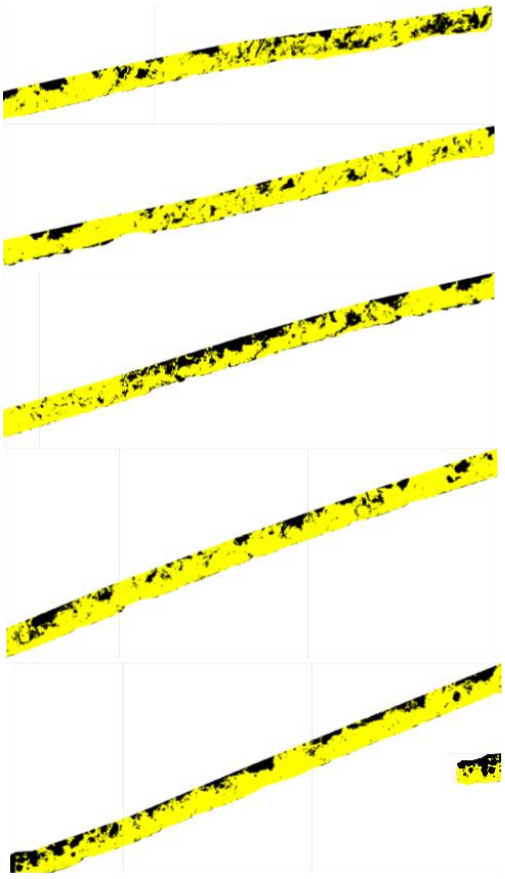

v-2. Plum Island (7. 2008)

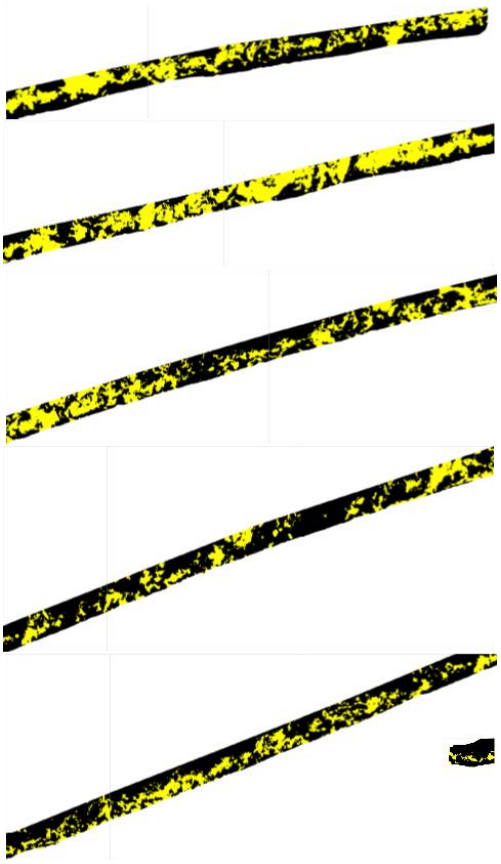

5.2 Summary of Fragstats metrics

Thirty-three metrics were calculated in Fragstats 4.0 using the images above. Metrics that were correlated at 0.90 or more were removed (Table 5.1). This left twenty-three metrics for further analyses in this study. Table 5.2 presents the values that were averaged from old and new images for each site.

Table 5.1. Twenty-three representative metrics used in this study.

Representative metric	Metrics category	Group members	Name (unit)*
PLAND	Area-Edge	LPI	Percentage of landscape (%)
PD	Aggregation		Patch density (number/100 ha)
ED	Area-Edge		Edge density (m/ha)
LSI	Aggregation		Landscape shape index
AREA_MN	Area-Edge		Mean area (ha)
AREA_AM	Area-Edge	AREA_RA, DIVISION, MESH	Area-weighted mean area (ha)
AREA_CV	Area-Edge		Coefficient variance of area
SHAPE_MN	Shape		Mean shape index
SHAPE_AM	Shape	SHAPE_RA	Area-weighted mean shape index
SHAPE_CV	Shape		Coefficient variance of shape index
FRAC_MN	Shape		Mean fractal dimension index
FRAC_AM	Shape		Area-weighted mean FRAC
FRAC_CV	Shape	FRAC_RA	Coefficient variance of FRAC
CIRCLE_MN	Shape	CIRCLE_CV	Mean of related circumscribing circle
CIRCLE_RA	Shape		Area-weighted mean CIRCLE
PAFRAC	Shape		Coefficient variance of CIRCLE
ENN_MN	Aggregation		Mean Euclidean nearest neighbor distance (m)
ENN_AM	Aggregation	COHESION	Area-weighted mean ENN (m)
ENN_RA	Aggregation		Range of ENN (m)
ENN_CV	Aggregation		Coefficient variance of ENN (m)
PLADJ	Aggregation	CIRCLE_AM, AI	Proportion of like adjacencies (%)
SPLIT	Aggregation		Splitting index
NLSI	Aggregation	CLUMPY, COHESION, AI	Normalized LSI

* Dimensionless unit is in blank

Table 5.2. Metrics used for this study. The values were averaged from old and new images.

Site*	PLAND	PD	ED	LSI	AREA_MN	AREA_AM	AREA_CV	SHAPE_MN	SHAPE_AM	SHAPE_CV	FRAC_MN	FRAC_AM	FRAC_CV
man	28.86	3916.04	1155.9	32.49	0.01	6.53	2855.50	1.14	20.91	68.30	1.10	1.55	44.40
net	2.30	1949.31	219.0	25.42	0.00	0.09	780.19	1.14	3.51	32.46	1.17	1.39	19.17
nes	7.79	3740.65	669.7	33.71	0.00	0.41	1378.01	1.27	6.92	49.60	1.22	1.49	43.52
coo	9.32	10372.12	1206.6	123.73	0.00	0.59	1882.64	1.16	5.59	35.58	1.19	1.43	22.12
stg	7.17	7128.66	911.3	67.78	0.00	0.16	865.38	1.18	4.29	36.43	1.20	1.40	20.25
eur	55.33	1861.65	1784.5	29.67	0.03	7.89	1621.88	1.35	21.22	95.45	1.19	1.51	17.11
pta	18.09	4905.02	1342.3	43.06	0.00	0.57	1025.89	1.27	6.88	52.51	1.22	1.44	18.63
tom	39.94	3351.82	1455.3	53.52	0.01	3.89	1779.97	1.27	10.97	62.60	1.20	1.46	16.15
mar	40.06	2583.31	1292.4	24.65	0.02	4.68	1472.88	1.26	12.69	68.60	1.21	1.48	17.23
mor	91.54	323.94	543.65	15.42	0.29	54.69	1385.48	1.28	14.23	78.76	1.19	1.40	12.67
stm	70.88	769.66	1639.9	43.01	0.09	14.21	1172.43	1.47	16.37	120.91	1.20	1.48	14.91
van	85.08	154.15	1074.0	23.04	0.77	37.55	786.45	1.50	22.69	183.63	1.15	1.48	14.53
pad	24.76	4713.49	1198.2	74.39	0.01	2.93	1629.82	1.25	7.84	47.84	1.20	1.40	16.02
stj	62.76	640.60	810.5	22.58	0.10	19.86	1255.03	1.28	13.57	77.72	1.17	1.42	13.03
bea	23.42	9008.13	1678.9	55.86	0.01	0.46	991.82	1.32	5.24	51.26	1.21	1.43	18.71
hat	36.22	4880.54	2119.8	68.71	0.01	3.97	2062.59	1.29	18.37	80.03	1.20	1.54	18.16
fal	42.52	2183.83	1644.0	44.34	0.02	11.79	2428.60	1.34	25.71	85.52	1.21	1.53	18.07
isl	56.44	1868.11	1109.2	27.45	0.10	14.72	1073.56	1.29	10.25	70.93	1.19	1.41	14.73
fir	35.42	2750.55	1519.9	41.20	0.01	0.86	765.70	1.37	6.63	64.75	1.21	1.42	16.45
cha	43.03	5650.89	1946.3	38.56	0.01	2.53	1805.98	1.26	10.82	59.77	1.20	1.46	19.29
bar	61.42	949.74	790.37	25.49	0.07	12.66	1379.24	1.33	9.48	60.03	1.19	1.38	15.67
plu	57.76	1284.73	962.71	35.66	0.05	36.86	1950.67	1.23	16.19	64.07	1.18	1.41	16.63

Table 5.2. continued.

Site*	CIRCLE_MN	CIRCLE_RA	PAFRAC	ENN_MN	ENN_AM	ENN_RA	ENN_CV	PLADJ	SPLIT	NLSI
man	0.30	0.99	1.36	3.07	1.53	43.37	7.45	91.92	26.40	0.08
net	0.31	0.93	1.44	4.83	3.25	81.35	3.66	58.38	456344.74	0.41
nes	0.39	0.98	1.40	2.91	1.71	42.07	8.44	81.98	915.20	0.18
coo	0.29	0.95	1.48	3.93	3.12	40.21	4.81	58.35	631451.69	0.41
stg	0.34	0.95	1.41	3.92	2.63	36.01	5.42	65.62	63858.92	0.34
eur	0.39	0.96	1.38	3.01	2.06	15.87	9.27	91.05	4.67	0.11
pta	0.40	0.96	1.40	3.64	2.31	38.71	6.75	80.09	1356.32	0.20
tom	0.41	0.96	1.38	3.46	2.09	27.71	7.25	89.97	48.26	0.10
mar	0.41	0.97	1.39	3.75	2.07	24.74	6.45	90.38	22.26	0.09
mor	0.46	0.98	1.36	3.21	2.00	7.21	7.73	97.93	1.21	0.21
stm	0.43	0.96	1.42	2.96	2.02	8.42	9.11	93.44	10.10	0.15
van	0.35	0.98	1.42	4.24	2.00	15.64	7.02	96.24	1.39	0.20
pad	0.42	0.96	1.36	3.72	2.30	43.32	6.74	84.49	1156.84	0.15
stj	0.44	0.97	1.31	5.13	2.07	28.18	5.53	96.17	8.77	0.06
bea	0.40	0.96	1.44	3.33	2.24	32.65	6.86	77.23	601.56	0.22
hat	0.38	0.97	1.43	3.02	2.07	44.55	8.02	83.84	54.45	0.16
fal	0.40	0.98	1.40	3.38	2.11	31.79	7.67	89.82	10.09	0.10
isl	0.42	0.94	1.33	3.51	2.13	22.74	8.00	92.59	71.85	0.12
fir	0.43	0.94	1.38	3.42	2.13	21.88	8.06	88.56	148.77	0.11
cha	0.36	0.96	1.40	2.76	2.06	17.79	8.96	87.62	22.51	0.12
bar	0.42	0.97	1.33	3.90	2.09	28.92	7.09	96.14	10.85	0.06
plu	0.37	0.96	1.32	3.75	2.20	26.40	7.33	94.80	81.79	0.10

* Site abbreviations: man: Manzanita, net: Netarts, nes: Nestucca, coo: Coos Bay, stg: Saint George, eur: Eureka, pta: Point Arena, tom: Tomales, mar: Marina, mor: Morro Bay, stm: Santa Maria, van: Vandenberg, pad: Padre Island, stj: Saint Joseph, bea: Bear Island, hat: Hatteras, fal: False Cape, isl: Island Beach, fir: Fire Island, cha: Chappaquiddick, bar: Barnstable, and plu: Plum Island.

5.3 Climate variables

There were twenty-four climate variables calculated for this study. Pearson's one-tailed correlation coefficient matrix for all the climate variables was made and it showed that eighteen variables were correlated by 0.90 or more, rounded after two decimal points (Table 5.3). All twenty-four climate variables are summarized in Table 5.4.

Table 5.3. Climate variables correlated by greater than 0.90. (See Table 4.2. for the description of climate variables.)

Representative climate variables	Variables with correlation > 0.9
PPT	MI, P:PET
PET	TEMP
PPT_SD	MI_SD
MB	OSMB
OSALLMB	OSMB
DP	MB_2
OSDP	OSRDP, $OSMB_2$
RDP	MB_2
PPT_CV	PET_CV
MI_CV	N/A
Vt/ALL	N/A
OS/ALL	N/A
RDP/DP	N/A
OSRDP/DP	N/A
PET_SD	N/A

Table 5.4. Climate variables used in this study.

Site	PPT	PET	MI	MI_SD	MI_CV	MB	OSMB	OsAllMB	Vt/ALL	OS/ALL	DP	RDP	RDP/DP	OSDP	OSRDP
man	1963.0	636.2	208.6	55.3	0.3	13.8	21.1	40.5	42.7	27.8	118.5	41.3	0.3	132.5	105.6
net	2183.5	630.0	246.6	58.9	0.2	8.3	20.7	17.3	28.7	20.6	96.4	74.4	0.8	77.6	67.6
nes	1857.6	641.7	189.5	47.8	0.3	9.3	22.8	28.6	26.9	17.8	59.3	18.3	0.3	42.6	27.6
coo	1688.7	653.7	157.9	48.2	0.3	18.2	27.5	97.3	47.0	33.4	160.4	58.6	0.4	110.7	82.0
stg	1793.9	657.2	172.8	61.5	0.4	13.9	20.2	192.8	38.1	21.0	72.8	7.9	0.1	41.9	25.5
eur	1035.1	657.5	57.4	43.3	0.8	29.3	39.4	439.7	46.1	28.6	167.2	88.9	0.5	72.2	19.9
pta	1043.0	656.7	58.4	52.2	0.9	36.9	36.7	550.3	58.6	34.1	268.8	60.4	0.2	156.1	108.4
tom	866.8	672.2	28.9	44.0	1.5	34.4	72.0	767.4	44.3	41.1	100.8	78.6	0.8	90.8	88.0
mar	425.8	706.9	-39.9	22.3	-0.6	13.1	126.2	147.3	7.9	6.0	6.0	1.3	0.2	4.0	2.3
mor	440.0	690.8	-36.5	26.5	-0.7	59.9	137.9	1165.8	38.1	33.5	72.9	46.5	0.6	60.5	54.6
stm	417.3	713.1	-41.6	23.7	-0.6	49.5	143.9	645.7	29.0	24.4	70.8	32.5	0.5	55.0	43.9
van	410.0	723.6	-43.4	22.8	-0.5	78.0	158.5	1256.9	44.2	39.7	100.5	74.6	0.7	90.3	83.0
pad	777.7	1256.5	-37.9	17.1	-0.5	45.9	62.1	60.2	28.4	10.9	55.0	37.7	0.7	21.8	17.1
stj	1488.9	1058.5	40.9	25.6	0.6	8.3	38.7	9.5	11.7	6.4	10.2	0.1	0.0	5.4	2.4
bea	1443.4	915.0	58.0	24.6	0.4	22.7	26.5	11.6	35.8	14.9	84.4	33.0	0.4	24.5	18.3
hat	1308.4	904.0	44.8	25.9	0.6	24.3	20.1	7.5	35.1	10.2	87.6	33.0	0.4	26.8	20.7
fal	1172.2	864.0	35.8	30.9	0.9	15.8	36.3	8.9	21.4	10.5	29.2	1.1	0.0	14.2	6.7
isl	1161.7	722.7	61.1	26.3	0.4	21.8	18.4	7.0	35.1	10.4	79.5	35.5	0.4	15.9	6.7
fir	1243.3	703.0	77.1	31.5	0.4	12.7	16.9	4.4	22.5	6.7	34.1	16.6	0.5	7.0	4.5
cha	1228.0	659.0	85.9	21.7	0.3	16.2	20.7	6.3	30.1	11.6	50.5	9.7	0.2	21.8	13.3
bar	1125.8	657.0	71.4	22.3	0.3	24.9	30.9	10.0	42.7	22.6	118.5	41.3	0.3	72.7	50.6
plu	1227.9	640.1	91.8	29.7	0.3	18.8	45.5	23.2	36.0	31.4	58.6	23.5	0.4	49.1	26.7

Table 5.4. continued

Site	OSRDP/DP	MB_2	$OSMB_2$	PPT_SD	PPT_CV	PET_SD	PET_CV	P:PET	TEMP
man	0.8	0.2	0.3	129.4	0.8	27.7	0.5	3.1	10.3
net	0.9	0.2	0.2	144.0	0.8	27.3	0.5	3.5	10.2
nes	0.6	0.1	0.1	121.4	0.8	26.7	0.5	2.9	10.7
coo	0.7	0.2	0.2	126.4	0.9	24.8	0.5	2.6	11.4
stg	0.6	0.1	0.1	141.2	0.9	22.4	0.4	2.7	11.7
eur	0.3	0.3	0.1	90.9	1.1	20.4	0.4	1.6	11.9
pta	0.7	0.3	0.3	105.8	1.2	19.8	0.4	1.6	11.9
tom	1.0	0.2	0.3	96.8	1.3	17.7	0.3	1.3	12.8
mar	0.6	0.0	0.0	45.8	1.3	21.8	0.4	0.6	13.9
mor	0.9	0.1	0.2	51.7	1.4	16.7	0.3	0.6	13.7
stm	0.8	0.1	0.1	49.6	1.4	18.7	0.3	0.6	14.4
van	0.9	0.2	0.3	49.2	1.4	21.4	0.4	0.6	14.7
pad	0.8	0.1	0.1	59.6	0.9	68.7	0.7	0.6	22.3
stj	0.5	0.0	0.0	76.0	0.6	60.6	0.7	1.4	20.0
bea	0.7	0.1	0.1	65.9	0.5	57.9	0.8	1.6	17.2
hat	0.8	0.1	0.1	52.3	0.5	58.3	0.8	1.4	17.0
fal	0.5	0.0	0.0	53.0	0.5	58.0	0.8	1.4	15.9
isl	0.4	0.1	0.0	46.1	0.5	54.4	0.9	1.6	12.0
fir	0.6	0.1	0.0	53.8	0.5	53.5	0.9	1.8	11.4
cha	0.6	0.1	0.0	50.9	0.5	50.6	0.9	1.9	10.2
bar	0.7	0.2	0.2	50.9	0.5	49.9	0.9	1.7	10.3
plu	0.5	0.1	0.1	58.6	0.6	50.9	1.0	1.9	9.4

5.4 Cluster analysis

In the cluster analysis, I used PLAND as a pivotal metric and added two to four other variables, each of which represented patch number, patch shape, or patch distribution. For example, I started the cluster analysis with PLAND and PD, a metric of a patch number, and then I added the patch shape metric PAFRAC or other metric for patch shape to PLAND and PD. If this showed a good result, then I added another metric such as ENN_MN, representing aggregation, to the result to see if the clusters changed or showed a better result. In this way, I tried up to five metrics (including PLAND) that can discern three to five clusters. I also tried two or three metrics representing the same characteristics. For example, I added NLSI and ENN_RA to PLAND at the same time. Both metrics are associated with patch distribution, although NLSI represents patch aggregation and ENN_RA represents the range of distance between patches.

After the many combinations that all the metrics could make were examined, I found four metrics, PLAND, PLADJ, NLSI, and ENN_RA (Figure 5.2, Table 5.5), that showed the most reasonable results because the results matched well with both geographical locations and sand patch patterns. The resultant hierarchical cluster analysis was completed using Ward's method with Euclidean distance and was standardized by z-scores.

Four clusters were obtained by cutting the dendrogram at between 5 and 10 of the rescaled distances. Cluster 1 had six sites: Manzanita, OR; Nestucca, OR; Pt. Arena, CA; Padre Island, TX; Bear Island, NC; and Hatteras, NC. Cluster 2 had three sites: Netarts, OR; Coos Bay, OR; and St. George, CA. Cluster 3 had three sites: Morro Bay,

CA; St. Maria, CA; and Vandenberg, CA. Cluster 4 had ten sites: Eureka, CA; Tomales, CA; Marina, CA; St. Joseph, FL; False Cape, VA; Island Beach, NJ; Fire Island, NY; Chappaquiddick, MA; Barnstable, MA; and Plum Island, MA. The dendrogram is shown in Figure 5.2 and the sites are presented geographically in Figure 5.3

Figure 5.2. Dendrogram created by SPSS 16.0 GP. Ward's method with Euclidean distance standardized z scores.

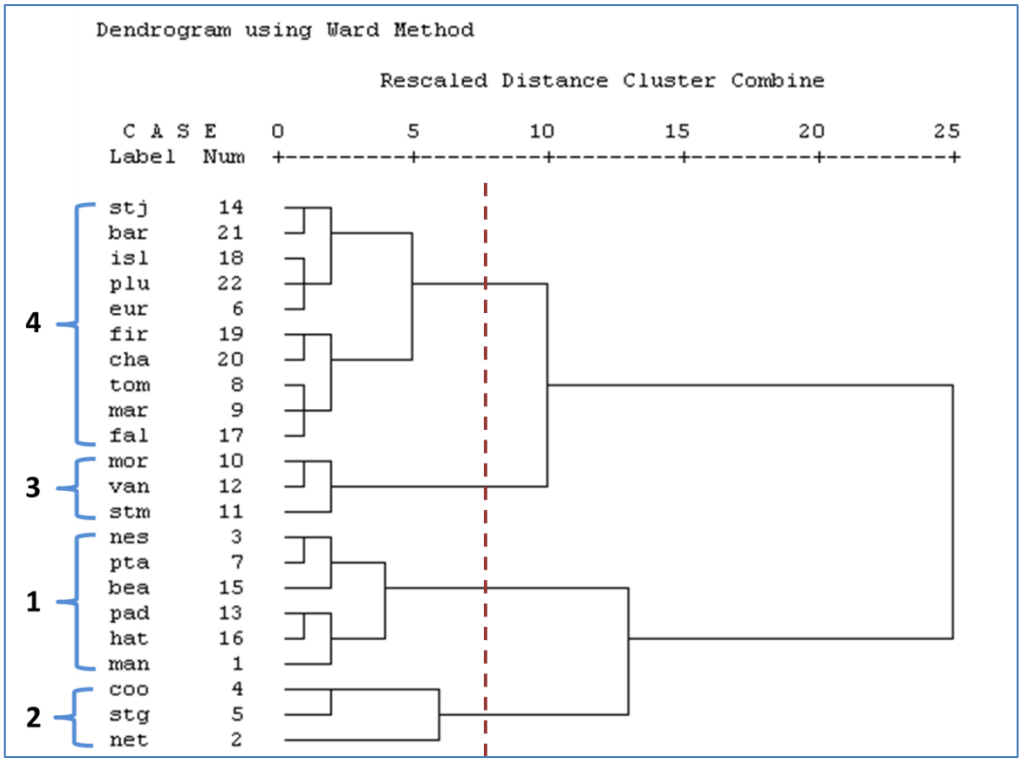

PLAND is the percentage of patch of the same class (sand in this study) of an entire landscape and a simple metric measuring the total amount of patches of the same type. PLADJ is the percentage of like adjacencies of the class of interest and equals the number of like adjacencies of a class of interest, divided by the total number of cell adjacencies, multiplied by 100. PLADJ equals 0 when the class is maximally

disaggregated (i.e. every cell is a different patch), and equals 100 when the landscape consists of a single patch and all the adjacencies are between the same class. NLSI is a normalized landscape shape index and is calculated as below.

$$NLSI = \frac{e_i - min\ e_i}{max\ e_i - min\ e_i} \quad (5.1)$$

where e_i equals the total length of the edge of class i, $min\ e_i$ equals the minimum total length of the edge of class i, and $max\ e_i$ equals the maximum total length of the edge of class i. NLSI equals 0 when the landscape consists of a single square or maximally compact (almost square) patch of a corresponding type; LSI equals 1 when the patch type is maximally disaggregated. ENN is Euclidean nearest-neighbor distance and equals the distance (m) to the nearest neighboring patch of the same type, based on shortest edge-to-edge distance (cell center to cell center). ENN approaches 0 as the distance to the nearest neighbor decreases. ENN is a simple measure of patch isolation and ENN_RA is the range of ENN. See the website of Fragstats for more detailed information (www.umass.edu/landeco/research/fragstats/fragstats.html).

Table 5.5. Four resulting metrics after hierarchical cluster analysis.

Name	Meaning	Unit	Range	Description	Note
PLAND	Percentage of landscape	%	0~100	Percentage of the areas of all sand patches	
PLADJ	Percentage of like-adjacencies	%	0~100	Number of like adjacencies involving the focal class, divided by total number of cell adjacencies involving focal class	0, when maximally disaggregated; 100, when only one single patch is in the landscape.
NLSI	Normalized landscape shape index	None	0~1	Simple measure of class aggregation or clumpiness	Increases as sand patches become increasingly disaggregated.

Table 5.5. continued

Name	Meaning	Unit	Range	Description	Note
ENN_RA	Range of Euclidean nearest neighbor	Meter	>0, no limit	Distance to the nearest neighboring patch based on cell center to cell center	Approaches 0 as the distance to the nearest neighbor decreases.

Figure 5.3. Geographical presentation of clusters: cluster 1 in red; cluster 2 in orange; cluster 3 in green; and cluster 4 in blue.

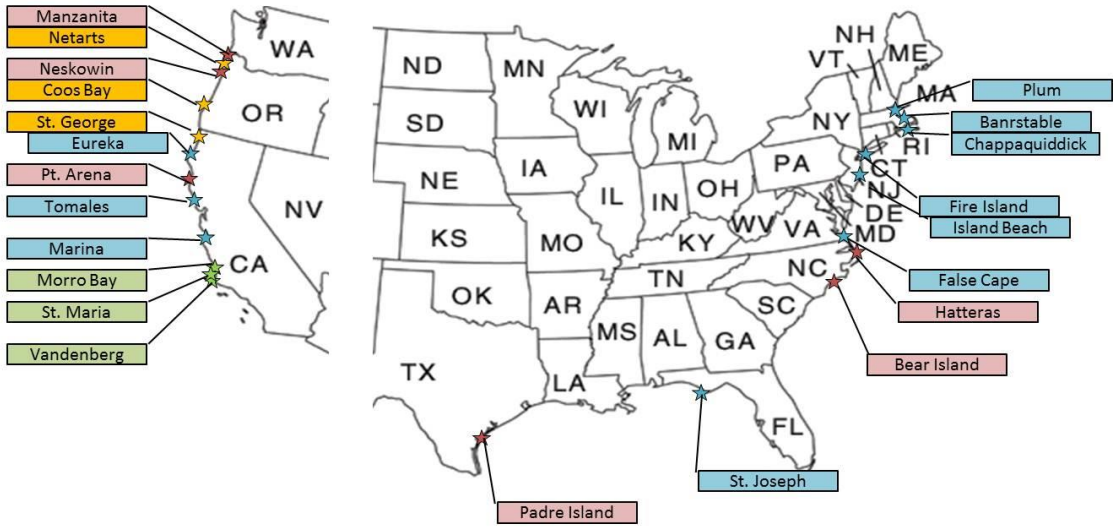

A scatter plot matrix (Figure 5.4) shows the characteristics of each site based on each metric. Cluster 3 (green circle) has the highest value of PLAND and PLADJ, and the lowest ENN_RA and consists of few, but very large sand patches. All sites in cluster 3 are located on the southwestern coast. Cluster 2 has the lowest value of PLAND and PLADJ, and the highest NLSI, and thus consists of sand patches that are small, irregularly shaped, and disaggregated. All sites in cluster 2 are located on the northwestern coast. Cluster 4 has high PLADJ and low NLSI, and mid PLAND and

ENN_RA and consists of few relatively large sand patches that are disaggregated. Ten sites are in cluster 4. Six of these sites are located on the eastern coast and the other sites are scattered. The value of the metrics of cluster 1 is around mid-range. Sites in cluster 1 are comprised of small and somewhat disaggregated patches, located on the southeastern and northwestern coasts and on the Gulf of Mexico. See Table 5.6 for a summary of the characteristics and sand patch pattern types of each cluster. Figure 5.5 shows the representative sites for each foredune type.

Figure 5.4. Scatter plot matrix of four metrics: PLAND, PLADJ, NLSI, and ENN_RA. Cluster 1 in red, 2 in orange, 3 in green, and 4 in blue.

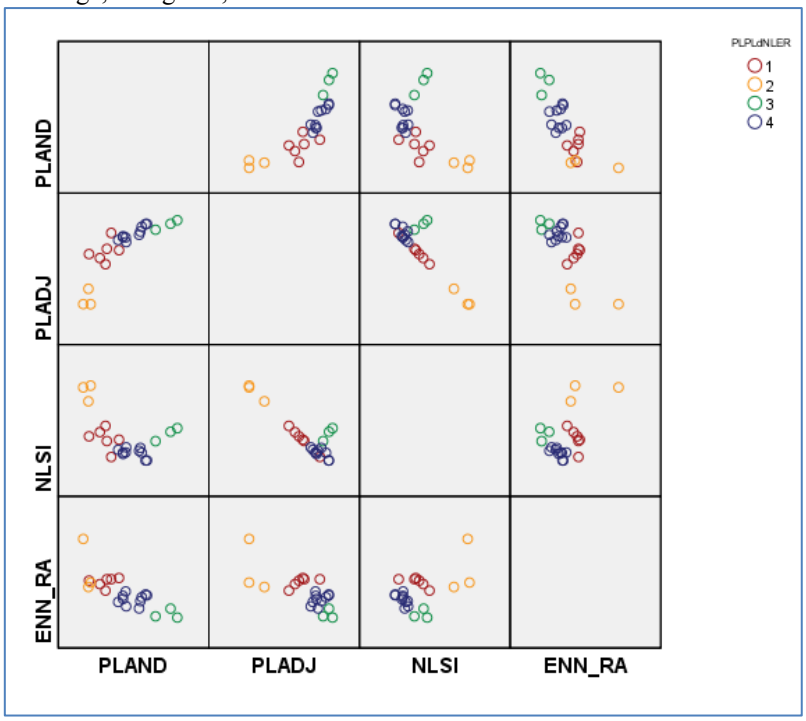

Table 5.6. Summary of characteristics of sand patch pattern types.

Patch type	Sites	Metrics				Characteristics
		PLAND	PLADJ	NLSI	ENN_RA	
1	man, nes, pta, pad, bea, hat	Low-mid	Mid-high	Mid	Mid	Small patches, somewhat aggregated
2	net, coo, stg	Low	Low	High	Mid	Small and irregular patches, disaggregated with long distance
3	mor, stm, van	High	High	Mid	Low	Very large, but few sand patches
4	eur, mar, tom, stj, fal, isl, fir, cha, bar, plu	Mid	High	Low-mid	Low-mid	Relatively large, but few sand patches, aggregated

Figure 5.5. Representative images for foredune types based on sand patch textures. See Table 5.6 for the characteristics of foredune types.

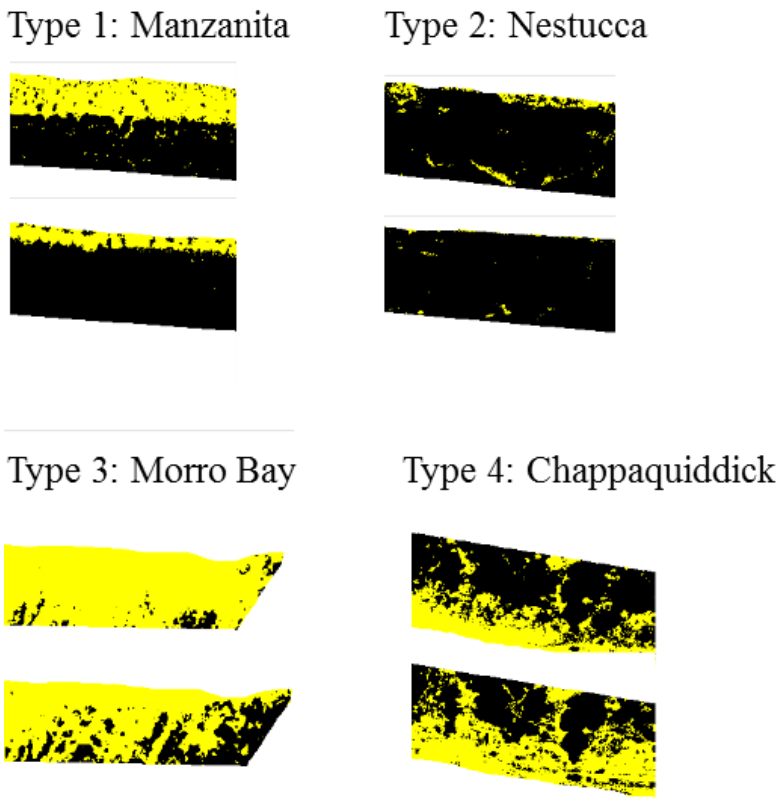

5.5 Patch pattern types and climate comparison

The four types of patch patterns that were created through cluster analysis were compared to climate variables in order to see the relationship between climate variables and each patch pattern type. A scatter plot matrix of all the climate variables marked by cluster numbers was made and I found that two scatter plots, one with PPT (annual average precipitation) and MB (Lancaster's mobility index) and another with PET (annual average potential evapotranspiration) and PPT_SD (standard deviation of annual average precipitation), better distinguished the types.

Figure 5.6. Scatter plots of four climate variables, marked by clusters: cluster 1 in red; cluster 2 in orange; cluster 3 in green; and cluster 4 in blue. Clusters were grouped by circles and called types1 through 4.

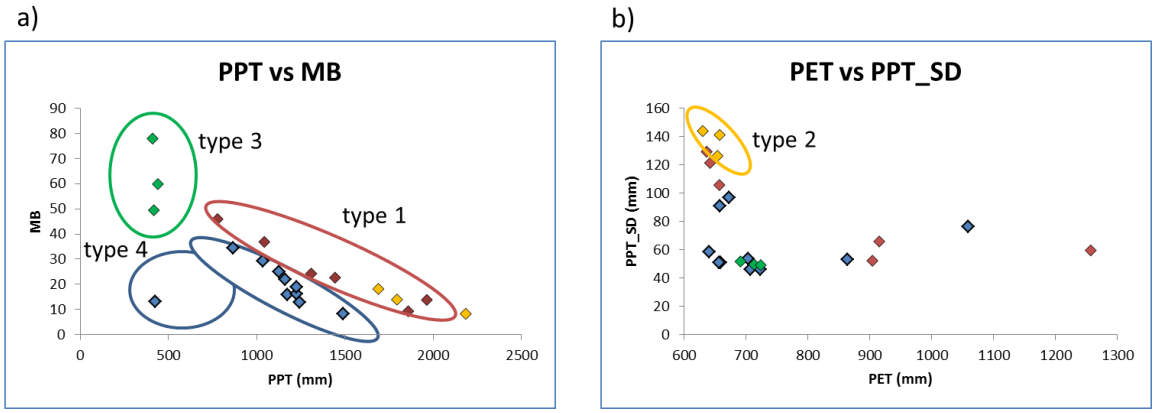

The scatter plot in Figure 5.6, a) shows that PPT and MB distinguished type 3 from the other types, and also type 1 from type 4. On the other hand, scatter plot b) shows that PET and PPT_SD distinguished type 2 from the other types. Overall, four climate variables (annual average precipitation and its annual variability, annual average potential transpiration, and Lancaster's mobility index, which includes PPT and PET,

and percentage of wind that blew above threshold velocity) were found to enable us to interpret the relationship between sand patch patterns and climate variables. Climate characteristics of each patch pattern type are shown in Table 5.7 and metrics and climate variables for each study site are shown in Table 5.8. The summary of statistics of metrics and climate variables for each texture type are shown in Table 5.9.

Table 5.7. Climate characteristics of each patch pattern type.

	Climate characteristics			
Type	PPT (mm)	PET (mm)	PPT_SD (mm)	MB
1	M (ca. 700-2000)			L-M
2		L (<700)	H (>120)	
3	L (<500)			MH (> ca. 50)
4	L-M (<1500)			LM (<40)

L: low, M: mid, H: high, LM: low to mid, and MH: mid to high

Table 5.8. Metrics and climate variables of each study site with patch pattern types.

Site	Type	Metrics				Climate variables			
		PLAND	PLADJ	NLSI	ENN_RA	PPT	PET	MB	PPT_SD
man	1	28.86	91.92	0.08	43.37	1963.04	636.23	13.83	129.35
net	2	2.30	58.38	0.41	81.35	2183.51	629.98	8.28	143.97
nes	1	7.79	81.98	0.18	42.07	1857.56	641.72	9.28	121.42
coo	2	9.32	58.35	0.41	40.21	1688.74	653.71	18.18	126.39
stg	2	7.17	65.62	0.34	36.01	1793.85	657.20	13.94	141.19
eur	4	55.33	91.05	0.11	15.87	1035.10	657.54	29.26	90.92
pta	1	18.09	80.09	0.20	38.71	1043.00	656.73	36.87	105.77
tom	4	39.94	89.97	0.10	27.71	866.80	672.17	34.36	96.75
mar	4	40.06	90.38	0.09	24.74	425.79	706.87	13.14	45.77
mor	3	91.54	97.93	0.21	7.21	439.99	690.84	59.87	51.73
stm	3	70.88	93.44	0.15	8.42	417.34	713.06	49.48	49.59
van	3	85.08	96.24	0.20	15.64	409.96	723.56	77.99	49.17
pad	1	24.76	84.49	0.15	43.32	777.68	1256.48	45.95	59.56
stj	4	62.76	96.17	0.06	28.18	1488.94	1058.49	8.35	76.03
bea	1	23.42	77.23	0.22	32.65	1443.35	915.00	22.66	65.87
hat	1	36.22	83.84	0.16	44.55	1308.36	903.96	24.27	52.26
fal	4	42.52	89.82	0.10	31.79	1172.23	863.99	15.76	53.02
isl	4	56.44	92.59	0.12	22.74	1161.70	722.71	21.82	46.14
fir	4	35.42	88.56	0.11	21.88	1243.26	703.03	12.71	53.77
cha	4	43.03	87.62	0.12	17.79	1227.97	659.01	16.16	50.88
bar	4	61.42	96.14	0.06	28.92	1125.80	656.96	24.90	50.89
plu	4	57.76	94.80	0.10	26.40	1227.86	640.14	18.75	58.58

Table 5.9. Summary of statistics of metrics and climate variables for each type

Type	PLAND				PLADJ				NLSI				ENN_RA			
	Mean	SD	Max	Min	Mean	SD	Max	Min	Mean	SD	Max	Min	Mean	SD	Max	Min
1	23.19	9.67	36.22	7.79	83.26	5.00	91.92	77.23	0.16	0.05	0.20	0.08	40.78	4.46	44.55	32.65
2	6.26	3.59	9.32	2.30	60.78	4.19	65.62	58.35	0.39	0.04	0.41	0.34	52.53	25.05	81.35	36.01
3	82.50	10.57	91.54	70.88	95.87	2.27	97.93	93.44	0.19	0.03	0.21	0.15	10.42	4.56	15.64	7.21
4	49.47	10.21	62.76	35.42	91.71	3.08	96.17	87.62	0.10	0.02	0.12	0.06	24.60	5.05	31.79	15.87

Type	PPT				MB				PPT_SD				PET			
	Mean	SD	Max	Min	Mean	SD	Max	Min	Mean	SD	Max	Min	Mean	SD	Max	Min
1	1398.83	458.56	1963.04	777.68	25.48	13.83	45.95	9.28	89.04	33.80	129.35	52.26	835.02	243.90	1256.48	636.2
2	1888.70	260.67	2183.51	1688.74	13.47	4.96	18.18	8.28	137.18	9.45	143.97	126.39	646.96	14.81	657.20	630.0
3	422.43	15.65	439.99	409.96	62.45	14.43	77.99	49.48	50.16	1.37	51.73	49.17	709.15	16.70	723.56	690.9
4	1097.54	284.27	1488.94	425.79	19.52	8.08	34.36	8.35	62.27	18.75	96.75	45.77	734.09	130.83	1058.49	640.1

5.6 Regression analysis of metrics and climate variables

Linear regressions with four metrics (PLAND, PLADJ, NLSI, and ENN_RA) and the four climate variables: PPT, PET, PPT_SD, and MB, identified in the scatter diagrams as distinguishing the foredune patch pattern types, were made in SPSS 16.0 GP to see which climate variables could explain the metrics (Table 5.10). In the regression, each metric is a dependent variable and each climate variable is an independent variable. Linear regression analysis reveals statistically important relationships between PLAND and PPT ($R^2 = 0.517$); PLAND and PPT_SD ($R^2 = 0.508$); PLADJ and PPT_SD ($R^2 = 0.507$); NLSI and PPT_SD ($R^2 = 0.353$); ENN_RA and PPT ($R^2 = 0.533$); and ENN_RA and PPT_SD ($R^2 = 0.42$).

Table 5.10. Linear regression analysis of metrics and climate variables.

Metrics		Climate variables			
		PPT	PET	PPT_SD	MB
PLAND	R^2	0.517	0.084	0.508	0.366
	Significance level	*0.000*	*0.449*	*0.000*	*0.001*
PLADJ	R^2	0.392	0.014	0.507	0.135
	Significance level	*0.001*	*0.299*	*0.000*	*0.046*
NLSI	R^2	0.155	0.036	0.353	0.000
	Significance level	*0.035*	*0.199*	*0.002*	*0.498*
ENN_RA	R^2	0.533	0.006	0.420	0.220
	Significance level	*0.000*	*0.363*	*0.001*	*0.014*

In addition, multiple regression analyses were done in SPSS 16.0 GP in which each metric was a dependent variable and the four climate variables were independent variables. The results of these multiple regressions are shown in Table 5.11. PLAND has the highest regression ($R^2 = 0.691$), but the rest of the metrics also had high regression

values. Only the significance level of NLSI was a bit higher ($R^2 = 0.035$), but its regression value was still high (0.439) at the 5 % significance level.

Table 5.11. Multiple regression results with four climate variables (PPT, PET, PPT_SD, and MB).

Metric		Value
PLAND	R^2	0.691
	Significance level	*0.003*
PLADJ	R^2	0.541
	Significance level	*0.000*
NLSI	R^2	0.439
	Significance level	*0.035*
ENN_RA	R^2	0.629
	Significance level	*0.001*

5.7 Climate (cumulative average) and bare sand area

To see how many years of climate data are optimal for the statistical prediction of the amount of bare sand area (PLAND), linear regressions were performed using SPSS. Metric PLAND from both old and new images was set as a dependent variable and each year of cumulative averages of PPT for both old and new images was set as an independent variable. Figure 5.7 a) shows that a plateau occurs after the 7th year and several abrupt breaks occur in the 15th, 20th and 27th years. Figure 5.7 b) is a scatter plot made with PLAND and cumulative averages of PPT for only 13 of the sites that have all 30 years of cumulative averages of PPT. The graph also shows that a plateau occurs after the 7th year.

Figure 5.7. Scatter plots showing regression with PLAND and PPT. a) all 44 old and new images, and b) only 13 new images that have all 30 years of PPT, because the original aerial photos were taken in 2009.

a)

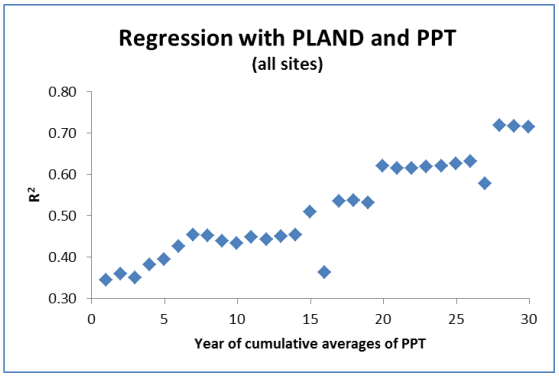

b)

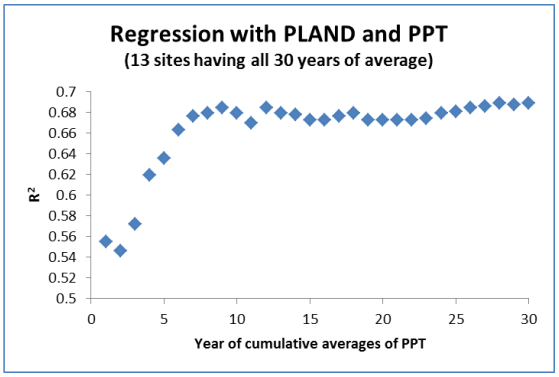

6 DISCUSSION

6.1 Section introduction

In this chapter the results presented in the previous chapter are discussed. The first section explains how foredune texture types obtained from cluster analysis are related to climate variables and how the types are distinguished one from another. Lancaster's (1988) and Tsoar's (2005) dune mobility indices are compared and then a better index for this study is discussed in more detail. Relationships between bare sand areas and mean annual precipitation are discussed and compared with Hugenholtz and Wolfe's (2005b) results. This chapter concludes with a discussion on foredune development resulting from climate change in the future.

6.2 Foredune texture types and climate controls

Figure 6.1 a) shows that plots of type 1 (red) that are small and somewhat aggregated in foredune texture, are located parallel to those of type 4 (blue). On the other hand, Figure 6.1 b) shows that plots of the two types (type 1 and 4) are distributed without any trend. Figure 5.4 (scatter plot matrix) shows that types 1 and 4 are close to each other in any metric combinations, while types 2 and 3 tend to be at the extreme sides. However, type 1 and type 4 can be divided by the line in Figure 6.1 a) whose slope and intercept are 0.035 and 68 respectively. Therefore, given the annual mean precipitation (PPT) and the mobility index (MB), if a site is up from the line ($y = 0.035x + 68$), the site falls into type 1; if a site is down from the line, the site falls into type 4.

Figure 6.1. Foredune texture types and climate controls. Type 1 is in red; 2 in orange; 3 in green; and 4 in blue. a) PPT vs MB marked by clusters and b) PET vs PPT_SD. Note: x axis of diagram b) starts from 600. Note: mar (Marina, CA), man (Manzanita, OR), and nes (Nestucca, OR).

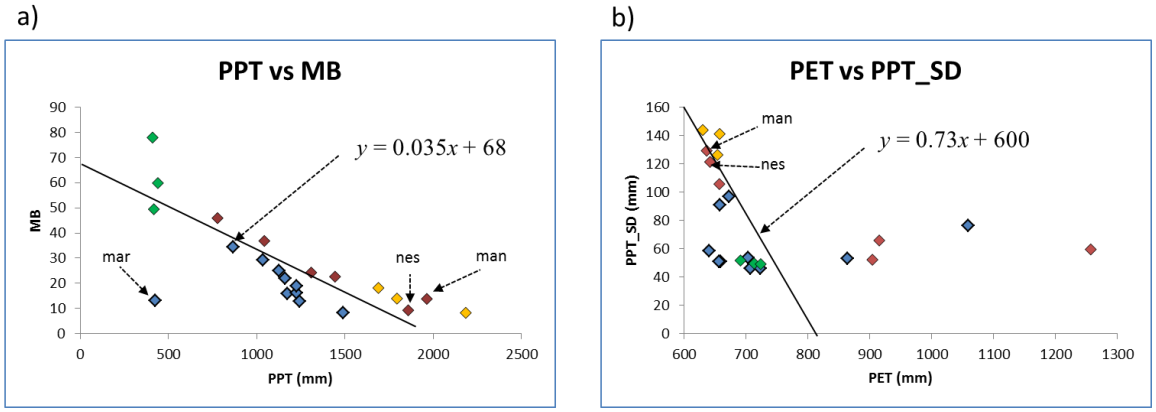

Type 2 (Nestucca, OR, Coos Bay, OR, and St. George, CA) that is small, irregular, and disaggregated in foredune texture, can be distinguished by a line whose slope and intercept are 0.73 and 600 respectively (Figure 6.1 b). However, as shown in Figure 6.1 a), type 2 is also above the line, but mixed with some type 1 sites. So in order for a site to fall into type 1 or 2, it is necessary to use both the lines shown in Figure 6.1 a) and b). The two type 1 sites that plot very close to type 2 sites are Manzanita, OR and Nestucca, OR. These three type 2 sites and two type 1 sites (Manzanita and Nestucca) are located near each other on the northwest coast of the United States (Figure 5.3). In terms of foredune texture, Manzanita and Nestucca are similar to type 2; the latter is more disaggregated. The values of PLAND (the percentage of bare sand area) demonstrate this, showing that the PLAND values of old images of the two (Manzanita and Nestucca) are greater than those of new images: old 36% and new 21% in Manzanita; and old 9% and new 6% in Nestucca. Therefore, it is suggested that the Manzanita and

Nestucca sites are in transition from type 1 to type 2 (to restoration status with more vegetation cover).

Sites of type 3 (Morro Bay, CA, St. Maria, CA, and Vandenberg, CA) that are very large, but few in foredune texture are all on the southwest coast of the United States. They received the smallest amount of rainfall–less than 500 mm annually (Figure 6.1 a). Although type 3 sites have higher annual mean potential evapotranspiration (PET: average PET is ca. 709 mm) than other sites on the west coast, (average annual PET is ca. 657 mm), PET values of all study sites except five (Padre Island, TX, St. Joseph, FL, Bear Island, NC, Hatters, NC, and False Cape, VA) are less than 800 mm (Table 3.1 and Figure 6.3). Therefore, PET does not play a significant role in distinguishing type 3 sites from others. Instead, a relatively high MB, greater than ca. 50, and low PPT, less than 500 mm, are the most important climate variables associated with type 3 sites.

Type 4 sites (Eureka, CA, Tomales, CA, Marina, CA, St. Joseph, FL, False Cape, VA, Island Beach, NJ, Fire Island, NY, Chappaquiddick, MA, Barnstable, MA, and Plum Island, MA) that are relatively large, but few and aggregated in foredune texture, have three sites on the west coast, one on the Gulf of Mexico, and the others are on the northeast coast of the United States. Type 4 sites can be distinguished from type 1 by the line in Figure 6.1 a). Both types 3 and 4 have similar climate characteristics: mid to high PPT (except Marina, Manzanita and Nestucca) and low to mid MB.

One site, Marina, a type 4, is located outside the majority of type 4s shown in plot a) in Figure 6.1. This is probably because Marina is located in Monterey Bay, CA (Figure 6.2), which is concave seaward. As Cooper (1967) mentioned, approaching wind

diffuses over the bay and its speed decreases. Table 3.1 shows that the mean wind speed of Marina, CA is 3.5 m/s, less than the sites nearby, and is the least wind speed among all other study sites. In addition to it, the invasion of non-native species, ice plant (*Carpobrotus edulis*) can account for this. Ice plant is a succulent and perennial plant introduced in early 1900s from South Africa into coastal dune fields in Monterey, U.S. to stabilize dunes (D'Antonio 1993; Guinon and Allen 1990). Marina dune field stabilized with the thick and mat-forming plant was probably more resistant to drier condition.

As described in the Background chapter, moisture and wind are the most important factors controlling coastal dune growth and development. The results of this study confirm this. Two moisture variables and a wind variable are associated with sand patch patterns in this study: annual mean precipitation (PPT), annual variability of precipitation (PPT_SD), and Lancaster's mobility index (MB), which contains the percentage of wind above threshold velocity (Vt) of all wind events (All). However, MB can be either a moisture or wind variable because it contains the terms PPT/PET and Vt/All (percentage of wind above threshold velocity).

Figure 6.2. Google image showing the Marina dune field that is located in Monterey Bay, CA.

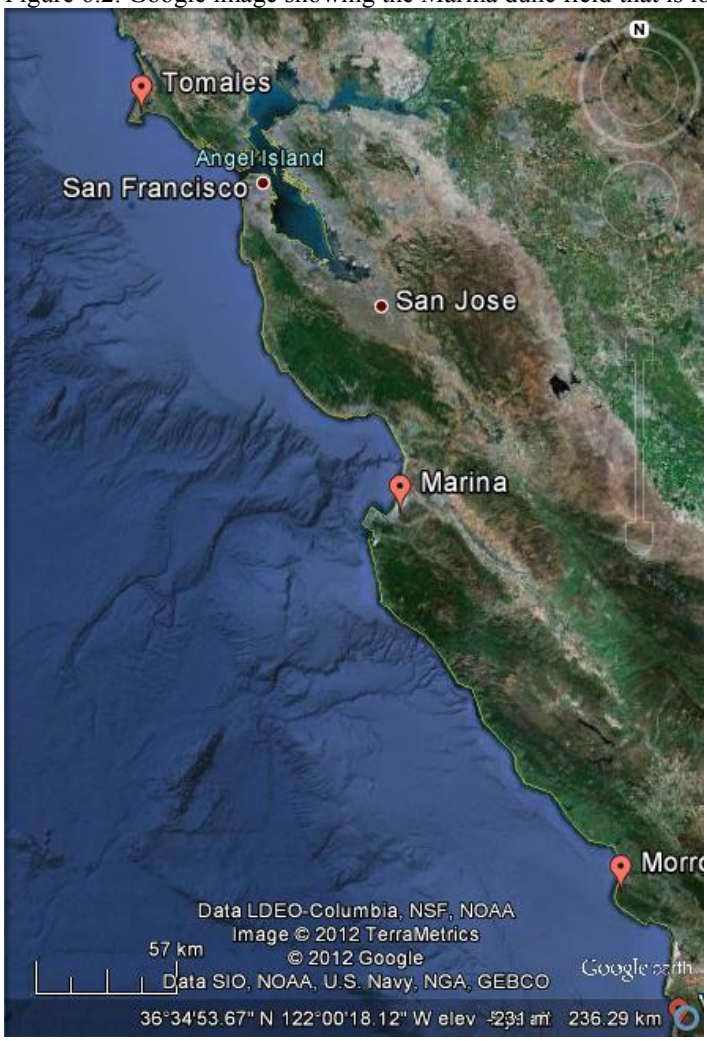

Figure 6.3. Potential evapotranspiration (PET) of all study sites. Except for five sites (pad, stj, bea, hat, and fal), all other sites measure less than 800 mm in PET.

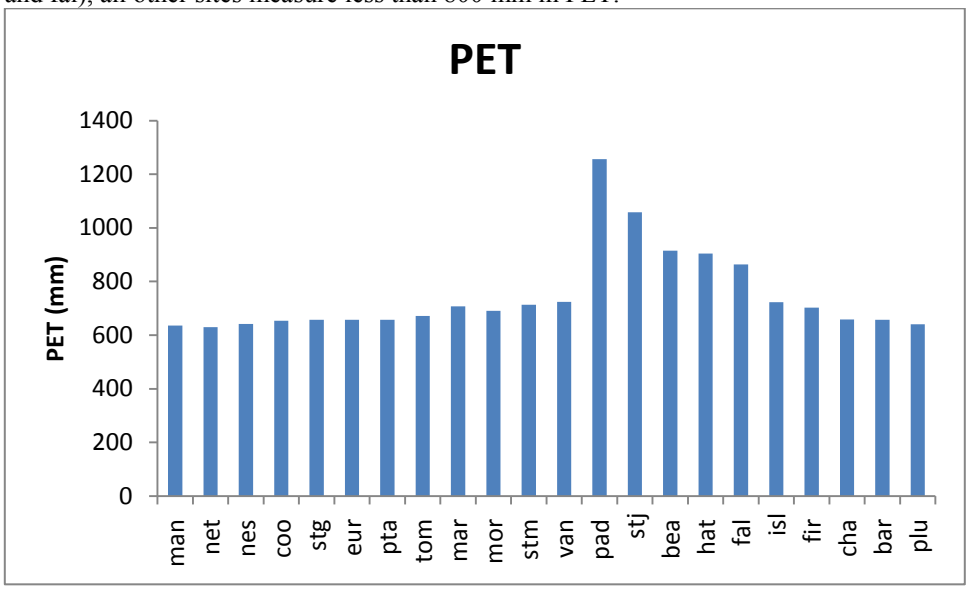

6.3 Dune mobility index and coastal sand dune fields

I evaluated the two mobility indices of Tsoar (2005) and Lancaster (1988). I found that Lancaster's mobility index (MB) is useful as one of the climate variables to distinguish sand patch pattern types, but I did not find any relationship between Tsoar's mobility index (MB_2) and sand patch patterns. The reason why Lancaster's mobility index works better for this study is because Lancaster's index contains a moisture component (P/PET), whereas Tsoar's index does not. Tsoar considered only wind power (drift potential: DP and resultant drift potential: RDP) in dune mobility because he said that moisture was not important due to sand's unique characteristics of high permeability and large pore space. This is probably true because he applied his index only to desert dunes. MB has been applied to arid environments and was successful (Muhs and Maat 1993; Muhs and Holliday 1995; Wolfe 1997).

In order to understand how MB influences foredune texture, it is necessary to understand how PPT/PET and Vt/All work in MB. First, I found that PPT:PET is strongly correlated with PPT (R = 0.95), so I made a scatter plot of PPT and inverse PPT:PET (PPT:PET/1) (Figure 6.4) to make it look similar to Figure 6.1 a). The patterns of the plot are similar to those of Figure 6.1 a), but the plot cannot distinguish type 4 from others because type 4 sites are more spread out than those shown in Figure 6.1 a) and mixed with sites of different types, for example types 1 and 3. I also calculated the correlation of Vt/All with each of four metrics (PLAND, PLADJ, NLSI, and ENN_RA) and found that there is no correlation between Vt/All and all the metrics. The R^2 of all metrics with Vt/All are less than 1 %. In this way, MB containing PPT:PET and Vt/All can explain a part of the sand patch patter types, but P:PET or Vt/All alone does not.

Figure 6.4. Plots with PPT and inverse P:PET. Inverse P:PET is used to compare with PPT and MB. Dots are marked by the type of foredune texture: type 1 in red, 2 in orange, 3 in green, and 4 in blue. Note that a site of type 1 (red arrow) is among type 4 and a site of type 4 (blue arrow) is among type 3. Compare this plot with Figure 6.1 a).

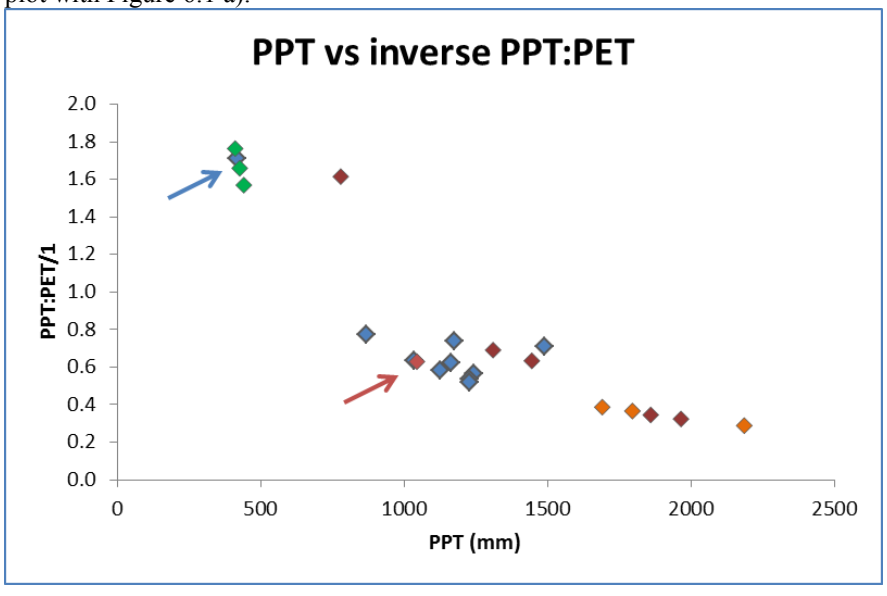

6.4 Relationship between bare sand area and mean annual PPT

Hugenholtz (2005b) investigated dune mobility and climate variations in southern Canadian prairies from the early 1900s to 1997. He compared average values for PPT:PET and wind speed with the decrease in dune mobility. R^2 values showed that the average annual wind speed explains only 4 % of the variability in dune stabilization and PPT:PET explains 28 % at the 95 % confidence level. Although only a small part of the variability can be explained by the small values of R^2 of the two climate variables (PPT:PET and average wind speed) in terms of dune stabilization, he suggested that dune activity can respond to recent climate variations, particularly aridity from the 1700s.

Prior to investigating the relationship between bare sand area (PLAND) and mean annual precipitation (PPT), a linear regression between average PPT:PET and PLAND was calculated and compared to the regression between PPT and PLAND (Figure 6.5). The R^2 of PLAND with PPT (0.52) is slightly greater than R^2 with PPT:PET (0.48) and both are at the 99 % confidence level. So I use PPT instead of PPT:PET to investigate the relationship between bare sand area and climate to compare Hugenholtz's results because PPT explains PLAND better than PPT:PET, and as described in the section above, PET is not a decisive factor in this study.

Figure 6.5. Plots of a) PLAND with PPT and b) PPT:PET. The R^2 values of both are at the 99 % confidence level.

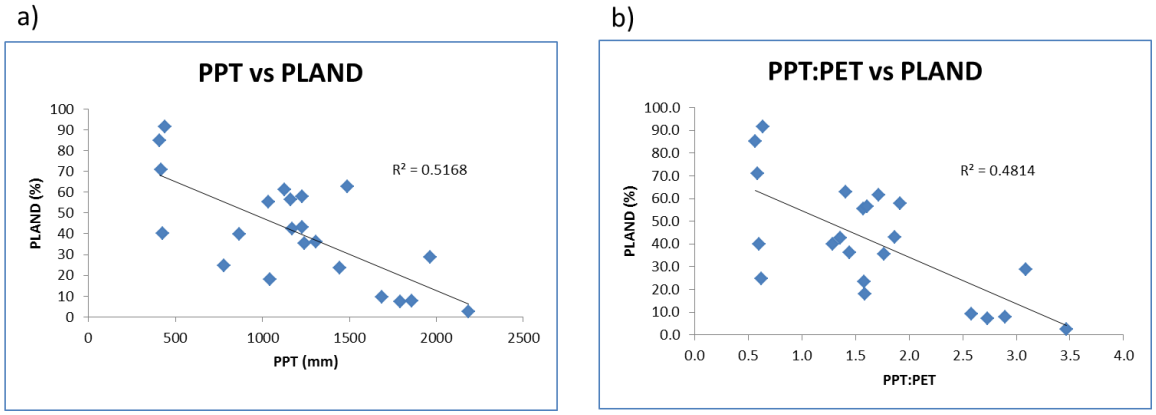

The R^2 value of PLAND and PPT (0.52) in this study is almost twice that of the decrease in dune activity and PPT:PET (0.28) in Hugenholtz (2005b). It is probably because coastal dune systems have much more rainfall than inland dune systems in the Canadian Prairie, so moisture availability is a decisive factor for dune mobility in coastal dune systems. A high correlation between PLAND and PPT_SD (0.51) shown in Table 5.9 demonstrates that moisture is very important to dune mobility expressed in the amount of bare sand area.

In order to understand the relationship between PLAND and wind power, linear regressions were conducted between PLAND and variables related to wind speed: DP (drift potential), OSDP (onshore drift potential), RDP (resultant drift potential), RDP/DP, OSRDP (onshore RDP), MB_2 (Tsoar's mobility index), OSRDP/DP (onshore RDP/DP), Vt/All (percentage of wind above threshold velocity out of all wind events), and OS/All (percentage of onshore wind out of all wind events). None of them showed a significant correlation. The maximum value of R^2 is only 0.04 (PLAND and DP), which

corresponds to Hugenholtz' result (0.04) conducted in a land dune system. This shows that a wind variable alone cannot explain PLAND. On the other hand, the R^2 value of PLAND and Lancaster's mobility index (MB) is 0.37 at a 99% confidence level (Figure 6.6). This shows that Lancaster's mobility index can explain some of the variability in terms of dune activity in coastal systems, which is different from the result of Hugenholtz. Considering all of these, I suggest that dune activity or stabilization in a coastal dune system is mainly controlled by vegetation cover, which is in turn affected by annual mean rainfall.

Figure 6.6. Positive correlations between PLAND and MB (Lancaster's mobility index)

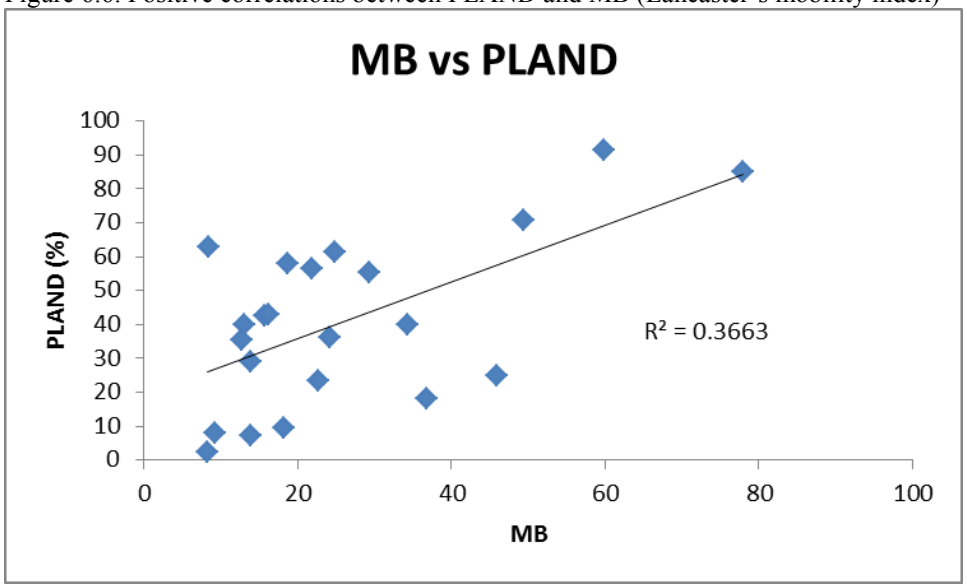

In addition, linear regressions were performed to find an optimal averaging period of PPT for PLAND. The R^2 value of PLAND and cumulative averages of PPT for all 44 sites of both old and new images is 0.45 at the 7^{th} year where the slope of the plot

starts to significantly decrease and become a plateau (Figure 6.7 a). On the other hand, the R^2 value for 13 sites that are new images having all 30 years of averages is 0.68 at the 7th year where the slope of the plot starts to decrease (Figure 6.7 b). Figure 6.7 a) shows abrupt breaks that occur at the 15th, 20th, and 27th years. This is because, as shown in Table 4.1, the years when old images were taken are different. The oldest image (St. George, CA) was taken in 1988, the next oldest ones in 1989, and then in 1993. From the 15th year (in 1993), five sites are eliminated, so the R^2 value increases and an abrupt break occurs. From the 20th year (in 1998), all the old images are eliminated and only the new images are left and so on. However, in Figure 6.7 b), no abrupt break is found, because all the images have 30 year cumulative averages. The result shows that no matter what the R^2 values are, 7 year PPT data is enough to investigate bare sand areas on coastal dune systems.

Figure 6.7. Plots showing the regression of PLAND and cumulative averages of PPT. a) all 44 old and new images, and b) only 13 new images that have all 30 years of PPT. The red arrows indicate the year when plateaus start; both occur at the 7th year.

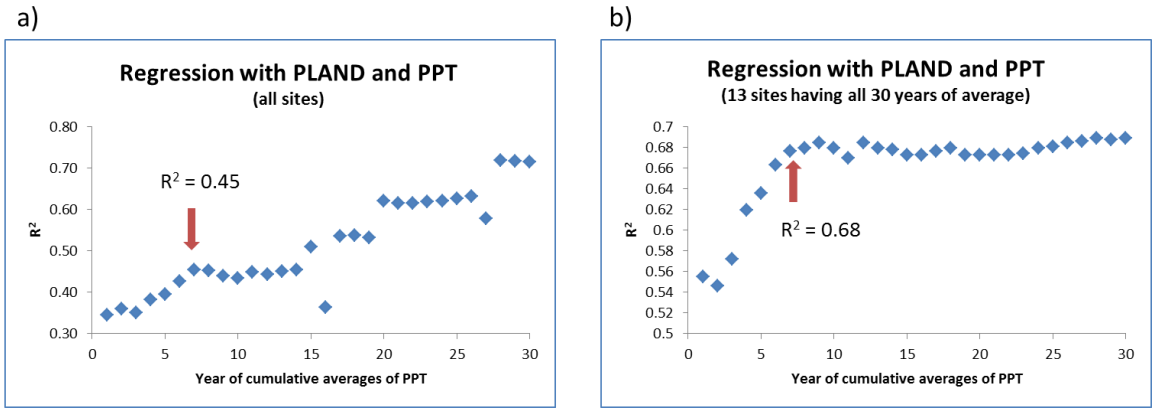

6.5 Comparison of bare sand area between old and new images

The amount of bare sand area (PLAND) of both old and new images for each site was examined and Island Beach, NJ and Plum Island, MA, showed the biggest differences between the old and new images (Figure 6.8). The values of the old PLAND for both sites are greater than those of the new PLAND, which indicates that the bare sand areas had been covered again with vegetation. However, climate data cannot account for the differences, because 30 year climate of the two sites have similar patterns to those of the close sites (Table 3.1 and 5.8).

The larger amount of bare sand areas of the old images of the east coast taken in 1995 can be explained by Northeasters in 1991 and 1992 that were major events damaging the east coast of the U.S. (Butman, Sherwood, and Dalyander 2008). The New Jersey coast was seriously damaged by the northeast storms that occurred on October 28 – November 2, 1991, followed by another storm on December 11 – 12, 1992 (Donnelly et al. 2004). Particularly, the December 1992 storm was severe on the New Jersey coast (Zhang, Douglas, and Leatherman 2001) and it generated a significant wave height of 7.6 m, maximum wind gusts at 24.7 m/s at Atlantic City, and a maximum water level elevation of 2.25 m above mean sea level which caused severe erosion of dunes (Nordstrom and Jackson 1995).

Figure 6.8. Comparison of bare sand area (PLAND). Island Beach, NJ ('isl') and Plum Island, MA ('plu') show the biggest differences between old and new images.

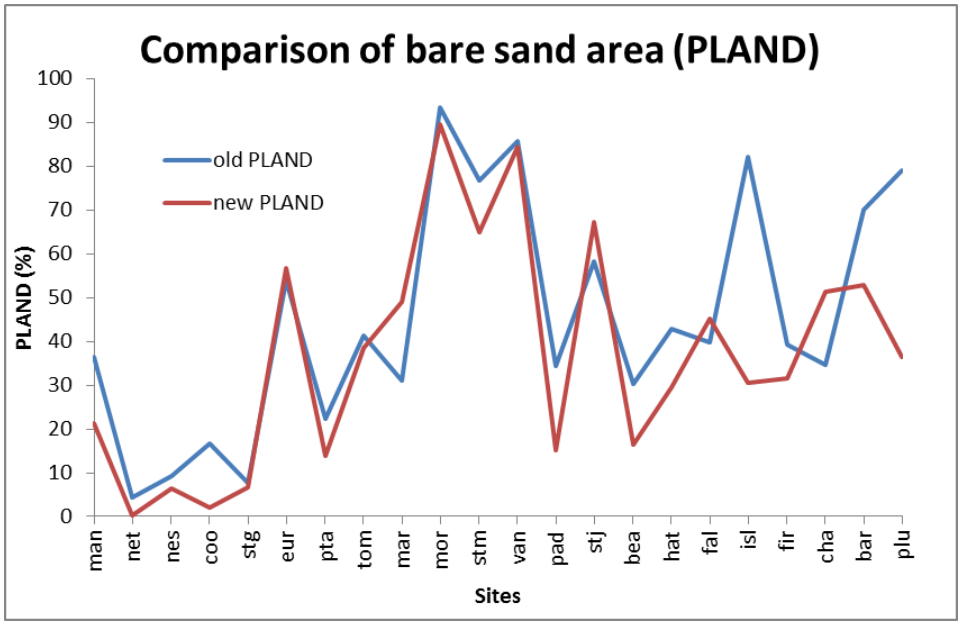

The November 1991 storm (aka Halloween Eve Storm or "Perfect Storm") was of unusually long duration and it generated high waves, a storm surge, and a high wind velocity of over 40 knots in combination with the remnants of Hurricane Grace (Davis and Dolan 1992). The 1991 storm damaged the east coast, from Cape Cod, NC through the coast of Maine and caused severe erosions of beaches and foredunes, particularly in Massachusetts (FitzGerald, van Heteren, and Montello 1994) where the cost of damage to the state reached $100,000,000's (McCown 2011).

Foredunes damaged by the storms have been restored through time by vegetation cover, which can be observed on the aerial photographs. The 1995 images for both Island Beach and Plum Island might still have shown that the areas were not fully recovered from the damage in three years, but 2008 images for both sites show that they

had significantly recovered from 82 % of PLAND to 36 % on Island Beach (Figure 5.1 r-1 and r-2) and from79 % to 36 % on Plum Island (Figure 5.1 v-1 and v-2). However, the damage of other east coast sites of the U.S. such as Hatteras, NC, False Cape, VA, Fire Island, NY, and Chappaquiddick and Barnstable, MA, might not have been to the same degree. This is probably because actual damage can be affected by many different local factors such as the ocean-bottom profile, the shoreline's orientation to the open ocean, tides, and the extent of dunes (Davis and Dolan 1993; Sallenger Jr 2000; Houser, Hapke, and Hamilton 2008).

6.6 Climate change and foredune development

According to the Fourth Assessment Report of Intergovernmental Panel on Climate Change (IPCC) (Christensen et al. 2007), annual mean precipitation will generally increase in North America, except for southwest and the south of the U.S. Researchers agreed that dune mobility is associated with vegetation cover and the vegetation is affected by precipitation and wind speed (Barchyn and Hugenholtz 2012; Hugenholtz and Wolfe 2006; Marin et al. 2005; Nield and Baas 2008). A drier climate, higher wind velocity, and concentrated wind direction accelerates dune activity caused by the destruction of vegetation cover.

Muhs and Maat (1993) investigated the relationship between dune activity and global climate change in Great Plains of the U.S. They used Lancaster's mobility index to observe the dune activity and found that the most dunes of the study sites were stabilized. They increased W (the time that wind above threshold velocity blew) by 20 % and found that dunes responded to increase in W. Thus, increased MB with increase in

W shows that the most dune fields would evolve into active dunes. This was demonstrated by comparing two aerial photographs taken in 1936 and 1983. In the 1930s, higher temperatures and wind speed and lower precipitation in this area cause 1936 aerial photographs to show fully active transverse and barchan dunes, although 1983 aerial photographs showed that most dunes were stabilized.

My study shows that four climate variables (PPT, PET, PPT_SD, and MB) are related to foredune textures. Particularly, Figure 6.1 a) shows that two climate variables (PPT and MB) are useful in explaining foredune textures. In order to investigate how foredune textures will change with PPT, I assumed that PPT will decrease by 10 %, 20 %, and 30 % and increase by 10 %, 20 %, and 30 % from the current average (1979 – 2008), but wind speed and temperature expressed in annual mean potential evapotranspiration (PET) will not change.

Figure 6.9. Diagrams showing decrease in PPT. Dots are foredune textures and circles are the original places of foredune textures. Texture type 1 is in red, 2 in orange, 3 in green, and 4 in blue.

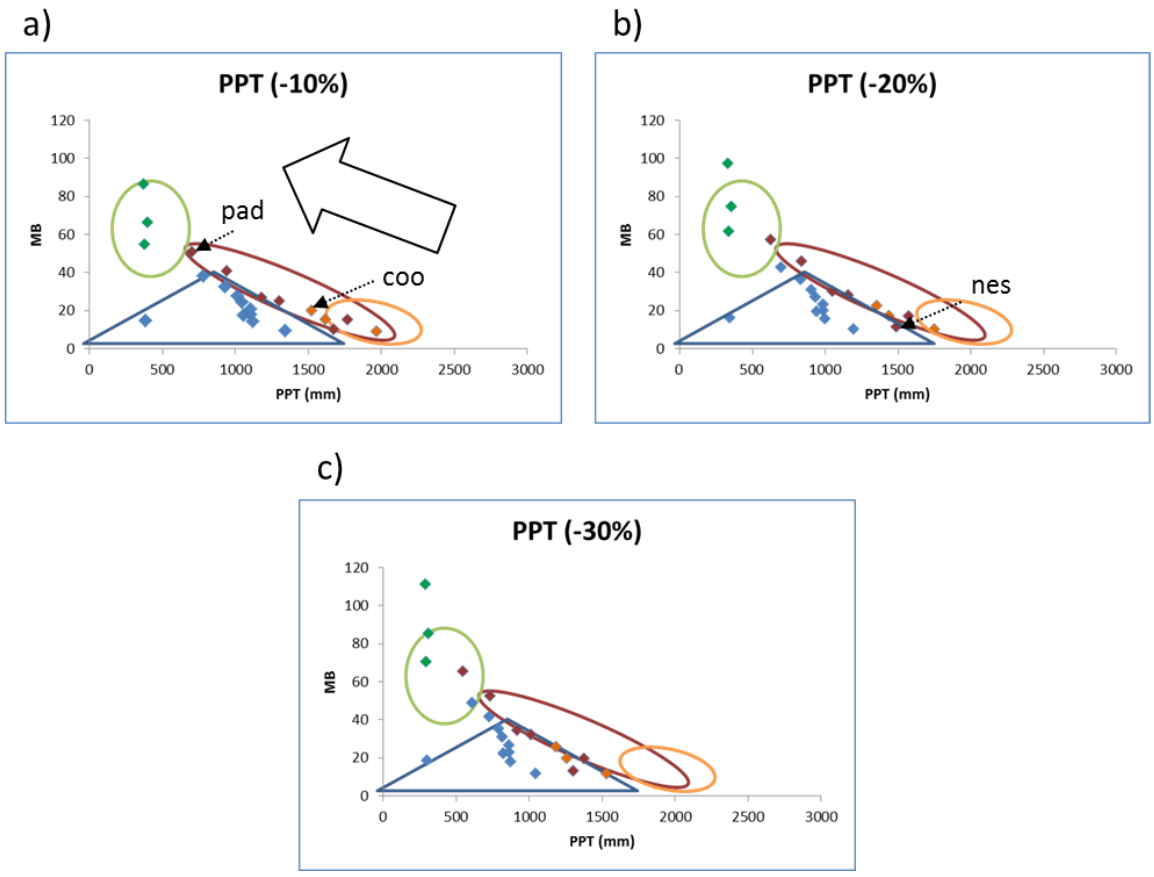

In this way, I made six plots of MB vs. PPT. The first three diagrams are plots that show decrease in PPT by 10 %, 20 %, and 30 % and the second three plots show increase in PPT by 10 %, 20 %, and 30 %. Circles are the original places of the plots under current climate conditions (1979 – 2008). The decrease in PPT causes foredune texture types to move left, and at the same time, the increase in MB causes patch types to move upward, because MB has PPT in the equation. When PPT decreases by 10 % (Figure 6.9 a), the overall movement of texture types is left. Decrease in PPT by 10 % does not cause foredune textures to change from one type to another except a site ('coo':

Coos Bay, OR) of type 2 (orange). When PPT decreases by 20 % (Figure 6.9 b), one site (Padre Island, TX) of type 1 (red) changes to type 3 (green) and one site ('nes': Nestucca, OR) of type 1 changes to type 4 (blue). However, most sites of type 4 remain in the current type. The decrease in PPT by 30 % (Figure 6.9 c) causes texture types to change significantly. Although sites of type 1 are likely to remain in the current type or around the boundary between type 1 and 4, all sites of type 2 (orange) change to texture types between type 1 and 4. Type 3 will move further toward upper left corner. Most sites of type 4 remain in the current type.

The increase in PPT causes foredune texture types to move right, and at the same time, the decrease in MB causes patch types to move downward, because MB has PPT in the equation. When PPT increases by 10 % (Figure 6.10 a), the overall movement of texture types is right. Increase in PPT by 10 % causes several sites ('man': Manzanita, OR of type 1, and 'stj': St. Joseph, FL of type 4) to move to other types, but most sites still remain in the current types. Increase in PPT by 20 % (Figure 6.10 b) causes two sites of type 1 to move to type 2 and most sites of type 4 to move toward type 1, but remain around the boundary between type 2 and 4. Increase in PPT by 30 % (Figure 6.10 c) causes most sites of type 4 except for Marina, CA ('mar') to move to type 1, but type 2 and 3 still remain in the current types, although type 2 move further right.

According to Figure 11.12 (p. 890) in the report of IPCC (Christensen et al. 2007, p. 890), the southwest and south of the U.S. will likely have less annual precipitation by about 5 to 10 %. Hence, the diagram of decrease in PPT by 10 % (Figure 6.9 a) will be applied to those sites (all type 3 sites (Morro Bay, St. Maria, and Vandenberg, CA) in

green and Padre Island ('pad') of type 1 in red), but those sites will remain in the current type, although they move toward upper left corner. The amount of bare sand area of type 3 sites is greater than 70 % and the average of them is about 83 %. Therefore, they seem to be responding to drier climate in the diagrams, but they will not change much, because the almost entire dune fields are already filled with sand patches. Increase in annual PPT by 10 % will likely occur in the northeast of the U.S. and hence, the diagram of increase in PPT by 10 % can be applied to the sites (Figure 6.10 a). However, the sites will remain in the type 4, although they move toward type 1. For the northeast sites to change their texture types, this result shows that PPT should increase by more than 10 %.

Figure 6.10. Diagrams showing increase in PPT. Dots are foredune textures and circles are the original places of foredune textures. Texture type 1 is in red, 2 in orange, 3 in green, and 4 in blue. Broken box indicates sites located on the northeast coast in the U.S., including Island Beach, NJ, Fire Island, NY, Chappaquiddick, MA, Barnstable, MA, and Plum Island, MA.

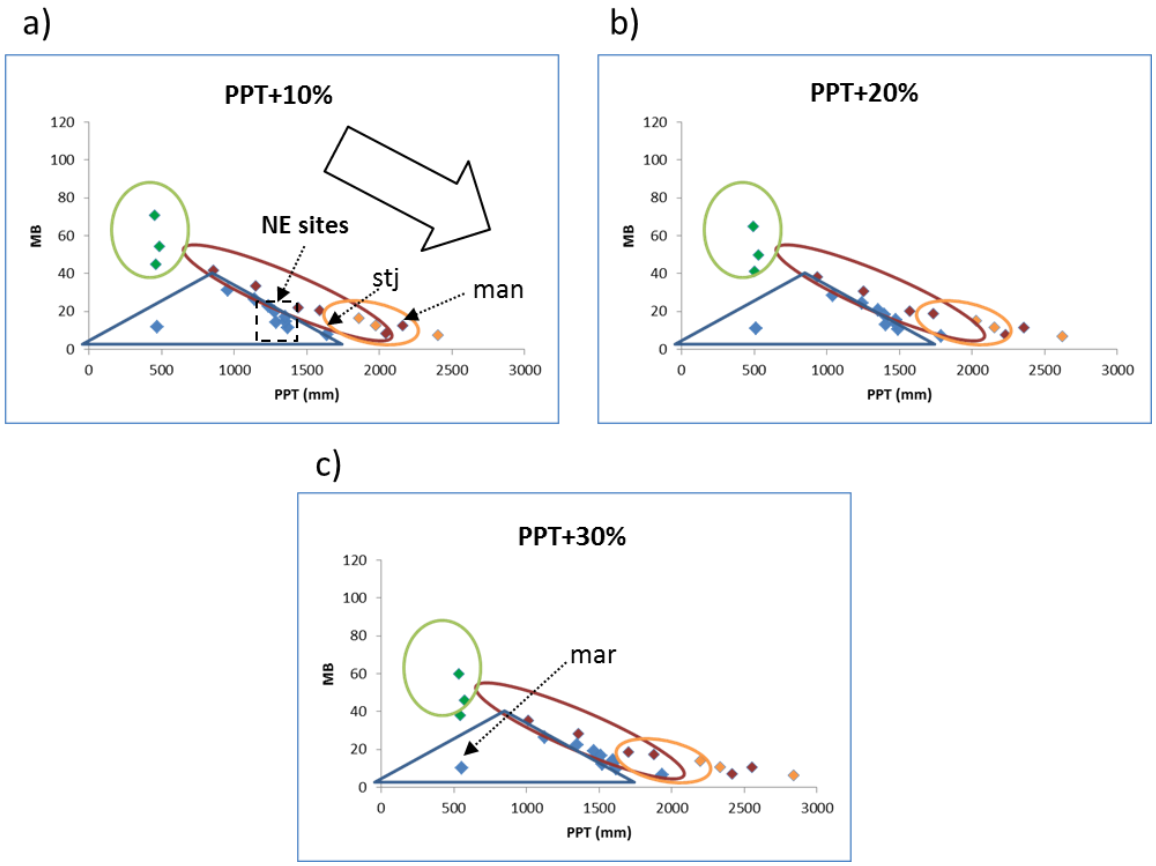

7 CONCLUSIONS

Digital aerial photographs of twenty-two dune fields on the coastal dune systems of the United States were quantified based on sand patch textures by applying the concepts and methodology of landscape ecology. Four foredune types were obtained through hierarchical cluster analysis and the metrics of PLAND (percentage of bare sand area), PLADJ (proportion of like adjacencies), NLSI (normalized landscape shape index), and ENN_RA (range of Euclidean nearest neighbor) were used to characterize in the foredune types. The characteristics of each type are as follows.

- Type 1 is comprised of small patches, somewhat aggregated mainly on the seaward slope of foredunes.
- Type 2 is composed of small and irregular patches, but foredune texture is disaggregated with a long distance between patches.
- Type 3 is made up of several, very large sized patches.
- Type 4 is relatively large, (smaller than type 3), but has few and aggregated sand patches.

Four climate variables (annual mean precipitation (PPT), annual mean potential transpiration (PET), Lancaster's mobility index (MB), and standard deviation of PPT (PPT_SD)) were found to be involved in the foredune types and in distinguishing one foredune type from another. The characteristics of climate for each foredune type are as follows.

- Type 1 is mid to high in PPT and low to mid in MB, and similar to type 4 in climate characteristics. Type 1 can be distinguished by a line ($y = 0.035x + 68$) of a plot of PPT and MB.
- Type 2 is high in PPT, low in MB, and low in PET, and can be distinguished from other types by a line ($y = 0.73x + 600$) of a plot of PET and PPT_SD.
- Type 3 is low in PPT and mid to high in MB. Because type 3 has unique climate characteristics, it can easily be distinguished from other types.
- Type 4 is mid in PPT and low to mid in MB. Type 1 and type 4 have similar climate characteristics and can be distinguished one from another by a line ($y = 0.035x + 68$) of a plot of PPT and MB.

Lancaster's mobility index (1988) works well for this study because it contains PPT and PET terms in the equation. However, Tsoar's mobility index (2005) does not show any relationships with the foredune types because it has only wind power terms (DP: drift potential and RDP: resultant drift potential). The R^2 value of the amount of bare sand area with PPT is 0.52, 0.51 with PPT_SD, and 0.37 with MB. MB, containing the ratio of PPT to PET (PPT:PET) and the percentage of threshold velocity of all wind events (Vt/All), can explain a part of the sand patch textures ($R^2 = 0.37$), but PPT:PET or Vt/All alone does not. The R^2 value (0.52) of PPT with PLAND suggested that dune activity or stabilization in coastal dune systems is mainly controlled by vegetation cover, which is in turn affected by PPT. Foredune types can be predicted in association with climate change. A drier climate will cause sand patches to become larger and more aggregated and eventually current foredune types will be similar to current type 3.

The optimal averaging period of precipitation for each bare sand area was obtained using linear regression between each cumulative averages of precipitation and PLAND. The R^2 values start to stabilize at the 7^{th} year of cumulative averages of PPT in both old and new images and new image with all 30 year averages. It was suggested that 7 year annual mean precipitation data is enough to investigate bare sand areas on coastal dune systems.

A foredune is a dynamic feature in a coastal system and forms and grows in association with vegetation. Climate variables such as wind (for sand transport) and rainfall or rainfall efficiency (for vegetation cover) are important for foredunes. However, vegetated dunes are susceptible to the effects of natural changes and those created by humans. This study demonstrates this in that climate variables, particularly annual mean precipitation and its variations, and mobility index, are important to foredune types classified by sand patch size and patterns, which enables prediction of the future development of foredune types in association with climate change.

REFERENCES

Arpin, O. E. 1970. Tidal inlet problems along the New England Coast. Paper read at Proceedings of 12th Conference on Coastal Engineering, at Washington, D.C.

Ash, J., and R. Wasson. 1983. Vegetation and sand mobility in the Australian desert dunefield. *Zeitschrift fur Geomorphologie Supplementband* 45:7-25.

Barbour, M. G., T. M. de Jong, and A. F. Johnson. 1976. Synecology of beach vegetation along the Pacific Coast of the United States of America: a first approximation. *Journal of Biogeography* 3 (1):55-69.

Barchyn, T. E., and C. H. Hugenholtz. 2012. Aeolian dune field geomorphology modulates the stabilization rate imposed by climate. *Journal of Geophysical Research* 117 (F2):F02035.

Bible, A. H. 1962. Padre Island National Seashore, Tex: Committee on Interior and Insular Affairs.

Bird, E. C. F., and M. L. Schwartz. 1985. *The world's coastline*. New York: Van Nostrand Reinhold.

Bonacker, G. L., R. C. Martin, and R. E. Frenkel. 1979. Preserve analysis: Netarts Sand Spit, 56: Oregon Natural Area Preserves Advisory Committee.

Bullard, J., D. Thomas, I. Livingstone, and G. Wiggs. 1997. Dunefield activity and interactions with climatic variability in the southwest Kalahari Desert. *Earth Surface Processes and Landforms* 22 (2):165-174.

Burel, F., and J. Baudry. 2003. *Landscape ecology: concepts, methods, and applications.* New Hampshire: Science Pub Inc.

Bush, D., N. Longo, W. Neal, L. Esteves, O. Pilkey, D. Pilkey, and C. Webb. 2001. *Living on the Edge of the Gulf*.

Butman, B., C. R. Sherwood, and P. S. Dalyander. 2008. Northeast storms ranked by wind stress and wave-generated bottom stress observed in Massachusetts Bay, 1990–2006. *Continental Shelf Research* 28 (10):1231-1245.

Capece, J. 2001. Land-use history of Cape Poge and Wasque, 17. Vineyard Haven, MA: The Trustees of Reservations.

Carls, E. G., R. I. Lonard, and D. B. Fenn. 1990. Impact of oil and gas operations on the vegetation of Padre Island National Seashore, Texas, USA. *Ocean and Shoreline Management* 14 (2):85-104.

———. 1991. Notes on the vegetation and flora of North Padre Island, Texas. *The Southwestern Naturalist* 36 (1):121-125.

Carlton, J. M. 1977. A survey of selected coastal vegetation communities of Florida, 44. St. Petersburg, FL: Florida Department of Natural Resources: Marine Research Laboratory.

Center for Earth Observation. *http://www.yale.edu/ceo/*

Chepil, W., D. Armbrust, and F. Siddoway. 1963. Climatic index of wind erosion conditions in the Great Plains. *Soil Science Society of America Journal* 27 (4):449-452.

Christensen, J. H., B. Hewitson, A. Busuioc, A. Chen, X. Gao, I. Held, R. Jones, R. K. Koli, W.-T. Kwon, R. Laprise, V. M. Rueda, L. Mearns, C. G. Menendez, J. Räisänen, A. Rinke, A. Sarr, and P. Whetten. 2007. Regional Climate Projections. In *Climate Change 2007: The Physical Science Basis. Contribution of Working Group I to the Fourth Assessment Report of the Intergovernmental Panel on Climate Change*, eds. S. Solomon, D. Qin, M. Manning, Z. Chen, M. Marguis, K. B. Averyt, M. Tignor and H. L. Miller. Cambridge, UK; New York, NY, USA: Cambridge University Press.

Cooper, W. S. 1958. *Coastal sand dunes of Oregon and Washington*. Baltimore, M.D: Geological Society of America - Memoir 72.

———. 1967. *Coastal dunes of California*. Boulder, CO: Geological Society of America.

D'Antonio, C. M. 1993. Mechanisms controlling invasion of coastal plant communities by the alien succulent Carpobrotus edulis. *Ecology* 74 (1):83-95.

Davis, R. A. J. 1997. Geology of the Florida Coast. In *The Geology of Florida*, eds. A. F. Randazzo and D. S. Jones, 155-168. Gainesville: University Press of Florida.

Davis, R. E., and R. Dolan. 1992. The" All Hallows' Eve" Coastal Storm: October 1991. *Journal of Coastal Research* 8 (4):978-983.

———. 1993. Nor'easters. *American scientist* 81 (5):428-439.

Dolan, R. 1972. Barrier dune system along the Outer Banks of North Carolina: a reappraisal. *Science* 176 (4032):286-288.

Dolan, R., P. J. Godfrey, and W. E. Odum. 1973. Man's impact on the barrier islands of North Carolina. *American scientist* 61 (2): 152-162.

Donnelly, J. P., J. Butler, S. Roll, M. Wengren, and T. Webb. 2004. A backbarrier overwash record of intense storms from Brigantine, New Jersey. *Marine Geology* 210 (1):107-121.

Doyle, L. J., D. Sharma, A. Hine, O. Pilkey Jr, W. Neal, O. Pilkey Sr, D. Martin, and D. Belknap. 1984. *Living with the West Florida shore*. Durham, NC: Duke University Press.

Fitzgerald, D. M., and S. Van Heteren. 1999. Classification of paraglacial barrier systems: coastal New England, USA. *Sedimentology* 46 (6):1083-1108.

FitzGerald, D. M., S. van Heteren, and T. M. Montello. 1994. Shoreline processes and damage resulting from the Halloween Eve storm of 1991 along the north and south shores of Massachusetts Bay, USA. *Journal of Coastal Research* 10 (1):113-132.

Forman, R. T. T. 1995a. *Land mosaics: the ecology of landscapes and regions*. Cambridge, UK: Cambridge University Press.

———. 1995b. Some general principles of landscape and regional ecology. *Landscape ecology* 10 (3):133-142.

Forman, R. T. T., and M. Godron. 1986. *Landscape ecology*. New York: John Wiley & Sons.

Fryberger, S. G., and G. Dean. 1979. Dune forms and wind regime. *A study of global sand seas* 1052:137-169.

Gares, P. A. 1987. Eolian sediment transport and dune formation on undeveloped and developed shorelines, Geography, Rugers University, New Brunswick, N.J.

———. 1992. Topographic changes associated with coastal dune blowouts at Island Beach State Park, New Jersey. *Earth Surface Processes and Landforms* 17 (6):589-604.

Gares, P. A., and K. F. Nordstrom. 1988. Creation of dune depressions by foredune accretion. *Geographical review*:194-204.

———. 1995. A cyclic model of foredune blowout evolution for a leeward coast: Island Beach, New Jersey. *Annals of the Association of American Geographers* 85 (1):1-20.

Godfrey, P. 1977. Climate, plant response and development of dunes on barrier beaches along the US east coast. *International Journal of Biometeorology* 21 (3):203-216.

Guinon, M., and D. Allen. 1990. Restoration of dune habitat at Spanish Bay. In *Environmental restoration: science and strategies for restoring the Earth.* ed. J. Berger, 70-80. Washington D.C.: Island Press.

Hargis, C. D., J. A. Bissonette, and J. L. David. 1998. The behavior of landscape metrics commonly used in the study of habitat fragmentation. *Landscape ecology* 13 (3):167-186.

Hennigar, H. F. 1977. Evolution of coastal sand dunes: Currituck spit, VA/NC. In *Coastal processes and resulting forms of sediment accumulations*, ed. V. Goldsmith, 403-422. Gloucester Point, VA: Society of Economic Paleontologists and Mineralogists and Virginia Institute of Marine Science.

Hesp, P. 1983. Morphodynaics of incipient foredunes in NSW, Australia. In *Eolian Sediments and Processes*, eds. M. E. Brookfield and T. S. Ahlbrandt, 325-342. Amsterdam: Elsevier.

———. 2002. Foredunes and blowouts: initiation, geomorphology and dynamics. *Geomorphology* 48 (1):245-268.

Hesp, P. A., and R. Hyde. 1996. Flow dynamics and geomorphology of a trough blowout. *Sedimentology* 43 (3):505-525.

Hofmann, E. E., L. J. Pietrafesa, and L. P. Atkinson. 1981. A bottom water intrusion in Onslow Bay, North Carolina. *Deep Sea Research Part A. Oceanographic Research Papers* 28 (4):329-345.

Houser, C., C. Hapke, and S. Hamilton. 2008. Controls on coastal dune morphology, shoreline erosion and barrier island response to extreme storms. *Geomorphology* 100 (3):223-240.

Hugenholtz, C., and S. Wolfe. 2005a. Biogeomorphic model of dunefield activation and stabilization on the northern Great Plains. *Geomorphology* 70 (1):53-70.

———. 2006. Morphodynamics and climate controls of two aeolian blowouts on the northern Great Plains, Canada. *Earth Surface Processes and Landforms* 31 (12):1540-1557.

Hugenholtz, C. H., N. Levin, T. E. Barchyn, and M. C. Baddock. 2012. Remote sensing and spatial analysis of aeolian sand dunes: a review and outlook. *Earth-Science Reviews* 111:319-334.

Hugenholtz, C. H., and S. A. Wolfe. 2005b. Recent stabilization of active sand dunes on the Canadian prairies and relation to recent climate variations. *Geomorphology* 68 (1):131-147.

Inman, D. L., and R. Dolan. 1989. The Outer Banks of North Carolina: Budget of sediment and inlet dynamics along a migrating barrier system. *Journal of Coastal Research* 5 (2):193-237.

Inman, D. L., and C. Nordstrom. 1971. On the tectonic and morphologic classification of coasts. *The Journal of Geology* 79 (1):1-21.

Jensen, J. R. 2000. Remote sensing of the environment: An earth resource perspective. Upper Saddle River, NJ: Prentice Hall

Jones, J. R., and B. Cameron. 1976. Comparison between sieving and settling-tube determinations of sand sizes by using discriminant analysis. *Geology* 4 (12):741-744.

Jones, J. R., and B. Cameron. 1977. Landward migration of barrier island sands under stable sea level conditions; Plum Island, Massachusetts. *Journal of Sedimentary Research* 47 (4):1475-1483.

Komar, P. D., D. Carpenter, and W. G. McDougal. 1995. The application of beach and dune erosion models to the high-energy Oregon coast: The Oregon Department of Land Conservation and Development. Accessed on May in 2012 from the website (http://www.oregon.gov/LCD/pages/index.aspx)

Lancaster, N. 1988. Development of linear dunes in the southwestern Kalahari, southern Africa. *Journal of Arid Environments* 14 (3):233-244.

Lancaster, N., and P. Helm. 2000. A test of a climatic index of dune mobility using measurements from the southwestern United States. *Earth Surface Processes and Landforms* 25 (2):197-207.

Leatherman, S. P. 1985. Geomorphic and stratigraphic analysis of Fire Island, New York. *Marine Geology* 63 (1-4):173-195.

Levin, N. 2011. Climate-driven changes in tropical cyclone intensity shape dune activity on Earth's largest sand island. *Geomorphology* 125 (1):239-252.

Li, X., L. Lu, G. Cheng, and H. Xiao. 2001. Quantifying landscape structure of the Heihe River Basin, north-west China using FRAGSTATS. *Journal of Arid Environments* 48 (4):521-535.

Losey, R. J. 2005. House Remains at the Netarts Sandspit Village, Oregon. *Journal of Field Archaeology* 30 (4):401-417.

Luck, M., and J. Wu. 2002. A gradient analysis of urban landscape pattern: a case study from the Phoenix metropolitan region, Arizona, USA. *Landscape ecology* 17 (4):327-339.

Marin, L., S. Forman, A. Valdez, and F. Bunch. 2005. Twentieth century dune migration at the Great Sand Dunes National Park and Preserve, Colorado, relation to drought variability. *Geomorphology* 70 (1):163-183.

Martin, W. E. 1959. The vegetation of Island Beach State Park, New Jersey. *Ecological Monographs* 29 (1):2-46.

Mazzullo, J., and S. K. Kennedy. 1985. Automated measurement of the nominal sectional diameters of individual sedimentary particles. *Journal of Sedimentary Research* 55 (4):593-595.

McAtee, J. W., and D. L. Drawe. 1980. Human impact on beach and foredune vegetation of North Padre Island, Texas. *Environmental Management* 4 (6):527-538.

McBride, J. R., and E. C. Stone. 1976. Plant succession on the sand dunes of the Monterey Peninsula, California. *American Midland Naturalist* 96 (1):118-132.

McCown, S. 2011. "Perfect Storm" damage summary, ed. National Climatic Data Center. National Oceanic and Atmospheric Administration.

McDonnell, M. J. 1981. Trampling effects on coastal dune vegetation in the Parker River National Wildlife Refuge, Massachusetts, USA. *Biological Conservation* 21 (4):289-301.

FRAGSTATS v4: Spatial Pattern Analysis Program for Categorical and Continuous Maps. Computer software program, Univ. Mass, Amherst.

McGarigal, K., S. A. Cushman, M. C. Neel, and E. Ene. 2002. FRAGSTATS: spatial pattern analysis program for categorical maps. Univ. Mass., Amherst.

McIntire, W. G., and J. P. Morgan. 1962. Recent geomorphic history of Plum Island. Massachusetts and adjacent coasts. In *Atlantic Coastal Studies Technical Report*. Baton Rouge: Coastal Studies Institute Louisiana State University.

Mendelssohn, I. A., M. W. Hester, F. J. Monteferrante, and F. Talbot. 1991. Experimental dune building and vegetative stabilization in a sand-deficient barrier island setting on the Louisiana coast, USA. *Journal of Coastal Research* 7 (1):137-149.

Miller, T. E., E. S. Gornish, and H. L. Buckley. 2010. Climate and coastal dune vegetation: disturbance, recovery, and succession. *Plant ecology* 206 (1):97-104.

Muhs, D., and P. Maat. 1993. The potential response of eolian sands to greenhouse warming and precipitation reduction on the Great Plains of the USA. *Journal of Arid Environments* 25 (4):351-361.

Muhs, D. R., and V. T. Holliday. 1995. Evidence of active dune sand on the Great Plains in the 19th century from accounts of early explorers. *Quaternary Research* 43 (2):198-208.

Muller, R. A., and G. W. Stone. 2001. A climatology of tropical storm and hurricane strikes to enhance vulnerability prediction for the southeast US coast. *Journal of Coastal Research* 17 (4):949-956.

Murcia, C. 1995. Edge effects in fragmented forests: implications for conservation. *Trends in Ecology & Evolution* 10 (2):58-62.

Nield, J. M., and A. C. W. Baas. 2008. The influence of different environmental and climatic conditions on vegetated aeolian dune landscape development and response. *Global and Planetary Change* 64 (1):76-92.

Nordstrom, K. F. 2004. *Beaches and dunes of developed coasts*. Cambridge, UK: Cambridge University Press.

Nordstrom, K. F., P. A. Gares, N. P. Psuty, J. Orrin H. Pilkey, W. J. Neal, and S. Orrin H. Pilkey. 1986. *Living with the New Jersey shore*. Durham, NC: Duke University Press Books.

Nordstrom, K. F., and N. L. Jackson. 1995. Temporal scales of landscape change following storms on a human-altered coast, New Jersey, USA. *Journal of Coastal Conservation* 1 (1):51-62.

Nordstrom, K. F., N. L. Jackson, and K. H. Korotky. 2011. Aeolian sediment transport across beach wrack. *Journal of Coastal Research* Special Issue (59):211-217.

Nordstrom, K. F., and E. L. Lotstein. 1989. Perspectives on resource use of dynamic coastal dunes. *Geographical review* 79 (1):1-12.

Orme, A. R. 2005. Morro Bay to Pint Conception. In *Living with the Changing California Coast*, eds. G. Griggs, K. Patsch and L. Savoy, 334-358. Berkeley and Los Angeles: University of California Press.

North Carolina State Parks. http://www.ncparks.gov.

Peterson, C. D., S. S. Williams, K. M. Cruikshank, and J. R. Dubè. 2011. Geoarchaeology of the Nehalem spit: Redistribution of beeswax galleon wreck

debris by Cascadia earthquake and tsunami (~ AD 1700), Oregon, USA. *Geoarchaeology* 26 (2):219-244.

Pilkey, O. H. 1998. *The North Carolina shore and its barrier islands: restless ribbons of sand*. Durham, NC: Duke University Press Books.

Pilkey, O. H. J., W. J. Neal, O. H. S. Pilkey, and S. R. Riggs. 1980. *From Currituck to Calabash: living with North Carolina's barrier islands*. 2nd ed. Durham, N.C.: Duke University Press.

Pitts, W. D., and M. G. Barbour. 1979. The microdistribution and feeding preferences of Peromyscus maniculatus in the strand at Point Reyes National Seashore, California. *American Midland Naturalist* 101 (1):38-48.

Priestas, A. M., and S. Fagherazzi. 2010. Morphological barrier island changes and recovery of dunes after Hurricane Dennis, St. George Island, Florida. *Geomorphology* 114 (4):614-626.

Raines, G. L. 2002. Description and comparison of geologic maps with FRAGSTATS—a spatial statistics program. *Computers & geosciences* 28 (2):169-177.

Riggs, S. R., W. J. Cleary, and S. W. Snyder. 1995. Influence of inherited geologic framework on barrier shoreface morphology and dynamics. *Marine Geology* 126 (1):213-234.

Riitters, K. H., R. O'neill, C. Hunsaker, J. D. Wickham, D. Yankee, S. Timmins, K. Jones, and B. Jackson. 1995. A factor analysis of landscape pattern and structure metrics. *Landscape ecology* 10 (1):23-39.

Roman, C. T., N. Jaworski, F. T. Short, S. Findlay, and R. S. Warren. 2000. Estuaries of the northeastern United States: habitat and land use signatures. *Estuaries and Coasts* 23 (6):743-764.

Rust, I. C., and W. K. Illenberger. 1996. Coastal dunes: sensitive or not? *Landscape and Urban Planning* 34 (3–4):165-169.

Sallenger Jr, A. H. 2000. Storm impact scale for barrier islands. *Journal of Coastal Research* 16 (3):890-895.

Savoy, L. E., D. Merritts, G. B. Griggs, and D. Rust. 1985. The Northern California Coast. In *Living with the California coast*, eds. G. B. Griggs, K. Patsch and L. E. Savoy, 163-191. Durham, N.C.: Duke University Press.

Schwab, W. C., E. R. Thieler, J. R. Allen, D. S. Foster, B. A. Swift, and J. F. Denny. 2000. Influence of inner-continental shelf geologic framework on the evolution

and behavior of the barrier-island system between Fire Island Inlet and Shinnecock Inlet, Long Island, New York. *Journal of Coastal Research* 16 (2):408-422.

Shennan, I., A. Long, M. Rutherford, J. Innes, F. Green, and K. Walker. 1998. Tidal marsh stratigraphy, sea-level change and large earthquakes—II: submergence events during the last 3500 years at Netarts Bay, Oregon, USA. *Quaternary Science Reviews* 17 (4-5):365-393.

Shumway, S. 1996. The swales of Sandy Neck. In *A report to the Massachusetts Natural Heritage and Endangered Species Program*, 46. Westborough, MA.

Exelis Visual Information Solutions. http://www.exelisvis.com/.

Stauble, D. K., and D. A. Warnke. 1974. The bathymetry and sedimentation of Cape San Blas shoal and shelf off Saint Joseph Spit, Florida. *Journal of Sedimentary Research* 44 (4):1037-1051.

Steiniger, S., and G. J. Hay. 2009. Free and open source geographic information tools for landscape ecology. *Ecological Informatics* 4 (4):183-195.

Stewart, R. A., and D. S. Gorsline. 1962. Recent Sedimentary History of St. Joseph Bay, Florida. *Sedimentology* 1 (4):256-286.

Talbot, M. 1984. Late Pleistocene rainfall and dune building in the Sahel. *Palaeoecology of Africa* 16:203-214.

Taylor, G. H., and C. Hannan. 1999. *The climate of Oregon: from rain forest to desert*. Corvallis: Oregon State University Press.

Thomas, D. S. G., M. Knight, and G. F. S. Wiggs. 2005. Remobilization of southern African desert dune systems by twenty-first century global warming. *Nature* 435 (7046):1218-1221.

Thomas, D. S. G., and H. Leason. 2005. Dunefield activity response to climate variability in the southwest Kalahari. *Geomorphology* 64 (1):117-132.

Thornthwaite, C. W. 1948. An approach toward a rational classification of climate. *Geographical review* 38 (1):55-94.

Tsoar, H. 2005. Sand dunes mobility and stability in relation to climate. *Physica A: Statistical Mechanics and its Applications* 357 (1):50-56.

Uuemaa, E., M. Antrop, J. Roosaare, R. Marja, and Ü. Mander. 2009. Landscape metrics and indices: an overview of their use in landscape research. *Living Reviews in Landscape Research* 3 (1):28.

Vallino, J., and J. Hopkinson, CS. 1998. Estimation of dispersion and characteristic mixing times in Plum Island Sound estuary. *Estuarine, Coastal and Shelf Science* 46 (3):333-350.

Van der Meulen, F., and A. Salman. 1996. Management of Mediterranean coastal dunes. *Ocean & coastal management* 30 (2):177-195.

Van Heteren, S., and O. Van de Plassche. 1997. Influence of relative sea-level change and tidal-inlet development on barrier-spit stratigraphy, Sandy Neck, Massachusetts. *Journal of Sedimentary Research* 67 (2):350-363.

Wasson, R. 1984. Late Quaternary palaeoenvironments in the desert dunefields of Australia. In *Late Cainozoic Palaeoclimates of the Southern Hemisphere*, ed. J. C. Vogel, 419-432. Rotterdam: A.A. Balkema.

Wiedemann, A. M. 1998. Coastal foredune development, Oregon, USA. *Journal of Coastal Research* Special Issue (26):45-51.

Wiggs, G. F. S., D. S. G. Thomas, J. E. Bullard, and I. Livingstone. 1995. Dune mobility and vegetation cover in the southwest Kalahari Desert. *Earth Surface Processes and Landforms* 20 (6):515-529.

Williams, W. T., and J. R. Potter. 1972. The coastal strand community at Morro Bay State Park, California. *Bulletin of the Torrey Botanical Club* 99 (4):163-171.

Wise, B. R., and W. A. White. 1980. *Padre Island National Seashore : a guide to the geology, natural environments, and history of a Texas barrier island*. Austin, TX: Bureau of Economic Geology, University of Texas at Austin.

Wolfe, S. 1997. Impact of increased aridity on sand dune activity in the Canadian Prairies. *Journal of Arid Environments* 36 (3):421-432.

Wu, J., and R. Hobbs. 2002. Key issues and research priorities in landscape ecology: an idiosyncratic synthesis. *Landscape ecology* 17 (4):355-365.

Zhang, K., B. C. Douglas, and S. P. Leatherman. 2001. Beach erosion potential for severe nor'easters. *Journal of Coastal Research* 17 (2):309-321.

APPENDIX

Köppen's Climate Classification System

Classification of major climatic types according to the Köppen-Geiger-Pohl scheme letter symbol

1st	2nd	3rd	criterion
A			temperature of coolest month 18 degrees Celsius or higher
	f		precipitation in driest month at least 60 mm
	m		precipitation in driest month less than 60 mm but equal to or greater than 100 – *r*/25)[1]
	w		precipitation in driest month less than 60 mm and less than 100 – (*r*/25)
B[2]			70% or more of annual precipitation falls in the summer half of the year and *r* less than 20*t* + 280, or 70% or more of annual precipitation falls in the winter half of the year and *r* less than 20*t,* or neither half of the year has 70% or more of annual precipitation and *r* less than 20*t* + 140[3]
	W		*r* is less than one-half of the upper limit for classification as a B type (see above)
	S		*r* is less than the upper limit for classification as a B type but is more than one-half of that amount
		h	*t* equal to or greater than 18 degrees Celsius
		k	*t* less than 18 degrees Celsius
C			temperature of warmest month greater than or equal to 10 degrees Celsius, and temperature of coldest month less than 18 degrees Celsius but greater than –3 degrees Celsius
	s		precipitation in driest month of summer half of the year is less than 30 mm and less than one-third of the wettest month of the winter half
	w		precipitation in driest month of the winter half of the year less than one-tenth of the amount in the wettest month of the summer half
	f		precipitation more evenly distributed throughout year; criteria for neither s nor w satisfied
		a	temperature of warmest month 22 degrees Celsius or above
		b	temperature of each of four warmest months 10 degrees Celsius or above but warmest month less than 22 degrees Celsius
		c	temperature of one to three months 10 degrees Celsius or above but warmest month less than 22 degrees Celsius
D			temperature of warmest month greater than or equal to 10 degrees Celsius, and temperature of coldest month –3 degrees Celsius or lower

Table continued

1st	2nd	3rd	criterion
	s		same as for type C
	w		same as for type C
	f		same as for type C
		a	same as for type C
		b	same as for type C
		c	same as for type C
		d	temperature of coldest month less than –38 degrees Celsius (d designation then used instead of a, b, or c)
E			temperature of warmest month less than 10 degrees Celsius
	T		temperature of warmest month greater than 0 degrees Celsius but less than 10 degrees Celsius
	F		temperature of warmest month 0 degrees Celsius or below
H[4]			temperature and precipitation characteristics highly dependent on traits of adjacent zones and overall elevation—highland climates may occur at any latitude

[1]In the formulas above, *r* is average annual precipitation total (mm) and *t* is average annual temperature (degrees Celsius). All other temperatures are monthly means (degrees Celsius), and all other precipitation amounts are mean monthly totals (mm).

[2]Any climate that satisfies the criteria for designation as a B type is classified as such, irrespective of its other characteristics.

[3]The summer half of the year is defined as the months April–September for the Northern Hemisphere and October–March for the Southern Hemisphere.

[4]Most modern climate schemes consider the role of altitude. The highland zone has been taken from Trewartha (1968).

Type A climates

- Af : Wet equatorial climate
- Am: Tropical monsoon and trade-wind littoral climate
- Aw: Tropical wet dry

Type B climates

- Bwh (part of BWk): Tropical and subtropical desert climate
- Bsh: Mid-latitude steppe and desert climate
- Bsk (part of BWk): Tropical and subtropical steppe climate

Type C and D climates

- Cfa, Cwa: Humid subtropical climate
- Csa, Csb: Mediterranean climate
- Cfb, Cfc: Marine west coast climate
- Dfa, Dfb, Dwa, Dwb: Humid continental climate
- Dfc, Dfd, Dwc, Dwd: Continental subarctic climate

Type E and H climates

- ET: Tundra climate
- EF: Snow and ice climate
- H: Highland climate

(Source: www.britannica.com)